THE ROLE OF INFLAMMASOME AND CASPASE-1 IN REGULATING ADAPTIVE

RESPONSE TO OXIDATIVE STRESS IN MOUSE HEPATOCYTES

by

Qian Sun

Bachelor of Medicine, Fudan University, 2008

Submitted to the Graduate Faculty of

the School of Medicine in partial fulfillment

of the requirements for the degree of

Doctor of Philosophy

University of Pittsburgh

2013

UNIVERSITY OF PITTSBURGH

SCHOOL OF MEDICINE

This dissertation was presented

by

Qian Sun

It was defended on

June 24, 2013

and approved by

Chairperson: Tim D. Oury, MD, PhD, Professor, Department of Pathology

Donna Beer Stolz, PhD, Associate Professor, Department of Cell Biology

Russell D. Salter, PhD, Professor, Department of Immunology

Yoram Vodovotz, PhD, Professor, Department of Surgery

Melanie J. Scott, MD, PhD, Assistant Professor, Department of Surgery

Dissertation Advisor: Timothy R. Billiar, MD, Professor and Chair, Department of Surgery

THE ROLE OF INFLAMMASOME AND CASPASE-1 IN REGULATING ADAPTIVE RESPONSE TO OXIDATIVE STRESS IN MOUSE HEPATOCYTES

Qian Sun

University of Pittsburgh, 2013

In myeloid cells, oxidative stress can induce the activation of caspase-1 through canonical inflammasome signaling, which leads to the release of proinflammatory cytokines IL-1β/IL-18 and a potentially damaging inflammatory response. However, little is known about the role of caspase-1 in the liver after oxidative stress. This is especially true for the hepatocyte, a cell type that expresses and can activate the inflammasome but produces low levels of IL-1β and IL-18. Paradoxically, during hemorrhagic shock with resuscitation (HS/R) in an *in vivo* mouse model associated with severe hepatic redox stress, caspase-1 activation is protective against liver injury independent of IL-1β and IL-18. We also demonstrate that caspase-1 activation protects against cell death after redox stress in hepatocytes induced by hypoxia/reoxygenation in an *in vitro* model of HS/R. Mechanistically, we show that caspase-1 activation leads to reduced mitochondrial respiration and reactive oxygen species (ROS) production by increasing mitochondrial autophagy and subsequent clearance of mitochondria in hepatocytes after hypoxia/reoxygenation. During redox stress, caspase-1 increases autophagic flux through upregulation of the autophagy initiator, beclin1.

Although others have shown that ROS generated by damaged mitochondria activate the NACHT, LRR and PYD domains-containing protein 3(NLRP3) inflammasome, caspase-1 activation in the liver after oxidative stress was independent of NLRP3. We show that while the NLRP1 inflammasome is responsible for caspase-1 activation in immune cells that leads to IL-18

release after HS/R, the protective effect of caspase-1 in hepatocytes is due to the formation of an AIM2-initiated inflammasome. Our *in vitro* results also suggest that AIM2 is essential for the upregulation of beclin1 and mitochondrial clearance during redox stress in hepatocytes. High-mobility group box 1 (HMGB1) is a universal sentinel for nucleic acid-mediated innate immune responses. We found that HMGB1 associates with AIM2 and it is required for caspase-1 activation in hepatocytes after redox stress.

Our findings suggest a novel role for the AIM2 inflammasome and caspase-1 in regulating cellular responses to oxidative stress. We provide an important advancement in our understanding of how AIM2 and caspase-1 activation is linked with mitochondrial function and stress-induced autophagy as protective mechanisms in cells where IL1β/IL18 are not highly expressed.

TABLE OF CONTENTS

LIST OF TABLES

LIST OF FIGURES

PREFACE

ACKNOWLEDGMENTS

As nearly five years of graduate study come to an end, I have the chance to reflect upon this long and fulfilling journey. My experience as a PhD candidate allowed me to evolve from a student without much research or life experience into a relatively independent scientist. During these years, numerous people helped make this work possible and made my PhD studies such an enjoyable journey.

I am very grateful for my experiences working in the Billiar lab, and I cannot express enough gratitude towards everyone there; it is the teamwork of the entire lab rather than the work I did alone that made this dissertation possible. First and foremost, I would like to thank my thesis advisor, Dr. Timothy Billiar, for his unwavering support and mentorship. He has always guided and supported me when my project did not work or the results differed from what I expected. More importantly, he gave me enough freedom to pursue the research that interested me the most. His dedication to science and his trainees will undoubtedly serve as a high bar for which I will continually be reaching. I would also thank another one of my mentors, Dr. Melanie Scott, for her enormous patience and support. She has spent countless hours not only teaching me how to design and troubleshoot experiments, but also supporting and guiding me through difficult times. Both Dr. Scott and Dr. Billiar allowed me to learn from my mistakes and grow as an independent researcher.

I also deeply appreciate the help and support from my committee: Drs. Russ Salter, Donna Stolz, Yoram Vodovotz, and Tim Oury. They have provided invaluable suggestions regarding experimental design, method optimization, and results interpretation. Their advice was a great help to me in every step toward the completion of my project, as well as in searching for a postdoctoral position.

I would like to thank the past and present members of the Billiar lab for making it such a collaborative place to work. In particular, I want to express my thanks to Hong Liao and Meihua Bo for their help and support throughout these years. They have not only provided enormous help with my experiments, but more importantly, they have always been there to advise and support me at difficult times in my life. I would also like to thank Rick Shapiro for his suggestions and discussions on experimental techniques; Patricia Loughran for her valuable help with imaging; Deb Williams and Kathy DiGiacomo for their tireless work managing the laboratory; Wentao Gao for his input regarding autophagy and adenoviral infection; and Alicia Frank, Lauryn Kohut, and Carol Meiers for their hard work and valuable assistance with hepatocyte isolation and hemorrhagic shock surgery. I would like to thank Savanh Chanthaphavong, Houming Cai, Christine Chen, John Pribis, Sun Young Kim, Meihong Deng, and many other past and present Billiar lab members for being such valuable resources and great friends during my graduate studies.

I originally took over this work from Christoph Menzel, a former member of the Billiar lab. I would like to thank him for being a patient teacher and a great friend. Also thank you to Aaron Gusdon, who provided great help with the mitochondrial analysis. I would like to thank Dr. Wendy Mars for her help and advice throughout all these years, especially with job searching.

Lastly, I want to express thanks and love to my parents, who have been my never-ending source of support and encouragement. They have always been great role models because of their care and passion for work and other people. Their unconditional love and support have given and will always give me the strength to pursue my dreams.

ABBREVIATIONS

ALT - alanine aminotransferase

ASC- apoptosis-associated speck-like protein containing a caspase-recruitment domain

AST - aspartate transaminase

Atg - autophagy-related gene

ATP- adenosine triphosphate

BCA - bicinchoninic acid

Bcl-2 - B-cell lymphoma 2

BM – bone marrow

BSA - bovine serum albumin

DAMP - damage-associated molecular pattern

DAPI - 4',6-diamidino-2-phenylindole

DCF – dichlorofluorescein

DMSO - dimethyl sulfoxide

dsDNA - double-stranded DNA

FMF - familial Mediterranean fever

GFA - green fluorescent protein

H&E - hematoxylin and eosin

HEPES - 4-(2-hydroxyethyl)-1-piperazineethanesulfonic acid

HMGB1- high-mobility group box 1

HNE - 4-hydroxyl-2-nonenal

HS – hemorrhagic shock

HSP- heat shock protein

HS/R- hemorrhagic shock with resuscitation

H_2O_2 - hydrogen peroxide

IFN - interferon

IL - interleukin

IPAF - ice protease activating factor

I/R - ischemia/reperfusion

KO - knockout

LPS - lipopolysaccharides

MAVS- mitochondrial antiviral-signaling protein

MAP - mean arterial pressure

MnTMPyP - manganese (III) tetrakis (1-methyl-4-pyridyl) porphyrin

MODS- multiple organ dysfunction syndrome

MPT- Mitochondrial permeability transition

mRNA – messenger RNA

MSU- monosodium urate monohydrate

mtDNA - mitochondrial DNA

NADPH - oxidase- nicotinamide adenine dinucleotide phosphate-oxidase

NLR- NOD-like receptor

NOD - nucleotide-binding oligomerization domain

NRF- nuclear respiratory factor

OCR - oxygen consumption rate

PAMP- pathogen-associated molecular pattern

PARP - poly (ADP-ribose) polymerase

PBS – phosphate buffered saline

PGC-1α - peroxisome proliferator-activated receptor γ coactivator 1α

PCR - polymerase chain reaction

PI - propidium iodide

PI3K-III- class III phosphatidylinositol 3-kinase

poly(dA:dT)- poly(dA-dT):poly(dA-dT)

PRR - pattern recognition receptor

RFP - red fluorescent protein

RIG-I- retinoic acid-inducible gene-I

RIPA - radioimmunoprecipitation assay buffer

RNS- reactive nitrogen species

ROI – region of interest

ROS - reactive oxygen species

SEM - standard error of the mean

SD - standard deviation

SDS - sodium dodecyl sulfate

TCA - trichloroacetic acid

TGF - transforming growth factor

TLR- Toll-like receptor

TMRM - tetramethylrhodamine

TNF- tumor necrosis factor

TOM 20 - translocase of outer membrane 20

USP- ubiquitin carboxyl-terminal hydrolase

UVRAG - UV radiation resistance-associated gene

VPS34- vacuolar sorting protein 34

WT - wild type

1.0   INTRODUCTION

The liver is a highly metabolically active organ and excessive oxidative stress is a common mechanism of various liver diseases, including liver ischemia/reperfusion (I/R)[1], acetaminophen-induced liver failure[2], septic-induced liver damage[3] and metabolic liver disorders[4]. In myeloid cells oxidative stress can induce the activation of innate immune response, such as that mediated by caspase-1 through canonical inflammasome signaling, which leads to the release of proinflammatory cytokines IL-1β/IL-18 and a potentially damaging inflammatory response. However, little is known about the role of caspase-1 in the liver after oxidative stress. This is especially true for hepatocytes, a cell type that expresses and can activate the inflammasome but produce low levels of IL-1β and IL-18. In my dissertation, I will focus on exploring the role of inflammasome and caspase-1 in regulating cell death and damage after oxidative stress in hepatocytes and the liver.

1.1   INNATE IMMUNITY IN STERILE INJURY

1.1.1   Pattern recognition receptors

The activation of innate immune pathways is crucial for host defense in response to invasive pathogens. In the setting of microbial infection, pathogen-associated molecular patterns

(PAMPs), which are conserved microbial motifs, can be recognized by pattern recognition receptors (PRRs) expressed by innate immune cells[5, 6]. This leads to the eradication of pathogens through numerous killing and clearance mechanisms that involve the production of inflammatory mediators and cell recruitment and activation. Similarly, the same PRRs can be activated in response to sterile injuries, such as tissue trauma and ischemia-reperfusion injury. In this case, signaling through PRRs is triggered by the recognition of damage-associated molecular patterns (DAMPs)[5].

In settings such as sterile injuries, DAMPs are released after tissue stress and injury and activate innate immune cells. This leads to the production of pro-inflammatory cytokines and chemokines in a response very similar to that seen during pathogen-induced inflammation. Instead of leading to the clearance of pathogens, the sterile inflammatory response is crucial for tissue repair and the initiation of adaptive cell stress responses[5, 7]. However, an unresolved or excessive pro-inflammatory response in response to persistent high levels of DAMPs or lack of anti-inflammatory response can be detrimental to the host[5].

1.1.2   Damage associated molecular patterns and sterile injury

There is accumulating evidence that PRRs of the innate immune system are involved in mediating inflammatory responses to sterile injury such as I/R injury. Multiple studies have shown the *in vivo* requirement for Toll-like receptor (TLR) signaling in tissue damage mediation after oxidative stress induced by liver I/R or hemorrhagic shock (HS)[8-10]. For example, inflammatory response and heart failure after cardiac I/R have been shown to result from the activation of TLR9 by mitochondrial DNA that escapes during autophagic mitochondrial degradation[11]. Tsung *et al.* have also demonstrated that high-mobility group box1 (HMGB1)

released from ischemic cells activates TLR4 and leads to liver inflammation as well as damage after liver I/R[12, 13]. Most of the studies reported so far have linked the activation of TLR signaling with exacerbated tissue damage after I/R due to an excessive inflammatory response.

Other PRR families can also recognize DAMPs and may be expected to be involved in the responses induced by I/R. For example, nucleotide-binding oligomerization domain (NOD)-like receptors (NLRs) are another recently described family of intracellular PRRs shown to respond to DAMPs, including extracellular adenosine triphosphate (ATP)[14], amyloid-β peptide[15], monosodium urate crystals[16], uric acid[17], elevated extracellular glucose[18] and extracellular matrix components[19]. However, it remains unknown as to whether NLRs can be activated by DAMPs and can contribute to the inflammatory response induced by I/R injury.

1.2   ACTIVATION OF INFLAMMASOME IN STERILE INJURIRS

1.2.1   Inflammasome structure and signaling

The discovery and characterization of inflammasome as well as pathways leading to caspase-1 activation by inflammasome scaffolds have been an exciting development in the field of innate immunity. As one of the proinflammatory caspases, the activity of caspase-1 is tightly regulated by signal-dependent autoactivation within multiprotein complexes called inflammasomes. Inflammasomes have been shown to be formed after activation of certain NLRs, including NLRP1, NLRP3, AIM2, and ice protease activating factor (IPAF) (or NLRC4), by pathogens and host-derived endogenous indicators of cellular stress. Whereas NLRP1 and IPAF have only

been shown to be activated by PAMPs such as muramyl dipeptide and flagellin, respectively, NLRP3 and AIM2 can be activated by a number of DAMPs, including ROS and endogenous DNA in addition to PAMPs[20]. A typical inflammasome contains an NLR, apoptosis-associated speck-like protein containing a caspase-recruitment domain (ASC), and pro-caspase-1. Inflammasome activation leads to autocleavage of caspase-1 to form the active caspase-1 p10/p20 tetramer[21]. Active caspase-1 is required for the proteolytic maturation and release of cytokines known to be involved in the injury response, including IL-1β and IL-18.

The secretion of IL-1β has been shown to mediate a variety of cellular events, including neutrophil infiltration, the regulation of sleep and appetite, and body temperature[21]. As a member of the IL-1 cytokine family, IL-18 is also a potent proinflammatory cytokine that enhances T-cell and natural killer cell maturation, as well as the production of other cytokines, chemokines, and cell adhesion molecules[22]. It has been shown to induce hepatic I/R injury by suppressing the production of the anti-inflammatory cytokines IL-4 and IL-10[23]. IL-18 has also, in several studies, been associated with obesity, insulin resistance, hypertension, and dyslipidemia[24, 25]. However, a recent study also suggested the anti-inflammatory role of IL-18 in upregulating IL-10 production to exert protection against lethal acute lung damage after burn injury[26]. Whereas the production of IL-1β requires two signals (synthesis of pro-IL-1β through the activation of TLRs and cleavage into its active form by caspase-1), the release of IL-18 is mainly regulated by activation of caspase-1, as the pro-form is constitutively present in the cytoplasm[27].

1.2.2   Inflammasome activation induced by ROS

Reactive oxygen species (ROS) serve as the major mechanism for NLRP3 inflammasome activation following sterile injury. ROS-dependent activation of the NLRP3 inflammasome has

been implicated in hyperoxia-induced acute lung injury[28] after the stimulation of α-synclein aggregates in patients with Parkinson's disease[29, 30] upon exposure to self double-stranded DNA (dsDNA), as in systemic lupus erythematosus patients[31], in a murine model of gout induced by monosodium urate monohydrate (MSU) crystal injection[32], and in arthritis associated with deposition of hydroxyapatite crystals[33]. However, controversy remains regarding the source of inflammasome-activating ROS. Early studies suggested that ROS responsible for inflammasome activation are derived from nicotinamide adenine dinucleotide phosphate (NADPH) oxidase[34]. However, this theory is contradicted by the fact that macrophages deficient in NADPH oxidase complex components show no defect in inflammasome activation[34]. More recent evidence from multiple groups suggests that mitochondria could be the major source of ROS required for inflammasome activation[35, 36]. Inhibition of mitochondrial autophagy, which removes ROS-generating mitochondria, leads to increased NLRP3 inflammasome activation and IL-1β release in macrophages[35, 37, 38]. More specifically, mitochondrial-derived ROS induce the association of NLRP3 with thioredoxin-interacting protein, thereby inducing activation of the NLRP3 inflammasome[18].

1.2.3   Inflammasome activation induced by other danger signals released during redox stress

In addition to ROS, other danger signals released during metabolic stress have been shown to induce inflammasome activation. These include mitochondrial DNA released from dysfunctional mitochondria and ATP from damaged cells or tissues. Mitochondria not only produce ROS, but are also the major target of ROS. Elevated ROS levels lead to opening of a mitochondrial permeability transition pore, causing the release of mitochondrial DNA (mtDNA) into the

cytosol[37]. Cytosolic mtDNA and more specifically, oxidized mtDNA, contribute to the secretion of IL-1β and IL-18 by activating the NLRP3 inflammasome[39]. Extracellular ATP released from necrotic cells can also lead to the formation of NLRP3 inflammasome through activation of the P_2X_7 receptor and decrease in intracellular K^+ levels[39]. The *in vivo* relevance of extracellular ATP was confirmed by recent animal studies with a newly developed bioluminescent ATP probe, which showed that the extracellular concentration of ATP in inflamed tissues *in vivo* was sufficient for P2 receptor activation[40]. Therefore, it would be intriguing to investigate whether mitochondrial DNA or ATP could serve as danger signals during redox stress induced by hemorrhagic shock with resuscitation (HS/R).

1.2.4 Non-canonical activation of inflammasome

In contrast to the well-established pathway discussed above where inflammasome formation is required for caspase-1 activation, there is emerging evidence that caspase-11 mediates the non-canonical activation of caspase-1. The first evidence was produced by Wang *et al.* when they demonstrated an essential role for caspase-11 in caspase-1 activation after septic shock *in vivo*[41]. More recently, Vishva Dixit's group showed that commercially available caspase-1 $^{-/-}$ mice actually lack both caspase-1 and caspase-11. These caspase-1 $^{-/-}$ mice were generated using strain 129 embryonic stem cells, which attenuated caspase-11 expression genetically[42]. These researchers demonstrated that caspase-11 is critical for the non-canonical activation of caspase-1 and IL-1β production in macrophages infected with Gram-negative bacteria and certain pore-forming toxins from organisms such as *Escherichia coli*, *Citrobacter rodentium*, or *Vibrio cholera*, but not after the stimulation of ATP or MSU. Caspase-11 was also shown to be involved in NLRP3- and caspase-1-independent macrophage cell death, which is required for

6

lipopolysaccharide (LPS)-induced lethality *in vivo*. The mechanism of caspase-11-mediated cell death was further explored by the group of Katherine Fitzgerald and Edward Miao, who showed that Gram-negative bacteria enter the cytosol and trigger caspase-11-dependent cell death involving Toll/Interleukin-1R domain-containing adapter-inducing interferon-β signaling[43, 44]. However, whether caspase-11 contributes to cell death after sterile injury is still unclear.

1.3   NON-CYTOKINE-MATURATION ROLE OF CASPASE-1

In addition to the well-established role of caspase-1 in cytokine maturation, recent research has begun to implicate caspase-1 as a regulator of the cellular response to stress by regulating cell death, tissue repair, and cytoprotective responses[7, 45]. This aspect of caspase-1 function may be especially important in non-immune cells such as the hepatocyte, the dominant cell type in the liver and a cell that does not produce IL-1β or IL-18.

1.3.1   Caspase-1 and pyroptosis

There are multiple ways in which a cell can die in response to cell stress, including by apoptosis, necrosis, and pyroptosis. Cells also employ multiple strategies to help them cope with stress and survive. The activation of the inflammasome in immune cells is often associated with pyroptosis, a caspase-1 dependent cell death[46, 47]. Pyroptosis is a form of proinflammatory cell death that was first described in macrophages after *Salmonella* infection[48, 49]. It is characterized by swelling and rapid lysis of the cells with the release of proinflammatory mediators IL-1β and IL-18.

However, it is still unknown whether this caspase-1 dependent cell death is mediated through caspase-1 itself or by its substrates, IL-1β and IL-18. Recent evidence suggests that pyroptosis can be induced by not only PAMPs but also DAMPs and ROS. Fernandes-Alnemri and colleagues have shown that cytoplasmic DNA triggers formation of the AIM2 inflammasome, which lead to pyroptotic cell death[50].

1.3.2   Caspase-1 and apoptosis

The activation of caspase-1 has been associated with cell death in the form of apoptosis in non-myeloid cells. In the model of neuronal I/R, caspase-1 induces apoptotic cell death through two possible mechanisms. First, caspase-1 mediates neuronal cell death through cleaving BH3 interacting-domain death agonist (BID), a pro-apoptotic protein, and activating the apoptotic caspase cascade[51]. Second, there is evidence that cerebral ischemia induces acute brain injury and apoptotic cell death through production of the proinflammatory cytokine IL-1β[52, 53]. Furthermore, caspase-1 induced caspase-6-mediated apoptosis after serum deprivation in human neurons[54]. In models of cardiac I/R, inflammasome formation and caspase-1 activation were found in myeloid cells such as leukocytes, as well as in nonmyeloid cells, including cardiomyocytes, endothelial cells, and fibroblasts in the peri-infarct region[55, 56]. Here, the inflammasome was activated through the P2X7 receptor and was associated with increased cardiomyocyte cell death after acute ischemia, which could be rescued by a noncompetitive antagonist of the P2X7 receptor, pyridoxalphosphate-6′-azopheny-2′,4′-disulphonate (PPADS)[55]. Syed *et al.* also demonstrated in cultured cardiac myocytes that caspase-1 activation after hypoxia led to cleavage of caspase-3 and subsequent apoptosis[56]. Taken together, these studies suggest a role for caspase-1 in mediating apoptosis in neurons and cardiomyocytes after hypoxic

insult such as that induced by ischemia. But whether caspase-1 activation regulates apoptotic cell death in hepatocytes after cell stress remains unclear.

1.3.3   Caspase-1 and necrosis

The role of inflammasome and caspase-1 in the induction of necrosis has been investigated in several studies, but the mechanism remains largely unclear. Squires *et al.* have shown that caspase-1 activation leads to the impairment of plasma membrane integrity and necrosis in macrophages after anthrax lethal toxin treatment[57]. However, cell death triggered by anthrax lethal toxin is characterized by rapid cell lysis, which is also a feature of pyroptosis. It is therefore unclear whether caspase-1 mediates cytolysis through a distinct pathway leading to necrosis or solely by inducing pyroptosis. Another study by Motani and colleagues demonstrated that caspase-1 promoted ASC-mediated necrotic cell death in monocytes independent of the catalytic activity of caspase-1[58]. Here, caspase-1 functions as a molecular determinant of cell death modes. Activation of ASC induces necrosis in cells that express caspase-1 while in cells, where caspase-1 is knocked down in the cells undergoing apoptosis. Moreover, this seems to represent a distinct pathway of cell death triggered by caspase-1, since previous studies showed that pyroptosis was a process that required catalytic activity of caspase-1[59].

1.3.4   Caspase-1 and protein secretion

There is emerging evidence that links caspase-1 activation with the unconventional secretion of proteins, which includes the substrates of caspase-1 IL-1β and IL-18, components of inflammasome such as caspase-1 itself, as well as many other proteins involved in inflammation,

cytoprotection, or tissue repair[60-62]. As the substrates of caspase-1, pro-IL1β and pro-IL18 lack signal peptide required for the conventional, endoplasmic reticulum /Golgi-dependent secretion pathway[63, 64]. Instead, their secretion has been shown to be mediated by caspase-1[60], which suggests the essential role of caspase-1 in IL-1β and IL-18 maturation and release. Interestingly, caspase-1 itself can be released from activated macrophages or UV-irradiated keratinocytes through this non-classical secretion pathway that requires the enzymatic activity of caspase-1[60]. However, the extracellular function of caspase-1 still remains largely unknown. It was speculated that this could serve as negative feedback mechanism to limit the concentration of caspase-1 in cells[60].

Caspase-1 also regulates the secretion of other proteins involved in inflammation and tissue repair, which help to restore tissue homeostasis after major stress. Among those proteins, the most well-studied are IL-1α and retinoic acid-inducible gene-I (RIG-I)[61, 62, 65]. Whether the enzymatic activity of caspase-1 is required for this unconventional secretion pathway for IL-1α remains controversial. Two studies have suggested the role of caspase-1 in mediating IL-1α secretion[60, 62]. The function of IL-1α is mostly unknown, except that it can trigger a sterile inflammatory response through the activation of Interleukin-1 receptor 1 (IL-1R1)[66]. Calpain-like proteases have also been suggested to cleave IL-1α, and both full-length and cleaved IL-1α are able to activate IL-1R1[67]. Nonetheless, it is likely that caspase-1 serves as the central regulator of IL-1α signaling, given that caspase-1-dependent IL-1α release is essential for the downstream signaling mediated by IL-1R1 after the simulation of inflammasome activators[62]. Indeed, NLRP3 inflammasome assembly and caspase-1 activation have been shown to induce IL-1α secretion, leading to increased basal keratinocyte proliferation through activation of the IL-1R1 and NF-κB pathway[65].

The secretion of RIG-I was thought to be another process mediated by caspase-1 activation. As a PRR, RIG-I recognizes non-self dsRNA[68] and initiates an antiviral response through activating mitochondrial antiviral-signaling protein (MAVS) and the production of type 1 interferon (IFN)[69]. Caspase-1 has been demonstrated to physically interact with full length RIG-I, and its activation results in reduced cellular level of RIG-I and inhibition of RIG-I-mediated signaling activity through enhanced secretion[61]. Therefore, caspase-1 activation was thought to be a checkpoint to prevent the overproduction of IFN and function to limit inflammation after viral and microbial infection[61]. However, *in vivo* experiments need to be performed to confirm the relevance of the finding in the settings of viral infection.

1.3.5 Caspase-1 cleaves proteins other than IL-1β and IL-18

Caspase-1 is an aspartate-specific cysteine protease and would be expected to cleave many proteins. Shao *et al.* utilized a diagonal gel proteomic approach to identify 41 proteins as potential targets of caspase-1[70]. This study and others have identified multiple caspase-1 direct targets, including proteins involved in different processes essential for energy metabolism and inflammation[71-73]. As the first study to investigate the relationship between caspase-1 activation and energy metabolism, Shao *et al.* identified proteins essential for mitochondrial respiration and glycolysis as targets of caspase-1 in their diagonal gel screen. These included beta subunit precursor of ATP synthase and a number of glycolysis enzymes which were further verified by *in vitro* caspase cleavage assays[70]. Their experiments using wild type (WT) and caspase-1 deficient cells also confirmed that caspase-1 activation after *Salmonella* infection results in the processing of the glycolysis enzymes and reduction of the cellular glycolytic rate in the

11

macrophage, a cell type that is highly dependent on glycolysis for energy demand[74]. This regulation of metabolism was suggested to contribute to caspase-1-dependent cell death[70].

In addition, after a high-fat diet, caspase-1 was shown to cleave SIRT1[72], a histone deacetylase that promotes insulin secretion by β cells[75] and increases insulin sensitivity in peripheral tissues[76] . The cleavage of SIRT1 by NLRP3 inflammasome-mediated caspase-1 activation results in a reduction of SIRT1 function in cells[72], providing one explanation for why mice lacking NLRP3 or caspase-1 are protected from high-fat diet-induced insulin resistance, metabolic dysfunction, and obesity[77].

Catalytic cleavage by caspase-1 also leads to the loss-of-function or gain-of-function of proteins involved in inflammatory responses, such as MAVS and pyrin[71, 73]. A study by Yu *et al.* demonstrated that caspase-1 cleaves MAVS at residue D429 after Dengue virus infection, abolishing its function in IFN production and induction of apoptosis through disruption of the mitochondrial membrane potential and activation of apoptotic caspases[73]. Another study by Chae and colleagues suggested pyrin, a familial Mediterranean fever (FMF) protein, can be cleaved be caspase-1 at D330. In contrast to MAVS, the cleavage of pyrin by caspase-1 produced a 330-residue N-terminal fragment that enhances ASC-independent NF-κB activation[71]. Moreover, their study suggested that pyrin variants with FMF-associated mutants are more susceptible to catalytic cleavage by caspase-1 than WT pyrin, suggesting a role for caspase-1 in inducing inflammation through the NF-κB pathway in the autoinflammatory disease FMF.

1.3.6   Caspase-1 and lysosomal function

Lysosomes are organelles that are responsible for the degradation of proteins, engulfed virus, and bacteria, as well as dysfunctional organelles such as mitochondria[78]. Caspase-1 has been shown

to promote lysosomal degradation in macrophages after *Legionella*[79] and *Salmonella* infection[80]. IPAF-mediated activation of caspase-1 restricts bacterial growth after *Legionella* infection by promoting the maturation of *Legionella*-containing phagolysosome and intracellular degradation of *Legionella*, thereby restricting the intracellular replication of the bacterium[79]. However, the exact mechanism by which caspase-1 promotes the fusion of Legionella-containing phagosome and lysosome is still not clear. Caspase-1 activation has also been shown to activate another step of the lysosomal degradation process, lysosome exocytosis, through increasing intracellular calcium levels during pyroptosis[80]. Since lysosomal degradation of mitochondria (or mitochondrial autophagy) is crucial for mitochondrial quality control after stress conditions[36], it would be of great interest to investigate the relationship between caspase-1 activation and lysosomal function after sterile injury.

1.4   CELL STRESS RESPONSES INDUCED AFTER REDOX STRESS

Adaptive cell stress responses are induced in tissues and organs such as the liver after major local or systemic perturbations. These responses are thought to be essential to protect the organ from further damage and to return the tissue back to state of metabolic homeostasis. Autophagy is one of the important adaptive cell stress responses that can protect the liver. Mitochondrial permeability transition (MPT), an indicator of mitochondrial dysfunction, has been demonstrated to be essential for hepatocellular cell death after I/R and can be prevented by autophagy[81]. My research has focused on the response of the liver to a hypoxic insult as seen in shock. Because autophagy is one of the well characterized cell stress responses in the liver after I/R injury, my thesis work has centered on autophagy and regulation of mitochondrial function.

1.4.1 Autophagy

Autophagy is one of the major adaptive responses used to cope with major stresses in the liver. It is a protective process by which the cell sequesters damaged proteins, organelles, or pathogens in a double-membrane compartment, the autophagosome, where the sequestered material is degraded and recycled[82]. Autophagy is induced by cellular stress such as nutrient deprivation, hypoxia[83], redox stress[84], and by the inflammatory mediator IFNγ[85, 86]. In recent studies using macrophages, autophagy has been shown to be cytoprotective through the inhibition of inflammasome activation. In these immune cells, this subsequently leads to reduced production of the inflammatory mediators IL-1β and IL-18[38]. More specifically, the effect has been shown to be mediated by autophagy and especially mitochondrial autophagy through reducing mitochondrial ROS production and eliminating DAMPs such as mitochondrial DNA[35, 37]. Thus, in cells that produce IL1β or IL18, this may serve as a protective mechanism to suppress the proinflammatory response in order to limit tissue damage. However, at the organ level it is likely that the protective effects of autophagy extend beyond just regulating the magnitude of the inflammatory response and may be cell-type specific. This is seen at the whole organ level after stresses such as HS/R and I/R where autophagy is upregulated in the brain[87], liver[88], and heart[89]. Under such conditions, autophagy is cytoprotective by clearing dysfunctional mitochondria[35], maintaining cellular ATP levels[90] and eliminating misfolded protein.

1.4.1.1 Autophagy process and beclin1

Autophagy is a dynamic, multi-step process that is characterized by nucleation of the initial phagophore, elongation of the phagophore to form the autophagosome, and fusion of the autophagosome and lysosome for degradation and recycling. Beclin1, which is essential for both

14

nucleation and elongation of phagophore, was shown to be upregulated in rat hepatocytes and confer protection after hypoxia/reoxygenation[81, 91]. In response to the induction of autophagy, the cytosolic LC3 is conjugated to phosphatidylethanolamine, which forms the outer and inner membranes of the autophagosome.

As a major component of class III phosphatidylinositol 3-kinase (PI3K-III) complex, beclin1 modulates the activity of vacuolar sorting protein 34 (VPS34), which is crucial for vesicle nucleation in autophagy[92]. Beclin1 is known to be regulated at the transcriptional and post-translational levels, as well as via protein-protein interaction. Transforming growth factor-β (TGF-β) and hepatitis C virus infection have been shown to increase beclin1 expression at the transcriptional level through the Smad4 pathway and by enhancing beclin1 promoter activity, respectively[93, 94]. Another study has demonstrated that Heat Shock Protein 90 (HSP90) inhibits beclin1 expression transcriptionally through the inactivation of NF-κB[95]. However, unbiased and more rigorous studies still need to be conducted to determine what transcription factors are responsible for messenger RNA (mRNA) synthesis of beclin1.

Aside from transcriptional regulation, the function of beclin1 in promoting autophagy is also regulated through protein-protein interaction. The best established interaction is with anti-apoptotic protein B-cell lymphoma 2 (Bcl-2). Beclin1 has been shown to associate directly with Bcl-2 and this interaction prevents beclin1 oligomerization and its association with VPS34, which results in the inhibition of VPS34 complex and decreased autophagy[96]. Moreover, the ability of beclin1 to modulate VPS34 kinase activity also depends on a network of beclin1 interacting proteins, namely UV radiation resistance-associated gene (UVRAG)[97], an activating molecule in beclin1-regulated autophagy (AMBRA1)[98] and autophagy-related protein 14-like

protein (ATG14L)[99]. Among these positive regulatory proteins, UVRAG and ATG14L serve as binding partners of beclin1 and are involved in the activation of VPS34 containing complexes[92].

Previous studies suggest that beclin1 can be degraded after its ubiquitination, and therefore affect VPS34 activity. Firstly, the steady-state concentration of beclin1 has been shown to be altered by developmentally down-regulated protein 4 (NEDD4)-mediated ubiquitination of beclin1 after its direct binding with beclin1 at the PY motif[100]. Secondly, a recent study based on screening for chemical inhibitors of autophagy discovered that ubiquitination of beclin1 and the stability of PI3K-III complex are affected by the peptidase activity of ubiquitin carboxyl-terminal hydrolase 10 (USP10) and USP13[101]. Thirdly, beclin1 was shown to undergo ubiquitination in a K48-dependent manner and this pathway can be inhibited by the molecular chaperone HSP90; therefore, HSP90 was responsible for the increase in beclin1 expression and VPS34 activity in monocytes[102].

1.4.1.2 Inflammasome activation and autophagy

Although extensive studies suggesting that autophagy inhibition leads to the activation of the NLRP3 inflammasome[35, 37] have been conducted, very few have focused on investigating the role of inflammasome formation in regulating autophagy. Suzuki *et al.* provided the first evidence suggesting an effect of inflammasome activation on the regulation of autophagy. These authors showed that caspase-1 activation mediated by the IPAF inflammasome after *Shigella* infection lead to inhibition of autophagy, which protects infected macrophages from pyroptosis[103]. However, conflicting evidence also suggests that inflammasome activation is responsible for the upregulation of autophagy. A study by Shi *et al.* showed that the AIM2 inflammasome induces autophagosome formation by activating the G protein RalB, which forms part of the protein platform required for the formation and maturation of autophagosome[104, 105].

Therefore, it seems likely that the activation of different inflammasomes has specific regulatory effects on autophagy under varying stresses.

1.4.2   Regulation of mitochondrial function

As the major source of ATP and ROS generation in the cell, mitochondria are believed to be adaptive organelles. Mitochondrial mass and oxidative phenotype are elaborately controlled to match the needs of various tissues in response to changes in the physiological environment and cellular adaptive responses after major stress[106]. It is generally considered that the production of mitochondrial ROS occurs as a consequence of aerobic metabolism. However, evidence is emerging that ROS can also serve as signaling molecules that lead to either cell death or a cytoprotective response. It has been suggested that low ROS levels may be critical in metabolic adaptation and pre-conditioning responses[107] while moderate to high levels of ROS production could result in enhanced inflammatory responses or cell death induced by MPT[108].

1.4.2.1 Mitochondrial danger signals and inflammasome activation

Several recent studies have demonstrated that danger signals derived from mitochondria, especially mitochondrial ROS, can induce inflammation through activation of the NLRP3 inflammasome[35, 37]. As the most well-studied NLR, NLRP3 can be activated by a plethora of diverse stimuli, including extracellular ATP[14], amyloid-β peptide[109], MSU[16], elevated extracellular glucose,[110] and extracellular matrix such as hyaluronan [111]. Given that many of the known activators of NLRP3 inflammasome also generate ROS, it seems likely ROS form a common pathway by which various NLRP3 agonists activate the NLRP3-inflammasome. Many studies have shown that ROS scavengers suppress NLRP3 inflammasome activation[112, 113].

Moreover, recent studies provide substantial evidence suggesting that ROS derived from mitochondrial complex I and complex III stimulate activation of the NLRP3 inflammasome and release of IL-1β in monocytes[35, 37]. The release of mitochondrial DNA into the cytosol, especially in its oxidized form, also induces NLRP3 inflammasome formation[37, 39]. However, the precise mechanism by which ROS production leads to NLRP3 activation is still largely unknown. Other than the NLRP3 inflammasome, AIM2 has also been shown to be activated by host derived dsDNA[114]. Work presented in this dissertation will show that mtDNA can act as a DAMP to activate AIM2 inflammasome.

1.4.2.2 Mitochondrial ROS and other inflammatory pathways

In addition to the role of mitochondrial ROS in mediating the production of IL-1β and IL-18 through inflammasome activation, ROS generated by mitochondria have also been shown to increase mRNA synthesis of pro-inflammatory cytokines through NF-κB and c-Jun N-terminal kinase pathways in various settings[115, 116]. Unlike IL-1β and IL-18, which require cleavage to be activated, pro-inflammatory cytokines such as tumor necrosis factor (TNF) and IL-6 are induced primarily at the transcriptional level[117]. As a major transcription factor in the innate immune response, NF-κB can be the target of ROS in various ways. In most studies, exogenous hydrogen peroxide (H_2O_2) and endogenous ROS generated after hypoxia-reoxygenation upregulates NF-κB activation, and it does so in part through alternative phosphorylation of IκBα[116]. Whereas IκBα is usually phosphorylated at serines 32 and 36, which leads to its ubiquitination and degradation, redox stress affects the phosphorylation of IκBα on Tyr42 or other tyrosine residues, resulting in its dissociation with NF-κB and subsequent activation of NF-κB[118, 119]. However, ROS can also lead to an inhibitory effect of NF-κB activation[116], suggesting complex interactions between ROS and NF-κB.

1.4.2.3 Mitochondrial ROS and cell death

Increased mitochondrial ROS could also induce direct hepatocellular cell death in the form of apoptosis or necrosis after I/R through MPT[81, 120]. Furthermore, MPT is the essential event in necroptosis induction, a specialized pathway of programmed necrosis characterized by the activation of receptor-interacting protein 1 (RIP1) after cardiac and cerebral ischemic injury[120]. MPT is associated with mitochondrial depolarization, uncoupling of oxidative phosphorylation, mitochondrial swelling, and subsequent necrotic and apoptotic cell death[121, 122]. However, cell death can be prevented over the short term if there is an alternative source of ATP produced through glycolysis[1]. Caspase-1 has been shown to cleave and inactivate enzymes involved in glycolysis and therefore inhibit glycolysis in macrophages after *Salmonella* infection[70]. But the role of inflammasomes and capase-1 in regulating mitochondria-derived cell death remains largely uninvestigated.

1.4.2.4 Mitochondrial biogenesis and mitophagy in mitochondrial quality control

Under stress conditions such as inflammation, calorie restriction, and oxidative stress, mitochondria are organelles that are particularly susceptible to oxidative damage and mitochondrial dysfunction, resulting in impaired ATP generation, excessive ROS production, and cell death[106, 123]. In response to these conditions, cells avoid major mitochondrial-mediated damage and preserve the quality of mitochondria through mitophagy, a process that identifies and targets dysfunctional mitochondria for degradation while concomitantly activating mitochondrial biogenesis.[106].

Mitochondrial biogenesis is controlled to a large extent by transcriptional mechanisms[106, 124]. Most of the genes involved in mitochondrial biogenesis are under the control of a nuclear network of transcription factors and coregulators that are responsible for fine-tuning gene

expression in response to changes in the physiological environment. Among these, peroxisome proliferator-activated receptor γ coactivator 1α (PGC-1α) has been demonstrated as the master regulator of mitochondrial biogenesis. It has been shown to co-activate nuclear respiratory factor 2 (NRF2) and nuclear respiratory factor 1 (NRF1), which leads to increased expression of mitochondrial transcription factor A as well as other nuclear-encoded mitochondria subunits of the electron transport chain complex, including β-ATP synthase and cytochrome c oxidase IV[125]. Although PGC-1α has been shown to be upregulated and mediate mitochondrial biogenesis after chronic hypoxia[126, 127], not much is known about its role in models of acute hypoxic stress such as that induced by I/R. In addition to its role in mitochondrial biogenesis, PGC-1α also induces the upregulation of antioxidant mechanisms and thereby protects cells from redox stress[128]. Therefore, it would be of great interest to assess whether PGC-1α is involved in cytoprotection after redox stress induced by HS with resuscitation.

1.5   HEMORRHAGIC SHOCK (HS)

Trauma is the third leading cause of death and morbidity worldwide. Much of the mortality and morbidity is caused by multiple organ dysfunction syndrome (MODS) resulting from systemic and end-organ inflammation secondary to HS/R, which is associated with global I/R injury[129]. The liver is one of the major organs that is affected by HS/R and liver damage is often associated with MODS[130]. It was estimated that approximately 20% of trauma patients admitted to hospitals with HS show liver dysfunction and develop hyperbilirubinemia[131]. Since the liver plays a key role in metabolism, HS also leads to alterations in synthesis of proteins such as acute phase protein and albumin[131].

1.5.1 HS and liver injury
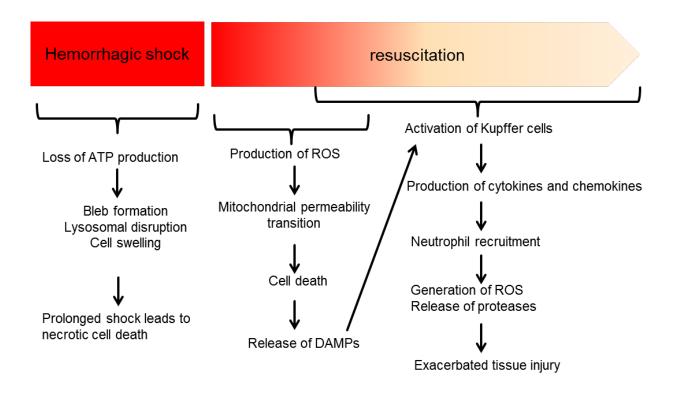
Figure 1. The time course of HS/R-induced liver injury

HS causes systemic hypoxia and low blood flow to the liver, resulting in insufficient local oxygen supply[132]. Mitochondrial respiration is suppressed during hypoxia due to lack of oxygen. This leads to the inhibition of oxidative phosphorylation with a subsequent reduction in ATP production[133]. Reduction of ATP causes cell swelling, rounding of mitochondria, lysosomal disruption, formation of plasma membrane blebs, and necrotic cell death, eventually resulting from disturbances in membrane ion translocation driven by ATP-dependent channels[134] (Figure 1).

Although HS itself primes cells for damage and will eventually cause cell death when the process is prolonged, the injury is more severe after the liver is reperfused/reoxygenated[133].

Production of ROS and reactive nitrogen species (RNS) has long been implicated in reperfusion injury. Even though low levels of ROS may be critical to signaling in cell stress and pre-conditioning responses[107], high levels of ROS contribute to hepatocellular cell death during liver I/R. During reperfusion/reoxygenation, the reestablishment of mitochondrial aerobic respiration results in excessive ROS production, which can trigger necrotic and apoptotic cell death through MPT and oxidation of essential molecules[132, 135]. After the onset of MPT, mitochondria depolarize and undergo large-amplitude swelling, which then leads to the rupture of the mitochondrial outer membrane and cytochrome c release[132]. Either apoptosis or necrosis can occur following MPT, depending on the level of intracellular ATP[133, 136]. Cyclosporin A, an inhibitor of MPT, has been reported to protect the liver from I/R injury by preventing mitochondrial depolarization and ATP depletion[137].

Tissue toxicity from excessive free radical generation can also result from its reactivity with various biological molecules, including inducing lipid peroxidation[138], mitochondrial DNA breaks,[139] and thiol oxidation in proteins[140]. Thiol oxidation of caspase-9, for example, promotes activation of caspase-9 and onset of apoptosis through the formation of disulfide bond linking caspase-9 with apoptotic protease-activating factor 1 (Apaf-1)[141]. Clinically, a few antioxidant agents have been shown to have a beneficial effect in the treatment of liver I/R injury, including thiol compound N-acetylcysteine[5] and a vitamin diet containing α-Tocopherol and ascorbate[136].

Compared to other cell types, hepatocytes express high levels of antioxidants such as glutathione, superoxide dismutase, and catalase, which make them relatively more resistant to injury induced by ROS and RNS under normal conditions[132]. However, hepatocytes show high levels of mitochondrial respiration with limited glycolysis during warm ischemia, which is

associated with excessive ROS production by mitochondria and imbalance of ROS production and endogenous antioxidant systems[132, 133].

1.5.2 HS and the innate immune response
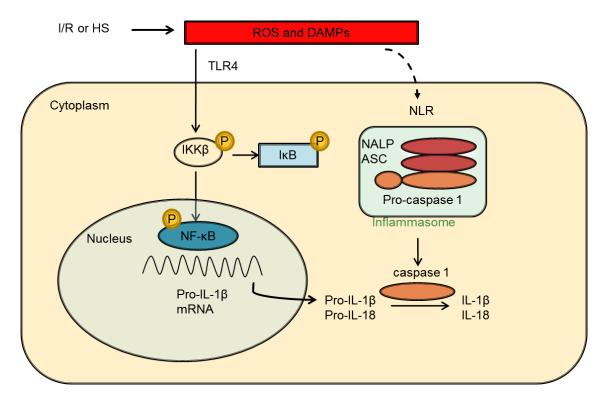
Figure 2: The role of the innate immune response after HS/R in macrophages

HS/R represents a global I/R phenomenon that contributes to end-organ dysfunction and damage[142].Other than cell death induced by prolonged hypoxia during ischemia and excessive ROS produced during reperfusion, I/R injury induces tissue damage through an excessive innate immune response. It has been well established that TLR signaling is involved in the profound systemic inflammatory response and the induction of tissue damage after HS/R. We have previously shown that TLR4-deficient mice were protected from liver injury following HS/R

with decreased production of pro-inflammatory cytokines associated with decreased NF-κB activation[143]. TLR4 $^{-/-}$ mice also demonstrated attenuated myocardial contractile depression and TNF-α expression in the heart after HS/R[144]. A study by Liu *et al.* showed that HMGB1 released during HS/R activated TLR4 and led to secretion of IL-23 and IL-17 by macrophages, which resulted in increased neutrophil infiltration[145]. We have shown that hypoxia alone triggers HMGB1 release via a TLR4-dependent mechanism in hepatocytes[13]. Therefore, as shown in Figure 2, danger signals such as ROS and DAMPs can activate TLR4 and lead to the mRNA synthesis of pro-inflammatory cytokines such as pro-IL1β and TNF-α through the activation of NF-κB. On the other hand, the release of mature IL-1β also requires the formation of inflammasome and activation of caspase-1. But it is still unknown whether NLRs can be activated after HS/R.

Moreover, although most studies have focused on the role of PRRs in immune cells during HS/R, parenchymal cells also seem to contribute to the inflammatory response following HS/R, as indicated by a study using bone marrow-chimeric mice[146]. However, the role of PRRs in nonmyeloid cells still remains largely unexplored.

2.0   CENTRAL HYPOTHESIS AND SPECIFIC AIMS

2.1   RATIONALE AND CENTRAL HYPOTHESIS

Emerging evidence suggests that caspase-1 activation can be induced by oxidative stress or the release of DAMPs after increased redox stress[35, 37]. Caspase-1 mediates the maturation of the pro-inflammatory cytokines IL1β/IL18 in immune cells and endothelial cells after oxidative stress. This is known to contribute to renal and myocardial I/R injury[147, 148]. However, our previous work demonstrated a protective effect of caspase-1 against liver injury during HS with bilateral femur fracture[149]. Moreover, recent research also implicates caspase-1 as a regulator of cellular responses to stress through the regulation of tissue repair and cytoprotective responses[7, 150]. This aspect of caspase-1 function is poorly characterized, but may be especially important in non-immune cells such as hepatocytes, which express and can activate inflammasome components[151], but are not known to produce significant amount of IL1β/IL18.

On a subcellular level, mitochondria are organelles central to the regulation of cell death and metabolic adaptation. Mitochondrial respiration is suppressed during hypoxia due to low oxygen tension. The reestablishment of mitochondrial aerobic respiration after reoxygenation results in excessive ROS production, which can trigger the release of pro-apoptotic proteins such as cytochrome *c* and can lead to cell death[135, 136]. Both general and mitochondrial autophagy are responsible for mitochondrial turnover and quality control[36] and have been shown to eliminate

dysfunctional mitochondria to reduce mitochondrial ROS production and therefore downregulate inflammasome and caspase-1 activation [35, 37].

Due to the important role of autophagy and mitochondrial function in regulating adaptive responses to prevent cell death after stresses, **we hypothesize that there is a significant role for the inflammasome and caspase-1 in regulating adaptive responses to oxidative stresses through either the release of inflammatory mediators or through regulating autophagy and mitochondrial function in the liver.**

2.2   SPECIFIC AIMS

Specific Aim 1: To investigate the mechanism by which caspase-1 is activated in hepatocytes *in vitro* and *in vivo.*

Specific Aim 2: To determine the role of inflammasome and caspase-1 activation in regulating apoptosis, autophagy, and mitochondrial function in hepatocytes.

3.0 METHODS

3.1 ANIMAL STUDIES

3.1.1 Mouse strains

Male C57BL/6 (WT), AIM2 $^{-/-}$, Interleukin-1 receptor $^{-/-}$ (IL-1R $^{-/-}$) and Interleukin-18 receptor $^{-/-}$ (IL-18R $^{-/-}$) mice were purchased from Jackson Laboratory (Bar Harbor, ME) and maintained at the University of Pittsburgh until eight weeks of age. NLRP3$^{-/-}$ mice were rederived from Millennium Pharmaceuticals (Boston, MA). Caspase-1$^{-/-}$ mice were obtained from Dr. Richard Flavell (Howard Hughes Medical Institute, Yale University) and were bred in our facility. Hepatocyte-specific HMGB1 $^{-/-}$ (HC-HMGB1$^{-/-}$) mice were obtained from Dr. Allan Tsung (University of Pittsburgh). Eight 12-week old mice weighing 21–30 g were used in the experiments.

3.1.2 Genotyping of caspase-1$^{-/-}$ and HC-HMGB1$^{-/-}$ Mice

Caspase-1 $^{-/-}$ mice were genotyped by reverse transcriptase–polymerase chain reaction (PCR) of digested tail tissue using the following primers: *caspase-1* forward: GAGACATATAAGGGAGAAGGG; *caspase-1* reverse: ATGGCACACCACAGATATCGG; and *caspase-1* neo: TGCTA AAGCGCATGCTCCAGACTG. PCR conditions used were as

27

follows: 94°C for three minutes; then 35 cycles of 94°C for 30 seconds, 62°C for 30 seconds and 72°C for 30 seconds; and then held at 72°C for five minutes before cooling to 4°C until run on 2% agarose gel. Bands were visualized using ethidium bromide. WT mice were identified by a single band at 500 bp. Caspase-1$^{-/-}$ mice were identified by a single band at 300 bp. Both bands were visible for heterozygous mice.

HC-HMGB1$^{-/-}$ mice were confirmed by genotyping both Albumin-Cre and HMGB1 using the primers: *HMGB1* forward: TGATGCGAACACGGCGTGCTCTA; *HMGB1* reverse: GCACAAAGAATGCATATGAGGAC; Albumin-Cre forward: GTTCGCAAGAACCTGATGG AACA; Albumin-Cre reverse: CTAGAGCCTGTTTTGCACGTTC. PCR conditions used were as follows: 94°C for two minutes; then 30 cycles of 94°C for 15 seconds, 62°C for 30 seconds and 72°C for 30 seconds; and then held at 72°C for five minutes before cooling to 4°C. WT mice for HMGB1-floxed strain were identified by a single band at 635 bp. HMGB1floxed mice were identified by a single band at 700 bp. Cre band is the only band that will show up at 342bp in size.

3.1.3   HS model

HS surgery was performed as previously described[152]. Mice were anesthetized intraperitoneally with sodium pentobarbital (50 mg/kg) and inhaled isofluorane (Abbott Laboratories). Unilateral groin dissections were performed, and femoral arteries were cannulated and flushed with heparin sulfate (Pharmacia, Uppsala, Sweden, and Upjohn, Kalamazoo, MI, USA), for a total of ~2 U heparin per animal. The groin catheter was connected to a blood pressure transducer (Micro-Med) for continuous mean arterial pressure (MAP) readings. Mice were allowed to recover from the inhaled anesthesia for 10 minutes before initiation of hemorrhage. After baseline blood-

pressure readings were repeated three times, mice were hemorrhaged to a MAP of 25 mmHg over 10 minutes. Total withdrawn blood was recorded every 10 minutes, and mice were maintained at a MAP of 25 mmHg for 90 minutes. The mice were then resuscitated over 10 minutes with three times the maximal shed blood amount in Lactated Ringer's solution through the arterial catheter. After post-resuscitation blood pressure readings, catheters were removed, vessels were ligated, and groin incisions were closed with 4-0 nylon sutures. Mice were sacrificed 1.5, 4.5, or 24 hours after resuscitation. Sham group mice underwent initial cannulation procedures and anesthesia only. Control mice were sacrificed without any procedures performed to obtain physiological baseline levels. All experimental protocols were approved by the University of Pittsburgh Institutional Animal Use and Care Committee. Experimental procedures were carried out in accordance with all regulations regarding the care and use of experimental animals published by the National Institutes of Health.

3.1.4 *In vivo* knockdown of NLRP1

NLRP1a was inhibited *in vivo* through the injection of NLRP1a-specific siRNA (50 µM/kg) (Invitrogen) as previously described, with modification[153]. The NLRP1a siRNA-Invivofectamine complex was prepared according to the protocol from Invitrogen and subjected to dialysis with a Float-A-Lyzer dialysis device (Spectrum labs). The complex was administered via tail vein injection two days before HS. Scrambled siRNA (50 µM/kg) was used as a control via tail vein injection.

3.1.5 Generation of bone marrow (BM) - chimeric mice

Chimeric mice were generated by adoptive transfer of donor bone marrow (BM) cells into irradiated recipient animals using combinations of WT (C57Bl/6) and knockout (KO) (Caspase-1 $^{-/-}$) mice. The following recipient/donor combinations were produced: WT/WT, WT/KO, KO/WT, and KO/KO. Recipient mice were exposed to an otherwise lethal 1000 cGy from a Cesium source (Nordion International) six hours before receiving 2.5×10^6 BM cells by tail vein injection. The BM cells were prepared in a sterile manner from the tibia and femur bones of the donor mice. All animals were monitored two to three times weekly for the first two weeks to ensure successful BM engraftment. Chimeric animals were maintained under the same conditions as described above and underwent HS 10–12 weeks after the adoptive transfer to ensure stable engraftment.

3.2 HEPATOCYTE ISOLATION AND BIOCHEMICAL ANALYSIS

3.2.1 Hepatocyte isolation and cell culture

Hepatocytes were isolated from mice by an *in situ* collagenase (type VI; Worthington) perfusion technique. Basically, mice were anesthetized intraperitonelly with 0.3ml of 14% Nembutal diluted in sodium chloride. A catheter was inserted into the vena cava and the liver was perfused with perfusion medium I (1.42M NaCl, 67mM KCl, 100mM Hepes, pH was adjusted to 7.5 with NaOH) for 10-15 minutes. The liver was then perfused with collagenase (the concentration was determined by optimization experiments for each batch) dissolved in perfusion medium II

(67mM NaCl, 6.7mM KCk, 100mM Hepes, 4.8mM CaCl2, and 1% Albumin, pH was adjusted to 7.6 with NaOH) for another 15 minutes. Liver cells were isolated with cell scraper and the crude cell preparation was filtered through a gauze funnel. The resulting cell suspension was centrifuged at 400rpm for two-three minutes to get rid of the non-parenchymal cells. The cell pellet was re-suspended in 30% percoll (GE Life Sciences) before the suspension was centrifuged at 400rpm for 10 minutes to remove the dead cells. Hepatocyte purity exceeded 99% as determined by flow cytometric assay, and viability was typically over 95% as determined by trypan blue exclusion. Hepatocytes (4×10^5 cells/ml for six-well plates) were plated on gelatin-coated culture plates in Williams medium E with 10% calf serum, 15 mM HEPES, 10^{-6} M insulin, 2 mM L-glutamine, 100 U/ml penicillin, 100 U/ml streptomycin. Hepatocytes were allowed to attach to plates for at least two hours before treatment. Hypoxia/reoxygenation treatment was performed as previously described[154]. Described briefly, hepatocytes were incubated in Krebs-Ringer–hydroxyethylpiperazine-N-2 ethanesulfonic acid (HEPES) buffer (KRH) containing 115 mM NaCl, 5 mM KCl, 2 mMCaCl$_2$, 1 mM KH$_2$PO$_4$, 1.2 mM MgSO$_4$, and 25 mM HEPES (all reagents were obtained from Sigma) at pH 6.2 in a hypoxia chamber. To simulate reoxygenation and return to the physiological pH of reperfusion, anaerobic KRH at pH 6.2 was replaced with hepatocyte culture media at pH 7.4.

3.2.2   Analysis of cell death

Hepatocytes (4×10^5 cells/ml of six-well plate) were cultured under hypoxia (1% oxygen) and then reoxygenated for one hour or kept for the same duration under normoxic condition with or without caspase-1 inhibitor pretreatment for one hour (15μM, Calbiochem). Cell death was measured using the Annexin V–FITC apoptosis detection kit (BD Biosciences) according to the

manufacturer's instructions. Described briefly, cells were collected after treatment, washed with phosphate buffered saline (PBS), stained with Annexin V–FITC and propidium iodide (PI) for 15 minutes in $1\times$ binding buffer (10 mM HEPES, pH 7.4, 140 mM NaCl, 2.5 mM $CaCl_2$), and analyzed by flow cytometry using Guava EasyCyte 8HT flow cytometer (Millipore).

3.2.3 Measurement of intracellular ROS

Intracellular ROS generation was assessed with CM-H_2DCFDA (10 µM). Microscopy or flow cytometry was performed. Images were acquired with a Zeiss 510 inverted confocal microscope. Dichlorofluorescein (DCF) fluorescence was measured in 15-20 randomly selected fields per group; fluorescence intensity was measured using Metamorph, and values are expressed with respect to the WT control cultured under normoxia. To normalize cell number, Hoeschst (Life Technologies) was used as a fluorescent marker for the nucleus and PI was used to exclude the dead cells. The experiments were repeated at least three times per treatment. Flow cytometry was performed using Guava EasyCyte 8HT flow cytometer.

3.2.4 Measurement of autophagic flux

Autophagic flux was assessed by increase in green fluorescent protein (GFP)–LC3 puncta or LC3II levels determined by Western blot after bafilomycin (50 nM, Sigma) treatment for one hour. In addition, autophagic flux was determined in hepatocytes transfected with red fluorescent protein-green fluorescent protein (GFP-RFP)-LC3 plasmid. Twenty-four hours after transfection, cells were imaged with Zeiss LSM 510 laser scanning confocal microscope using a $63\times$ oil lens.

The numbers of GFP and RFP double positive (early autophagic vacuoles) and RFP only (late autophagic vacuoles) puncta were counted for each cell.

3.2.5　Liver homogenization

Snap-frozen liver tissue was homogenized in radioimmunoprecipitation assay buffer (RIPA) buffer (50 mM Tris-HCl, 150 mM NaCl, pH 7.4) containing protease inhibitors (1 mM phenylmethylsulfonyl fluoride, 0.1 µM aprotinin, 1 µg/ml leupeptin and 1 µM pepstatin) with glass/Teflon homogenizer (15 up-and-downs) to obtain all soluble proteins. The whole liver lysate was then pelleted by centrifugation at 10,000 x g for 15 minutes at 4 ^{o}C and the supernatant was saved and stored at -80 ^{o}C until use.

3.2.6　Western blot analysis

Treated hepatocytes were washed twice in PBS and lysed with 1× cell lysis buffer (Cell Signaling Technologies) containing 20 mM Tris-HCl (pH 7.5), 150 mM NaCl, 1 mM Na$_2$EDTA, 1 mM EGTA, 1% Triton, 2.5 mM sodium pyrophosphate, 1 mM β-glycerolphosphate, 1 mM Na$_3$VO$_4$, 1 µg/ml leupeptin, and 1 µg/ml phenylmethylsulfonyl fluoride on ice for 30 minutes. Protein content of cell lysates was determined by bicinchoninic acid (BCA) protein assay (Pierce). For Western blot, equal protein amounts (30µg) were separated by sodium dodecyl sulfate polyacrylamide gel electrophoresis (SDS-PAGE) and transferred onto a polyvinylidene fluoride membrane followed by probing with optimized dilutions of primary antibody overnight at 4°C (see Table 1). Horseradish peroxidase-conjugated secondary antibodies were then used at

1:20,000 in a standard enhanced chemiluminescence reaction according to the manufacturer's instructions (Pierce).

Table 1. Primary Antibodies and Conditions for Immunoblotting

Protein	Company	Catalog #	Dilution (in 1% milk)
Caspase-1	Millipore or Cell signaling	06-503 or 2225	1:1000
Beclin1	abcam	Ab55878	1:2000
Cleaved caspase-3	Cell signaling	9664	1:1000
Cleaved poly (ADP-ribose) polymerase (PARP)	Cell signaling	9544	1:1000
PARP	Cell signaling	9542	1:1000
Caspase-3	Cell signaling	9662	1:1000
Atg3	Cell signaling	3415	1:1000
Atg12-5	Cell signaling	2630	1:1000
Atg7	Cell signaling	2631	1:1000
Cytochrome c	BD Biosciences	556432	1:1000
AIM2	Santa cruz	sc-137967	1:500
PGC-1α	Cell signaling	2178	1:1000
HMGB1	Abcam	Ab18256	1:1000
Nlrp1	Cell signaling	Ab3683	1:1000
ASC	Santa cruz	Sc-33958	1:500
GAPDH	Abcam	Ab9484	1:10000

3.2.7 Immunofluorescence and confocal microscopy

Liver tissue from mice was removed after perfusion with cold PBS and 2% paraformaldehyde. Tissue was fixed in 2% paraformaldehyde for two hours followed by cryopreservation with 30% sucrose overnight before freezing in liquid nitrogen–cooled isopentane and stored at −80 °C until use. Liver sections (6 μm) were permeabilized with 0.3% Triton X-100 for 20 min and stained as previously described[155]. Immunofluorescence staining began by rehydrating slides with PBS. Nonspecific binding was blocked using 2% bovine serum albumin (BSA) for 45 minutes followed by rinses with 0.5% BSA. The level of lipid peroxidation was determined by 4-hydroxyl-2-nonenal (HNE) staining using HNE antibody for 60 minutes at room temperature followed by incubation for 60 minutes with fluorescently labeled secondary antibodies (1:1000; Invitrogen). After nuclear staining for 40 seconds with 4',6-diamidino-2-phenylindole (DAPI), slides were covered using gelvatol, a water-soluble mounting medium (21 g polyvinyl alcohol, 52 ml water, sodium azide, and 106 ml 0.2 M Tris buffer). Images were taken from six random fields per section with a Fluoview 500 confocal microscope (Olympus) at the Center for Biologic Imaging. Imaging conditions were maintained at identical settings with original gating performed using the negative control (no primary antibody). The relative HNE adducts per cell were quantitated using a Metamorph image acquisition system (Universal Imaging) and normalized to fluorescence intensity of β-actin.

Table 2: Primary antibodies and conditions for immunofluorescence

Protein	Company	Catalog #	Dilution (in 1% milk)
HNE	Calbiochem	393204	1:200
AIM2	Santa cruz	sc-137967	1:200

HMGB1	Abcam	Ab18256	1:250

3.2.8 Transfection with siRNA

Cells were transfected using Lipofectamine 2000 (Invitrogen) according to the manufacturer's instructions. A non-silencing siRNA pool (siCtrl, Dharmacon) was used as a control. To knock down beclin1 or caspase-1 expression in hepatocytes with Dharmacon smartpool siRNA (20 nM, Dharmacon) targeting mouse beclin1 or caspase-1 (sibeclin1 or siCasp-1), cells were transfected with 10nM of either control siRNA or targeting siRNA for 24 hours. Efficiency of gene silencing was determined by Western blot.

3.2.9 ATP measurement

Steady-state ATP levels in hepatocytes was measured as previously published[156]. Described briefly, hepatocytes were lysed with 1X cell lysis buffer (Cell Signaling Technology) supplemented with 1.5% trichloroacetic acid (TCA) for 10 minutes at 4°C. Cell lysates were diluted 1:50 in Tris buffer (0.1mM) and ATP levels were measured by luciferin-luciferase assay with ATP determination kit according to the manufacturer's instructions (Invitrogen). The results were normalized to the protein content in each sample.

3.2.10 Real-time PCR

Total RNA was extracted from hepatocytes using RNeasy mini extraction kits from Qiagen (Valencia) according to the manufacturer's protocol. Comparative DNA (cDNA) was synthesized using 1μg RNA and oligo dT primers (Qiagen) and Omniscript™ reverse transcriptase (Qiagen). PCR reaction mixtures were prepared using SYBR Green PCR master mix (PE Applied Biosystem). SYBR Green two-step real-time RT-PCR was performed using forward and reverse primer pairs prevalidated and specific for beclin1 (Qiagen). The default program was performed on a CFX Connect RT system (Bio-rad) and consisted of 95 °C for 10 minutes, and 35 cycles of 95 °C for 10 seconds, 60 °C for 30 seconds, and 72°C for 30 seconds. All samples were run in triplicate. The level of gene expression for each sample was normalized to β-actin mRNA expression using the comparative Ct method.

3.2.11 Immunoprecipitation

Whole cell lysates were incubated overnight with goat anti-ASC antibody, and immune complexes were then precipitated with protein A/G-agarose beads(Santa cruz) for four hours and then washed several times with immunoprecipitation buffer (20 mM Tris-HCl (pH 7.5), 150 mM NaCl, 1 mM Na_2EDTA, 1 mM EGTA, 1% Nonidet P-40, 1% sodium deoxycholate, 2.5 mM sodium pyrophosphate, 1 mM β-glycerophosphate, 1 mM Na_3VO_4, 1 μg/ml leupeptin, and 1 mM PMSF). Immunoprecipitated proteins were eluted with 2× sodium dodecyl sulfate (SDS) loading buffer (0.5 M Tris-HCl (pH 6.8), 2 ml of glycerol, 10% (w/v) SDS, 0.1% (w/v) bromphenol blue, and 5% β-mercaptoethanol in water) and then analyzed by Western blot as described above.

3.2.12 Mouse caspase-1 plasmid

To generate mouse caspase-1 plasmid, mouse caspase-1 was cloned by PCR from cDNA prepared by reverse transcription of normal mouse hepatocyte mRNA. The primers (Integrated DNA Technologies) used for PCR were as follows: forward 5'-CAT GGC TGA CAA GAT CCT GAG GGC-3' and reverse 5'-GTT TAA TGT CCC GGG AAG AGG TAG-3'. The amplimer was subcloned into pAdlox.

3.2.13 Mouse beclin1 adenoviral vector

To generate adenoviral vectors expressing mouse beclin1, the Open Reading Frames of murine beclin1 were inserted into a shuttle plasmid pAdlox at HindIII and BamHI sites and the sequences were confirmed. E1/E3-deleted adenoviral vector was then constructed using Cre-lox recombination system in the adenovirus-packaging cell line CRE8. The recombinant adenoviruses were propagated in 293 cells, purified by cesium chloride density gradient centrifugation and dialysis. Adenovirus particle concentration was determined by spectrophotometric analysis. Ad-beclin1 or ad-GFP was injected through the tail vein at 4×10^{10} viral particles for each mouse. Two days after injection, mice were subjected to HS and 4.5 hours of resuscitation.

3.2.14 Electron microscopy

For electron microscopy, mice were perfused with cold PBS, then with 2% paraformaldehyde and 2% glutaraldehyde in 0.1 mol/L phosphate buffer (pH 7.4) and processed for transmission

38

electron microscopy as described[157]. After dehydration, sections were stained with uranyl acetate and lead citrate for observation under a JEM 1011CX electron microscope (JEOL). Images were acquired from a randomly selected pool of 10-15 fields under each condition.

3.2.15 Reagents

Caspase-1 inhibitor (Ac-YVAD-CMK) came from Millipore. Pan caspase-1 inhibitor (Z-VAD-FMK) came from R&D Systems. Manganese (III) tetrakis (1-methyl-4-pyridyl) porphyrin (MnTMPyP) came from Enzo Life Sciences. Caspase-1 activity was determined using caspase-1 activity colorimetric kit (R&D Systems). Caspase-3 activity was determined by caspase-3 activity fluorometric kit (R&D Systems).

3.3   MITOCHONDRIAL ASSAYS

3.3.1   Measurement of mitochondrial and cytosolic ROS in hepatocytes

To assess mitochondrial and cytosolic-specific ROS production at the single cell level, hepatocytes were transfected with mitochondrial-targeted HyPer-Mito or cytoplasm-targeted HyPer-Cyto (Evrogen), which is a genetically encoded fluorescent sensor capable of highly specific detection of mitochondrial or cytosolic H_2O_2 in live cells. At 36 hours after transfection, hepatocytes were subjected to hypoxia (1% O_2) for six hours and reoxygenated or kept under normoxia for the same duration. The green fluorescent signal was observed by fluorescent microscopy in 30 random cells per treatment using an EVOS® fluorescence microscope (AMG).

Fluorescence intensity was assessed by Image J software and expressed as fold increase to WT control. The experiments were repeated at least three times per treatment.

3.3.2 Mitochondrial volume and mitochondrial DNA copy number

Mitochondrial volume was determined by MitoTracker Red staining (Life Technologies) and divided by cell volume marked by calcein (BD Biosciences) as previously described with modifications[158]. Hepatocytes were loaded with 1µM of calcein and 100µM of MitoTracker Red for 30 minutes before imaged in Zeiss LSM 510 laser-scanning confocal microscope using a 63× oil lens. Z-stacks acquired individual hepatocytes at 5µm intervals. The mitochondrial volume of a random portion of cytoplasm was determined as a fraction of cytoplasm using ImageJ's 3D Object Counter macro (Fabrice Cordelires & Jonathan Jackson).

mtDNA copy number was measured by quantitative PCR as previously described [159]. Primers (Integrated DNA Technologies) were as follows: forward 5'-CCC AGC TAC TAC CAT CAT TCA AGT-3' and reverse 5'-GAT GGT TTG GGA GAT TGG TTG ATG-3'. The primers used were against part of the mitochondrially-encoded nicotinamide adenine dinucleotide hydride dehydrogenase subunit 6 (mt-Nd6), and the results shown are normalized to nuclear DNA copy number.

3.3.3 Citrate synthase activity assay

Citrate synthase activity was measured in the liver using citrate synthase assay kit (Sigma). Described briefly, livers were collected from control mice or mice that underwent HS/R and immediately homogenized in RIPA buffer (Sigma) with 50 µg of liver protein loaded per well of

a 96-well plate; citrate synthase activity was measured according to the manufacturer's instructions.

3.3.4 Measurement of cytochrome c release

Cytosolic fractions of liver tissue from WT and capsase-1^{-/-} mice were prepared as previously described[160]. Described briefly, livers from control mice or mice subjected to HS/R were excised, homogenized, and centrifuged to pellet the mitochondria. The supernatant was collected and protein concentration was determined by BCA assay (Thermo Scientific).

3.3.5 Measurement of mitochondrial respiration

Mouse primary hepatocytes were seeded at 1×10^4 cells per well in hepatocyte growth media (Williams medium E containing 10% calf serum) on XF-24 cell culture plates (Seahorse) coated with gelatin. WT and caspase-1 [-/-] (or AIM2 [-/-]) hepatocytes were treated with hypoxia (1% oxygen) for six hours before the growth media was changed to unbuffered running Dulbecco's modified Eagle's medium (DMEM) (40μM GlutaMax-1, 20μM Sodium Pyruvate, 25mM glucose, 60mM NaCl, pH=7.4). The plates were kept in non-CO2 incubator at 37C for 1 hour before running on XF-24 Analyzer to measure cellular oxygen consumption rate. The concentrations of oligomycin, trifluorocarbonylcyanide phenylhydrazone, and rotenone were 1μM, 0.3μM, and 1μM, respectively. The results shown are presented as cellular oxygen consumption rate normalized to protein content in each well as determined by BCA assay.

3.3.6 Measurement of mitochondrial potential

Mitochondrial potential was determined as previously described[161]. Primary hepatocytes plated on four-well chamber slides (Thermo Scientific) were incubated with 50nM tetramethylrhodamine (TMRM, Invitrogen) for 30 minutes at 37°C. Cells were washed with Krebs-Ringer Bicarbonate buffer with 10 mM glucose and the images were taken in buffer containing 12.5 nM TMRM to maintain the equilibrium distribution of TMRM[162]. Images were collected using a Nikon A1 inverted laser scanning confocal microscope with a 60x oil immersion objective. Cells were kept at 37°C for the duration of imaging with a stage adaptor. Mitochondrial membrane potential was measured by calculating the fluorescence of eight-10 mitochondrial regions of interest (ROIs) and the results were normalized with one ROI in the nucleus in the same optical plane as a measure of loading.

3.4 STATISTICAL ANALYSIS

Results are displayed as mean ± standard deviation (SD) or mean ± standard error of the mean (SEM) from at least three independent experiments. Two-tailed Student's *t*-test was used to calculate statistical significance of two experimental groups. P values of less than 0.05 were considered significant.

4.0   RESULTS-CASPASE-1 REGULATES AUTOPHAGY AND BECLIN1 AFTER REDOX STRESS

4.1   CASPASE-1 IS ACTIVATED AND HEPATOPROTECTIVE AFTER HS

To investigate the role of the inflammasome and caspase-1 in regulating liver injury after oxidative stress, we utilized a HS/R model known to induce oxidative stress in the liver[163, 164]. We subjected WT and caspase-1^{-/-} mice to HS for 1.5 hours as described in the Methods section, and sacrificed mice without resuscitation (HS alone), or after 1.5 hours, 4.5 hours, or 24 hours of fluid resuscitation. As shown in Figure 3A, IL-18 levels were significantly increased at all the time points after HS in the WT mice, indicating activation of inflammasome and caspase-1. As expected, caspase-1^{-/-} mice did not express any detectable IL-18, even after HS/R. Moreover, we used Western blotting to assess the activation of caspase-1 in WT livers. The results show that caspase-1 was activated (cleaved) in the liver in a time-dependent manner after HS (Figure 3B).
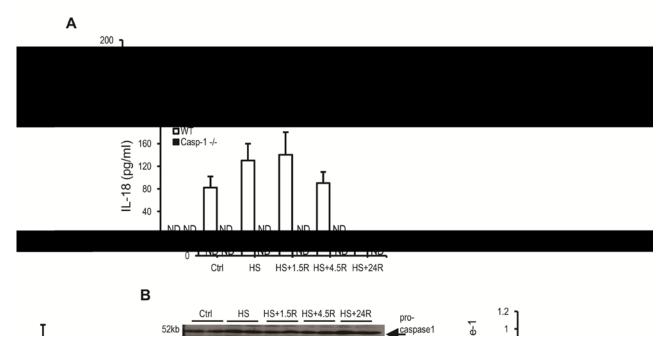
Figure 3: Caspase-1 is activated in the liver after HS/R

(A) IL-18 levels in the plasma of control (Ctrl) WT and caspase-1 -/- mice and mice subjected to HS only or HS and different time points of resuscitation. (n=3 for control groups; n=7-8 for experimental groups; mean±SEM; ND=not detected). (B) Representative Western blot and quantification of cleaved caspase-1 normalized to GAPDH expression. (mean±SD)

Consistent with the results we previously reported in an HS model with bilateral femur fracture[149], caspase-1^{-/-} mice had significantly increased levels of plasma ALT and aspartate transaminase (AST) (Figure 4A), compared with WT mice after 4.5 hours of resuscitation, indicating increased liver damage. Similarly, hematoxylin and eosin (H&E) staining of liver sections demonstrated more extensive centrilobular necrosis in caspase-1^{-/-} mice in comparison with WT mice (Figure 4B). Caspase-1^{-/-} mice also had more neutrophil infiltration in the liver compared with WT 4.5 hours after resuscitation, which persisted even after 24 hours of resuscitation and suggests increased inflammatory responses and tissues damage in caspase-1^{-/-} mice (Figure 4C). Inflammatory cytokines, such as IL-6 and MCP-1, were significantly elevated

after HS/R in the plasma of WT mice as expected, with significantly increased IL-6 and MCP-1 levels in caspase-1$^{-/-}$ mice after HS/R (Figure 4D). Increased inflammatory cytokine levels corresponded well with increased liver damage. Taken together, these data suggest that caspase-1 is activated in the liver during HS/R, and plays a hepatoprotective role in this model of global I/R and oxidative stress.
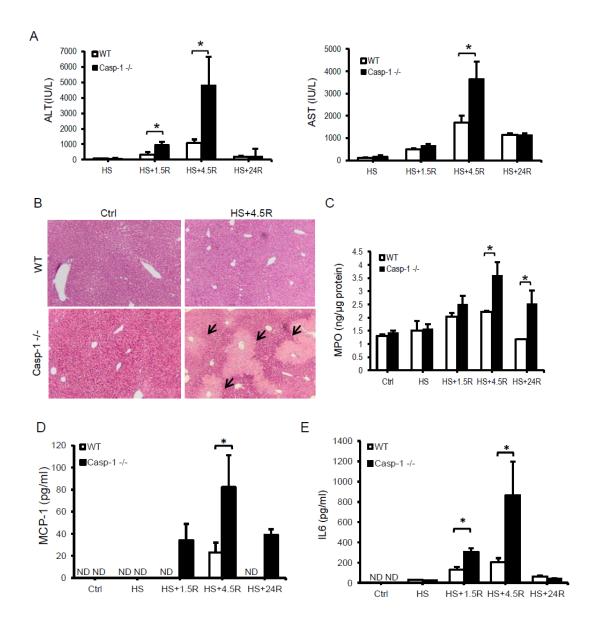
Figure 4: Caspase-1 is liver protective after HS/R

45

(A) ALT and AST levels in mice subjected to HS only and HS/R (n=3 for control groups; n=7-8 for experimental groups; mean±SEM; *P<0.05, WT vs. caspase-1 -/-). (B) H&E staining of liver sections of control mice and mice treated with HS and 4.5 hours of resuscitation. Caspase-1 -/- mice demonstrated extensive centrilobular necrosis (black arrows). Representative images for every group (n=7-8) are shown (original magnification, X100). (C) Myeloperoxidase (MPO) levels were compared in the liver between WT and caspase-1 -/- mice (n=3 for control groups; n=7-8 for experimental groups; mean±SEM ; *P<0.05, WT vs. caspase-1 -/-). (D) MCP-1 and (E) IL6 levels in the plasma of control (Ctrl) WT and caspase-1 -/- mice and mice subjected to HS only or HS and different time points of resuscitation. (n=3 for control groups and n=7-8 for experimental groups; mean±SEM; ND=not detected).

4.2 CASPASE-1 PROTECTS HEPATOCYTES AGAINST CELL DEATH AFTER HYPOXIA-REOXYGENATION

Since the major role of caspase-1 is to produce IL-1β and IL-18, we next assessed whether the protective effect of caspase-1 in the liver is dependent on IL-1 or IL-18, which are produced mostly by immune cells such as macrophages. IL-18R^{-/-} and IL-1R^{-/-} mice showed similar levels of plasma ALT after HS/R, suggesting the hepatoprotective effect of caspase-1 is not dependent on its downstream cytokines (Figure 5).
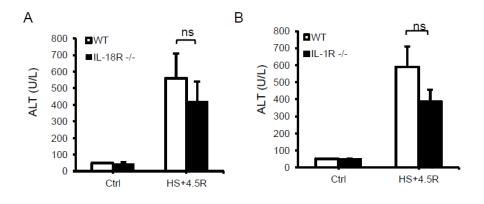
Figure 5: The protective effect of caspase-1 is not dependent on IL-1 or IL-18

46

(A) and (B) ALT levels in mice subjected to HS/R (n=2 for control groups; n=7-8 for experimental groups; mean±SEM).

A recent study also demonstrated that caspase-1 and inflammasome can be activated in response to endotoxin and fatty acids in hepatocytes, the major cell type in the liver[151]. To assess whether the protective effect of caspase-1 during HS/R and oxidative stress is driven by caspase-1 activation in hepatocytes, we subjected primary hepatocytes isolated from WT and caspase-1^{-/-} mice to hypoxia/reoxygenation as previously described[154]. Hepatocytes were cultured under hypoxic conditions (1% hypoxia) for six hours and reoxygenated for one hour to mimic I/R induced by HS/R. Caspase-1 activity was measured in WT hepatocytes by determining the cleavage of a colorimetric peptide substrate. Both hypoxia alone and hypoxia/reoxygenation induced the activation of caspase-1 in WT hepatocytes (Figure 6A). To further confirm the role of caspase-1 in hepatocytes after oxidative stress, caspase-1 was knocked down by approximately 51% in WT hepatocytes treated with caspase-1 siRNA as assessed by Western blotting at 24 hours (Figure 6B). Acute knockdown of caspase-1 significantly decreased caspase-1 activity after hypoxia/reoxygenation as expected (Figure 6A). Moreover, reversal studies confirm that transfection with mouse caspase-1 is able to significantly restore caspase-1 activity in caspase-1 [-/-] hepatocytes (Figure 6A and 6B).

Consistent with our previous *in vivo* results showing increased liver cell death after HS/R and peripheral tissue injury, caspase-1-deficiency and acute knockdown resulted in higher levels of hepatocyte apoptosis and necrosis as determined by increased caspase-3 activity (Fig 6C and 6D) and Annexin V/PI staining after hypoxia/reoxygenation (Fig.6E). To confirm that altered levels of cell death were dependent on caspase-1 activation, we repeated the experiment comparing Annexin V/PI staining in WT hepatocytes with WT hepatocytes pretreated for one

hour with caspase-1 inhibitor Ac-YVAD-CMK (15μM) and obtained similar results, with increased levels of hepatocyte apoptosis/necrosis in caspase-1 inhibitor treated cells (Figure 6F). Moreover, pan caspase inhibitor Z-VAD-FMK (15μM) was able to rescue excessive cell death in caspase-1 $^{-/-}$ hepatocytes to levels similar as those seen in WT cells after hypoxia-reoxygenation, indicating that caspase-1 protects hepatocytes through the inhibition of apoptosis after redox stress (Figure 7).
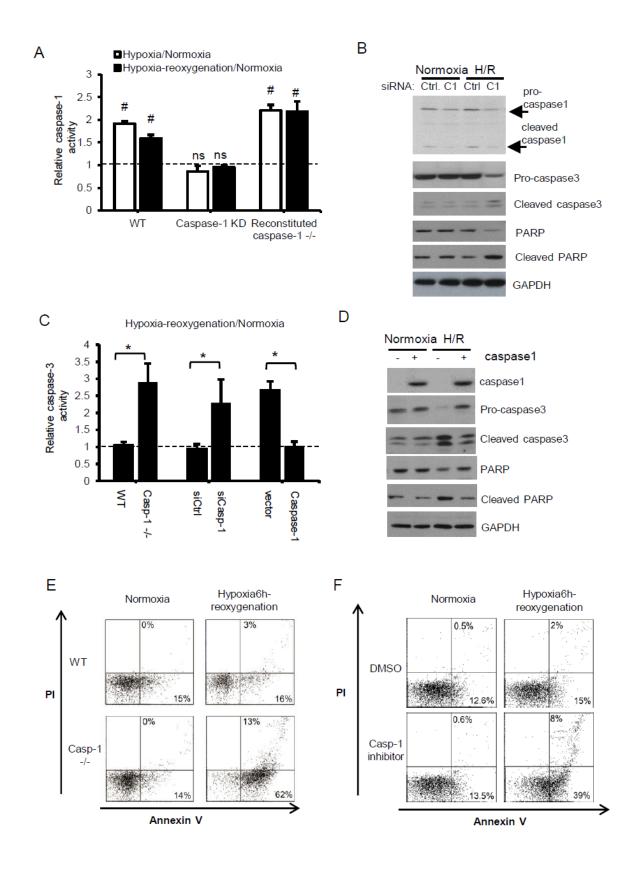
Figure 6: Caspase-1 is protective in hepatocytes after hypoxia/reoxygenation

(A) Relative caspase-1 activity in WT hepatocytes, WT hepatocytes treated with caspase-1 siRNA and caspase-1 [-/-] cells transfected with mouse caspase-1plasmid after normoxia, six hours hypoxia or six hours hypoxia/one hour reoxygenation. Data are shown as percentage of normoxic levels (mean±SD n=3; [#]P<0.05, normoxia vs. hypoxia-reoxygenation; ns=not significant). (B) Relative caspase-3 activity in WT and caspase-1^{-/-} hepatocytes, WT hepatocytes treated with caspase-1 siRNA and caspase-1 [-/-] cells expressing mouse caspase-1 after six hours hypoxia/one hour reoxygenation. Data are shown as percentage of normoxic levels (mean±SD; n=3; *P<0.05). (C) Representative Western blot (left) and quantification (right) of caspase-1, cleaved caspase-3, and PARP in WT hepatocytes treated with control siRNA (siCtrl) or caspase-1 siRNA (siC1) 24 hours before six hours hypoxia/one hour reoxygenation (H/R) treatment (mean±SEM; n=3; **P<0.01). (D) Representative Western blot (left) and quantification (right) of caspase-1, cleaved caspase-3, and PARP in caspase-1 [-/-] hepatocytes and caspase-1 reconstituted cells subjected to hypoxia/reoxygenation (H/R) (mean±SEM; n=3; *P<0.05). (E) Representative Annexin V/PI flow cytometry dot plots for hepatocytes cultured under normoxia or after six hours hypoxia/one hour reoxygenation. (F) Representative Annexin V/PI analysis of WT hepatocytes pretreated with dimethyl sulfoxide (DMSO) or caspase-1 inhibitor (15μM), then six hours hypoxia/one hour reoxygenation. Data shown are representative of three independent experiments.
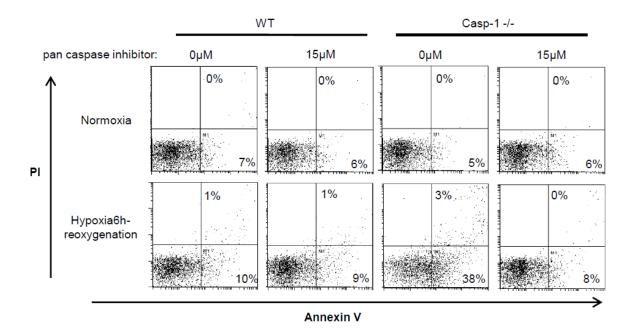
Figure 7: Caspase-1 protects hepatocytes through the inhibition of apoptosis after hypoxia/reoxygenation

Representative Annexin V/PI analysis of WT and caspase-1 -/- hepatocytes pretreated with pan caspase-1 inhibitor (Z-VAD-FMK,15µM), then six hours hypoxia/one hour reoxygenation. Data shown are representative of three independent experiments.

4.3   CASPASE-1 DEFICIENCY INCREASES MITOCHONDRIAL ROS PRODUCTION DURING OXIDATIVE STRESS

Excessive oxidative stress is one cause of hepatocellular cell death after hypoxia/reoxygenation and HS/R[163, 165]. We hypothesized that caspase-1 may regulate oxidative stress after hypoxia/reoxygenation and therefore we assessed intracellular ROS production by DCF staining. As expected, hypoxia/reoxygenation leads to oxidative stress as measured by increased intracellular ROS production (Figure 8A). We found that ROS production was greater in hepatocytes isolated from caspase-1 -/- mice or WT hepatocytes treated with caspase-1 inhibitor than WT hepatocytes alone following hypoxia/reoxygenation (Figure 8A and B). The central role of caspase-1 in regulating intracellular ROS production was further confirmed by the acute knockdown and reconstitution studies (Fig. 8C).

Since ROS can originate from mitochondria or from cytosolic NADPH oxidase/xanthine oxidase, we used fluorescent sensors capable of specifically detecting mitochondrial or cytosolic H_2O_2[166] to determine the source of excessive ROS in caspase-1-/- cells. Hypoxia/reoxygenation significantly increased both mitochondrial and cytosolic H_2O_2 as expected (Figure 8D). Levels of mitochondrial-derived ROS were significantly higher in caspase-1-/- hepatocytes compared with WT, with no difference in cytosolic ROS levels, suggesting that caspase-1 regulates

mitochondrial ROS production after hypoxia/reoxygenation. The results were further confirmed by caspase-1 knockdown with siRNA (Figure 8D).
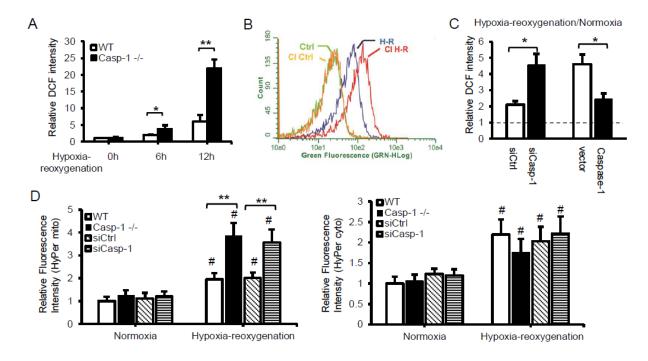
Figure 8: Caspase-1 deficiency increases mitochondrial ROS production during hypoxia/reoxygenation.

(A) Intracellular ROS estimated by DCF staining in hepatocytes after normoxia or hypoxia for six or 12 hours and one hour of reoxygenation. Fluorescence intensity was quantified and normalized to normoxic WT levels (mean±SEM; *P<0.05, **P<0.01). (B) DCF fluorescence measured by flow cytometry in WT hepatocytes pretreated with vehicle DMSO or caspase-1 inhibitor (CI) and then six hours hypoxia/one hour reoxygenation (H-R). Data shown are representative histograms from two independent experiments. (C) Relative intracellular ROS estimated by DCF staining in WT hepatocytes treated with caspase-1 siRNA and caspase-1 [-/-] cells expressing mouse caspase-1 after normoxia or six hours hypoxia/one hour reoxygenation. Data are shown as percentage of normoxic levels (mean±SD; n=3; *P<0.05). (D) Mitochondrial (left) and cytoplasmic H_2O_2 (right) in hepatocytes treated with six hours hypoxia/one hour reoxygenation (mean±SEM; [#]P<0.05, hypoxia-reoxygenation vs. normoxia; **P<0.01, WT vs. caspase-1 [-/-] or siCtrl vs. siCasp-1).

To confirm that excessive mitochondrial ROS contributed to increased cell death in caspase-1^{-/-} hepatocytes, we treated cells with MnTMPyP, a mitochondrial-specific ROS scavenger[167], prior to hypoxia/reoxygenation treatment. MnTMPyP treatment decreased cell death of caspase-1 [-/-] hepatocytes to levels similar to those seen in WT hepatocytes after hypoxia/reoxygenation (Figure 9). Altogether, these findings show a role for caspase-1 in mediating protection against mitochondrial-derived oxidative stress in hepatocytes.
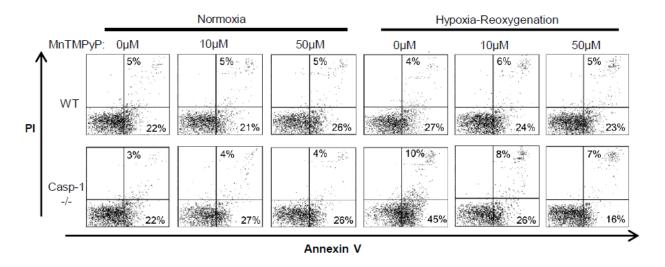
Figure 9: Caspase-1 -/- cells were rescued by mitochondrial ROS scavenger

Annexin V/PI staining in WT and caspase-1 [-/-] hepatocytes pretreated with zero, 10, or 50µM MnTMPyP for one hour and subjected to six hours hypoxia/one hour reoxygenation or normoxia. Data are representative of two independent experiments.

4.4   CASPASE-1 DEFICIENCY RESULTS IN IMPAIRED MITOCHONDRIAL CLEARANCE AFTER HYPOXIA-REOXYGENATION

One adaptive mechanism employed to protect cells from harmful ROS is through regulation of mitochondrial oxidative phosphorylation that generates ROS as a byproduct[168]. We analyzed

mitochondrial oxygen consumption rate (OCR) using the Seahorse Extracellular Flux Analyzer and confirmed that OCR in WT cells was reduced after hypoxia/reoxygenation as expected (Figure 10). In contrast, basal OCR in caspase-1$^{-/-}$ hepatocytes was significantly lower than WT hepatocytes, and remained unchanged after hypoxia/reoxygenation (Figure 10), suggesting an important role for caspase-1 in regulating mitochondrial respiration in both basal and hypoxic states.
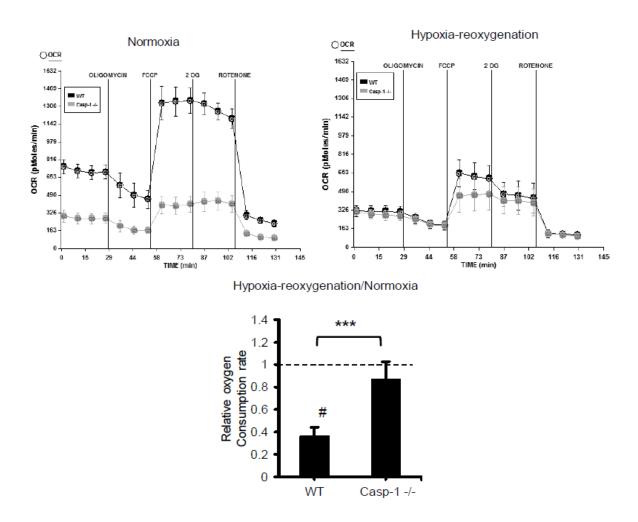
Figure 10: Activation of caspase-1 decreases oxygen consumption after hypoxia/reoxygenation

OCR in hepatocytes cultured under normoxia or treated with six hours hypoxia/one hour reoxygenation. OCR was normalized to protein content and shown as percentage of normoxic control (mean±SD; n=3; #P<0.05, hypoxia-reoxygenation vs. normoxia; ***P<0.001, WT vs. caspase-1$^{-/-}$).

Mitochondrial respiration is a main source of ATP energy in cells, so we also determined steady-state levels of ATP in WT and caspase-1^{-/-} hepatocytes. ATP levels decreased significantly in WT hepatocytes after hypoxia as expected, but interestingly remained unchanged in caspase-1^{-/-} hepatocytes, correlating with similarly unchanged mitochondrial respiration in these cells (Figure 11A). However, no significant difference was seen in mitochondrial membrane potential between WT and Caspase-1 [-/-] hepatocytes after hypoxia-reoxygenation (Figure 11B).
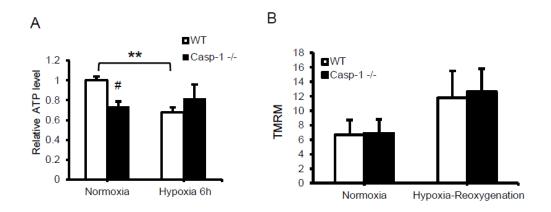
Figure 11: Mitochondrial function in WT and caspase-1 -/- hepatocytes after hypoxia-reoxygenation
(A) Steady-state ATP levels were measured by luciferin-luciferase reaction and normalized to protein content. (mean±SD; n=3. **$P<0.01$, hypoxia six hours vs. normoxia. #$P<0.05$, WT vs. caspase-1 [-/-]). (B) Mitochondrial membrane potential was measured by TMRM staining in hepatocytes cultured under normoxic conditions or treated with hypoxia for six hours followed by reoxygenation (mean±SD; n=3).

One explanation for the reduced mitochondrial respiration and ROS production during hypoxia/reoxygenation could be initiation of a rapid decrease in mitochondrial content[169, 170]. We found significantly decreased mitochondrial volume in WT hepatocytes after hypoxia/reoxygenation, measured by quantitation of 3D-confocal microscopy images. In

contrast, mitochondrial volume in caspase-1$^{-/-}$ and caspase-1 knocked down cells remained unchanged (Figure 12A), and was consistent with observed mitochondrial respiration. Our results showing a role for caspase-1 in the reduction in mitochondrial volume after hypoxia were further confirmed in caspase-1 reconstituted cells and WT hepatocytes pretreated with caspase-1 inhibitor (Figure 12A and 12B). To ensure that changes in mitochondrial volume were not secondary to mitochondrial swelling, mitochondrial content was also determined by measuring mtDNA copy number. Like before, mtDNA was significantly decreased in WT hepatocytes after hypoxia or hypoxia/reoxygenation compared with normoxia, whereas caspase-1$^{-/-}$ cells had significantly increased mtDNA content in comparison with normoxic level (Figure 12C), further suggesting an important role of caspase-1 in regulating mitochondrial mass. The effect of caspase-1 on regulating mitochondrial content was further confirmed by 1.65 fold increase in the levels of translocase of outer membrane 20 (TOM 20) in caspase-1 knockdown cells (Figure 12D). Given the critical role of PGC-1α in regulating mitochondrial biogenesis, we next assessed whether caspase-1 activation regulates the levels of PGC-1α. As shown in Figure 13, both WT and caspase-1 $^{-/-}$ hepatocytes had increased PGC-1α expression early after hypoxia, suggesting an upregulation in mitochondrial biogenesis after acute hypoxia. However, we did not observe a significant difference in PGC-1α levels between WT and caspase-1$^{-/-}$ cells. Altogether, caspase-1 appears to play a vital role in reducing mitochondrial content during hypoxia/reoxygenation, which may form part of the protective mechanism of caspase-1.
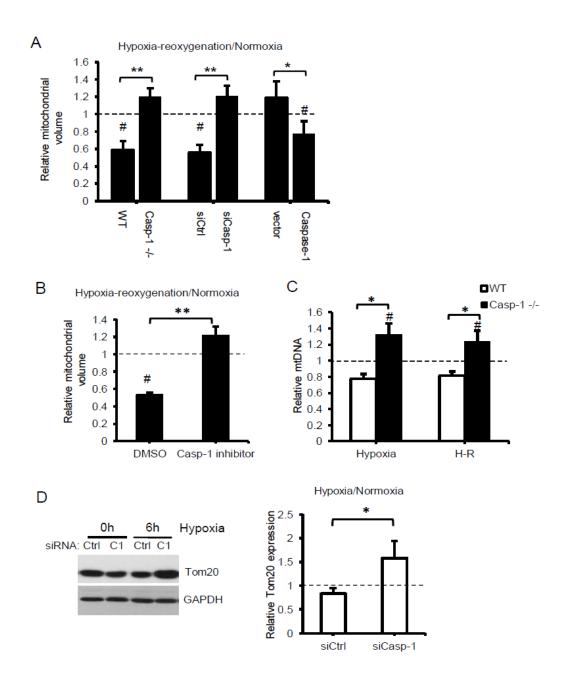
Figure 12: Defective mitochondrial clearance in caspase-1-deficient cells during oxidative stress

(A) Mitochondrial volume in hepatocytes cultured under normoxia or treated with six hours hypoxia/one hour reoxygenation. Data are shown as percentage of normoxic levels (mean±SEM; [#]P<0.05, normoxia vs. hypoxia-reoxygenation. **P<0.01, WT vs. caspase-1 [-/-] or siCtrl vs. siCasp-1; *P<0.05, vector vs. caspase-1). (B) Mitochondrial content in WT hepatocytes pretreated with DMSO or caspase-1 inhibitor before normoxic culture or treated with hypoxia/reoxygenation. Data are shown as percentage of normoxic levels (mean±SEM; [#]P<0.05, normoxia vs. hypoxia-reoxygenation. **P<0.01, WT vs. caspase-1 inhibitor). (C) Mitochondrial DNA copy number

57

was shown as percentage of normoxic levels (mean±SEM; n=3; [#]P<0.05, normoxia vs. hypoxia or hypoxia-reoxygenation. *P<0.05, WT vs. caspase-1 [-/-]). (D) The expression (left) and quantification (right) of TOM 20 was assessed in WT hepatocytes transfected with control siRNA (siCtrl) or caspase-1 siRNA (siC1) 24 hours before they were treated with hypoxia (mean±SEM; n=3;*P<0.05).
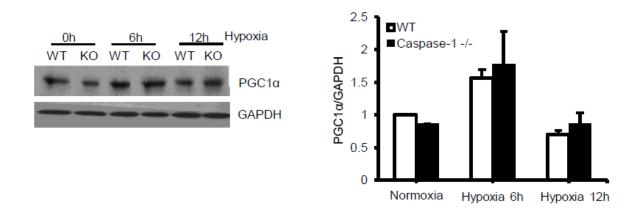
Figure 13: caspase-1 deficiency does not have an effect on PGC-1alpha expression after hypoxia

The expression (left) and quantification (right) of PGC-1α was assessed in WT and caspase-1 -/- hepatocytes treated with zero, six, or 12 hours of hypoxia.

4.5   DEFICIENCY IN CASPASE-1 DECREASES AUTOPHAGIC FLUX IN HEPATOCYTES AFTER HYPOXIA-REOXYGENATION

Mitochondrial autophagy is responsible for mitochondrial turnover and clearance of dysfunctional or damaged mitochondria[36, 171]. We observed mitochondria-containing autophagosomes in WT hepatocytes after hypoxia-reoxygenation (Figure 14, left), and this number was increased by blocking degradation of autolysosomes with bafilomycin A1 (Figure 14, right). Given our findings above, we hypothesized that caspase-1 would regulate autophagic

flux during hypoxia/reoxygenation. Autophagic flux is controlled by both induction and maturation/degradation of autophagosomes. To quantify autophagy we inhibited lysosomal degradation (with bafilomycin) and analyzed the accumulation of GFP-LC3 puncta (autophagic vacuoles) by microscopy or LC3II by Western blot. This, together with assessment of steady-state autophagy, allowed us to monitor changes in autophagic flux[172]. WT and caspase-1^{-/-} hepatocytes showed similar levels of autophagic flux under normoxic conditions as well as after starvation (Figure 15A and 15B). However, after hypoxia/reoxygenation, caspase-1^{-/-} and caspase-1 knocked down hepatocytes had fewer autophagosomes compared with control groups, and this number did not increase with bafilomycin treatment, suggesting that caspase-1 is important for autophagy induction (Figure 15A and 15B). Reversal studies confirm that transfection with mouse caspase-1 is able to significantly restore autophagic flux in caspase-1^{-/-} hepatocytes.
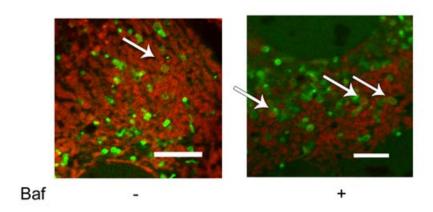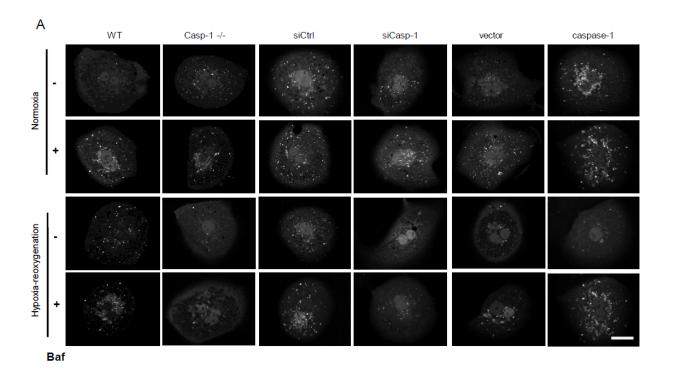
Figure 14: Mitochondrial autophagy in WT hepatocytes after hypoxia-reoxygenation

Mitochondria (MitoTracker-Red) contained autophagosomes (GFP-LC3) in WT hepatocytes after six hours hypoxia/one hour reoxygenation +/- bafilomycin (50nM). Images are representative of at least three separate experiments. Scale bar=10µm.

The maturation of autophagosomes after caspase-1 activation was further analyzed using a tandem RFP-GFP-LC3 construct[173]. GFP fluorescence is quenched in acidic lysosomes while RFP is relatively more resistant to acidic conditions. Therefore, co-localization of green and red puncta indicates early autophagic vacuoles, while red puncta alone indicate late autophagic vacuoles. Caspase-1^{-/-} hepatocytes had a significantly reduced number of early autophagic vacuoles after hypoxia/reoxygenation compared with WT hepatocytes (Figure 16), further confirming a role for caspase-1 in promoting autophagy induction.

B
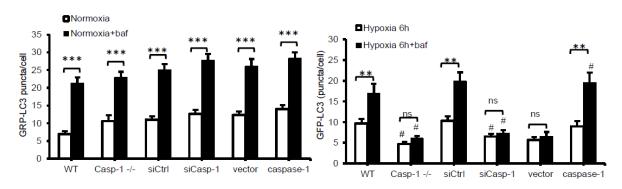
Figure 15: Caspase-1 regulates autophagic flux in hepatocytes after oxidative stress

(A) Autophagosomes (GFP-LC3 puncta) in hepatocytes after six hours hypoxia/one hour reoxygenation +/- bafilomycin (50nM). Scale bar=100µm. (B) Quantification of autophagosomes (GFP-LC3 puncta) in hepatocytes after six hours hypoxia/one hour reoxygenation +/- bafilomycin (50nM) (mean±SEM; **P<0.01, ***P<0.001, steady state vs. bafilomycin treatment; [#]P<0.05, WT vs. caspase-1 [-/-], siCtrl vs. siCasp-1 or vector vs. caspase-1; ns=not significant).
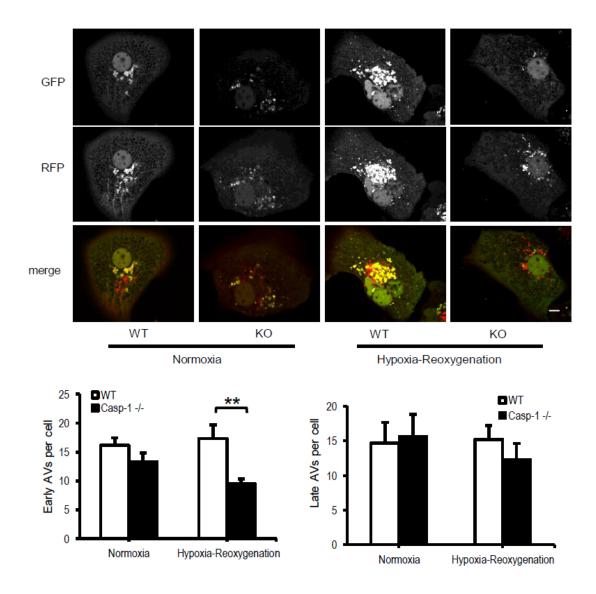
Figure 16: Caspase-1 upregulates induction of autophagy in hepatocytes after oxidative stress

WT and caspase-1 [-/-] hepatocytes were transfected with GFP-RFP-LC3 for 24 hours before they were subjected to six hours of hypoxia and reoxygenation. Cells were fixed and imaged using confocal microscopy. Early (GFP and RFP positive puncta) and late (RFP positive only puncta) autophagic vacuoles were quantified (mean±SEM; **P<0.01, WT vs. caspase-1 [-/-]). Scale bar=20μm.

To determine whether protection against oxidative stress-induced cell death conferred by caspase-1 activation correlates with upregulation of autophagic flux, we blocked autophagic flux

using a lower concentration of bafilomycin (20nM) that doesn't cause significant cell death under basal level, and subjected cells to hypoxia/reoxygenation with subsequent analysis of cell death. As shown in Figure 17, the low concentration of bafilomycin treatment did not significantly increase cell death in either WT or caspase-1$^{-/-}$ hepatocytes under normoxic conditions. As previously shown, hypoxia/reoxygenation increased WT cell death compared with normoxic levels and this was further increased with bafilomycin treatment (Figure 17). Cell death in caspase-1$^{-/-}$ hepatocytes was higher than in WT cells as previously noted, but was not altered by blocking autophagic flux with bafilomycin. Collectively, these data suggest that caspase-1 is protective in hepatocytes after hypoxia/reoxygenation by upregulating autophagic flux, and that autophagic flux is hepatoprotective during oxidative stress.
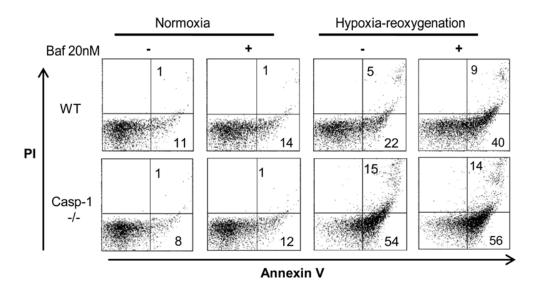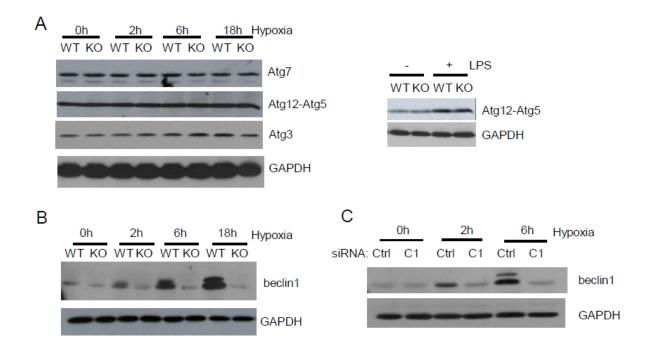
Figure 17: Caspase-1 protects hepatocytes by upregulating autophagy after hypoxia-reoxygenation

WT and caspase-1 -/- hepatocytes were subjected to hypoxia-reoxygenation with or without bafilomycin (20nM). Cell death was analyzed by Annexin V/PI and representative result of three experiments was shown.

4.6   DEFICIENCY IN CASPASE-1 IMPAIRS BECLIN1 UPREGULATION AFTER HYPOXIA-REOXYGENATION

Next, we determined the mechanism by which caspase-1 regulates autophagy induction. There was no difference in levels of Atg3, Atg12-Atg5 conjugate, or Atg7, which are key proteins involved in regulating the initiation of autophagy induction, between WT and caspase-1$^{-/-}$ hepatocytes during oxidative stress (Figure 18A, left) and after LPS treatment (Figure 18A, right). However, expression of beclin1, a key autophagy initiator, was induced in WT but was significantly lower in caspase-1$^{-/-}$ hepatocytes after hypoxia (Fig.18B), suggesting a previously unidentified role for caspase-1 in regulating beclin1 expression. Similarly, beclin1 expression was significantly lower in caspase-1 knocked down hepatocytes after hypoxia/reoxygenation (Figure 18C). Moreover, WT hepatocytes showed increased levels of beclin1 mRNA after hypoxia, whereas the levels remained unchanged in caspase-1 $^{-/-}$ and caspase-1 knocked down cells (Figure 18D).

Beclin1 has been previously shown to be cleaved by caspase-8[174]. To determine if caspase-1 induces beclin1 levels through regulation of caspase-8, we assessed the activity of caspase-8 by Western blot. WT and caspase-1 $^{-/-}$ hepatocytes showed increased caspase-8 after hypoxia, but no difference in caspase-8 cleavage was observed between WT and caspase-1 $^{-/-}$ cells (Figure 19). To confirm a role for beclin1-mediated autophagy in reducing mitochondrial content and subsequent ROS production during hypoxia/reoxygenation in hepatocytes, we knocked down beclin1 in WT hepatocytes (Figure 20A). Mitochondrial ROS but not cytosolic ROS production was significantly higher in sibeclin1-treated cells compared with controls (Figure 20B), similar to the results observed in caspase-1$^{-/-}$ cells.
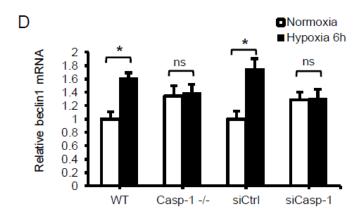
Figure 18: Caspase-1 is required for beclin1 upregulation after HS/R and hypoxia/reoxygenation

(A) Atg7, Atg12-Atg5 conjugates, and Atg3 expression in WT and caspase-1 [-/-] hepatocytes cultured under normoxia or hypoxia for two, six, and 18 hours was assessed by Western blot (left). The expression of Atg12-Atg5 in WT and caspase-1 [-/-] hepatocytes treated with LPS for six hours is shown in the right as positive control. Images are representative of at least three independent experiments. (B) Representative Western blot of beclin1 in WT and caspase-1 [-/-] hepatocytes cultured under normoxia or hypoxia for two, six, and 18 hours. (C) Representative Western blot of beclin1 in WT hepatocytes treated with control siRNA or caspase-1 siRNA after normoxia or hypoxia for

two and six hours. (D) Beclin1 mRNA levels in hepatocytes after normoxia or six hours hypoxia (mean±SEM; n=3; *P<0.05; ns=not significant).
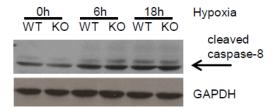
Figure 19: Representative caspase-8 expression in WT and caspase-1 -/- hepatocytes cultured under normoxia or treated with hypoxia for six or 18 hours
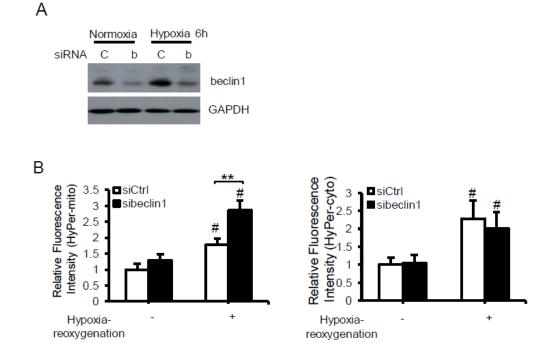
Figure 20: Beclin1 knockdown results in increased mitochondrial ROS production in mouse hepatocytes after hypoxia-reoxygenation

(A) Beclin1 expression in WT hepatocytes transfected with siControl (C) or sibeclin1 (b) for 24 hours before they were subjected to six hours of hypoxia (B) mitochondrial (left) and cytosolic H_2O_2 (right) production in WT

hepatocytes transfected with control siRNA (siCtrl) or siRNA targeting beclin1 (sibeclin1) and six hours hypoxia/one hour reoxygenation (mean±SEM; #$P<0.05$, hypoxia-reoxygenation vs. normoxia; **$P<0.01$; siCtrl vs. sibeclin1).

4.7 CASPASE-1 ACTIVATION IS PROTECTIVE IN THE LIVER AFTER HS/R THROUGH UPREGULATING BECLIN1 AND SUBSEQUENT CLEARANCE OF MITOCHONDRIA

To determine if it is by a similar mechanism that caspase-1 exerts protection *in vivo* after HS/R, we assessed oxidative stress in the liver by measuring a major aldehyde product of lipid oxidation, HNE Michael adducts[175]. Increased liver injury in caspase-1 $^{-/-}$ mice after HS/R was associated with greater liver lipid peroxidation (Figure 21), suggesting increased oxidative stress in the livers of these mice. We also found higher cytosolic cytochrome c levels in caspase-1 deficient livers after HS/R compared with WT (Figure 22A). The results are consistent with increased mitochondrial ROS in caspase-1$^{-/-}$ hepatocytes and suggest increased mitochondria-triggered cell death due to caspase-1 deficiency.
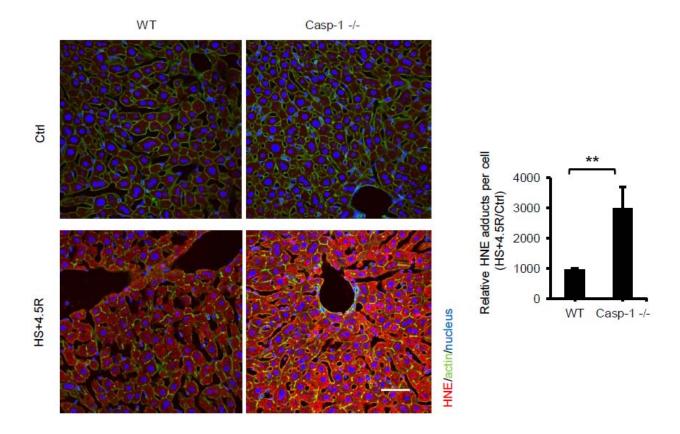
Figure 21: Caspase-1 activation reduced liver injury and oxidative stress after HS/R

Representative staining (scale bar=100µm) and quantification of 4-HNE adducts in livers of control mice (Ctrl) and mice subjected to HS and 4.5 hours of resuscitation (HS+4.5R) (mean±SEM; n=3 for Ctrl, n=5 for HS+4.5R; **P<0.01). Quantification is shown as fold increase to Ctrl groups. (D) Cytochrome c release was determined by Western blot of liver cytosolic fraction.

To assess mitochondrial content *in vivo*, we measured activity of citrate synthase, a mitochondrial enzyme relatively resistant to oxidative modification, which can therefore be used as an indicator of mitochondrial content[176]. We found that mitochondrial content was significantly decreased in WT livers but remained unchanged in caspase-1 [-/-] livers following HS/R (Figure 22B). Mitochondrial autophagy in WT liver after HS/R was confirmed by electron microscopy analysis (Figure 22C). Moreover, beclin1 levels increased in WT and caspase-1 [-/-]

68

livers following HS/R. But consistent with our findings *in vitro*, beclin1 expression was significantly lower in caspase-1 $^{-/-}$ livers compared with WT livers (Figure 22D).
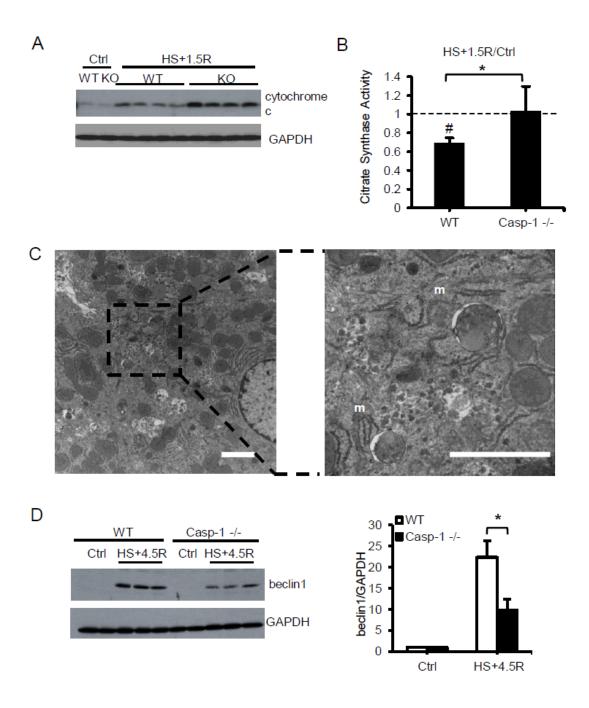
Figure 22: Caspase-1 deficiency results in increased mitochondrial content and decreased beclin1 in the liver after HS/R

(A) Liver mitochondrial content was determined by citrate synthase activity and normalized to controls (mean±SEM; n=4; [#]P<0.05, HS+1.5R vs. Ctrl. *P<0.05, WT vs. caspase-1 [-/-]). (B) Electron microscopy images of WT liver treated with HS and 4.5 hours of resuscitation. Mitochondria-containing autophagosomes are indicated as m (scale bar=2µm). (C) Western blot and quantification of beclin1 levels in livers of control mice or mice subjected to HS+4.5R (mean±SD; n=3 for control groups, n=6 for HS+4.5R groups; *P<0.05).

Taken together, our results suggest that caspase-1 deficiency *in vivo* leads to increased oxidative stress and suppressed mitochondrial clearance in the liver after HS/R. To determine if this can be rescued by beclin1 overexpression, we constructed an adenovirus encoding full-length mouse beclin1 (ad-beclin1) and injected it or ad-GFP as control intravenously into mice 48 hours prior to HS/R. Liver ad-GFP expression was confirmed in control mice (Fig.23A), and liver beclin1-overexpression was confirmed by immunoblotting (Fig.23B). Beclin1 overexpression in caspase-1 [-/-] livers led to significantly increased autophagy indicated by the levels of LC3II (Figure 23C).
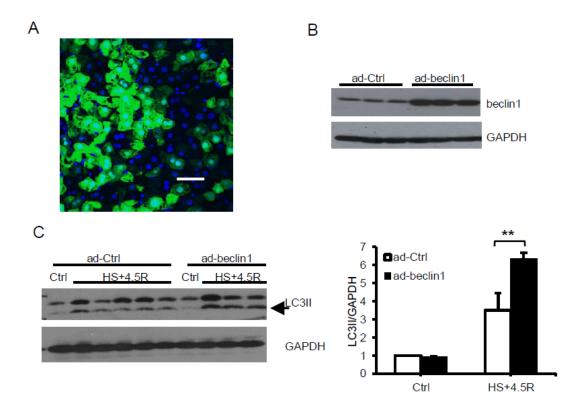
Figure 23: Beclin1 overexpression leads to increased autophagy in caspase-1 -/- mice after HS/R

(A) Effectiveness of adenoviral gene expression in liver after tail vein injection with adenovirus encoding GFP as control (ad-Ctrl) (left; scale bar=50μm) or mouse beclin1 (ad-beclin1) (right). (B) Western blot and quantification of LC3II in livers of caspase-1 [-/-] mice given control adenovirus (ad-Ctrl) or mouse beclin1 adenovirus (ad-beclin1) 48 hours prior to no surgery (Ctrl) or HS and 4.5 hours of resuscitation (HS+4.5R) (mean±SD; n=5, **P<0.01).

Moreover, overexpression of beclin1 was hepatoprotective in caspase-1^{-/-} mice, but did not confer further protection in WT mice where beclin1 can be upregulated normally (Figure 24A). We also confirmed that beclin1-overexpression reduced oxidative stress in caspase-1^{-/-} livers as assessed by HNE adducts (Figure 24B). Decreased cytosolic cytochrome *c* levels (Figure 24C) in caspase-1^{-/-} livers with beclin1-overexpression further suggests prevention of mitochondria-triggered cell death by beclin1. Taken together, our results indicate a previously unrecognized role for caspase-1 in the upregulation of beclin1 to initiate mitochondrial

autophagy in hepatocytes and to reduce excessive mitochondrial ROS production. This is

consistent with a known protective role of beclin1 during hypoxia/reoxygenation [177].
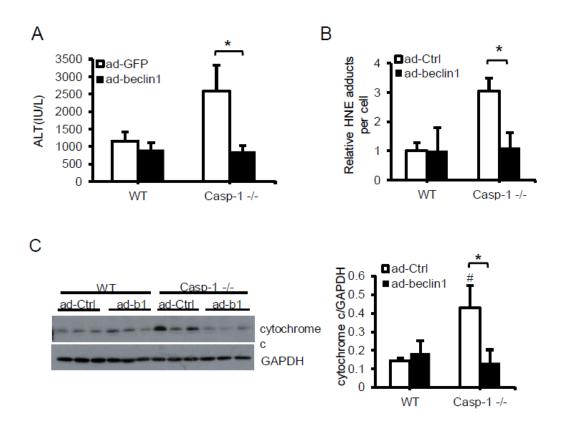
Figure 24: Beclin1 overexpression rescues caspase-1 -/- mice from excessive liver injury

(A) Plasma ALT (n=6; mean±SEM; *P<0.05), (B) liver HNE adducts (mean±SEM; n=5, *P<0.05), and (C) liver

cytoplasmic cytochrome c (n=5; mean±SD; #P<0.05, WT vs. caspase-1 -/-. *P<0.05, ad-Ctrl vs. ad-beclin1) in mice

given ad-GFP or ad-beclin1 (ad-b1) 48 hours prior to HS+4.5R.

4.8　GENERATION OF BONE MARROW (BM) CHIMERIC MICE TO DETERMINE THE CELL TYPE RESPONSIBLE FOR ACTIVATION OF CASPASE-1 IN THE LIVER

To confirm the role of parenchymal cells in mediating the activation and protective effect of caspase-1, we generated BM chimeric mice by adoptive BM transfer into irradiated hosts using WT and caspase-1$^{-/-}$ (KO) mice. Combinations included WT/WT (recipient/donor), WT/KO, KO/WT, and KO/KO. WT/WT and KO/KO mice served as positive and negative controls, respectively. Following HS/R, circulating IL-18 levels were measured to assess the activation of caspase-1. As expected, the KO/KO combination resulted in a near-complete absence of cytokine release after HS/R (Figure 25A). The test combinations of WT/KO and KO/WT led to similar IL-18 levels as WT/WT mice following HS/R, suggesting that both parenchymal cells and BM-derived immune cells contribute to caspase-1 activation. However, KO/KO mice did not show higher levels of liver injury compared with WT/WT mice, as we have shown in caspase-1 $^{-/-}$ mice (Figures 25B and 25C). Moreover, basal beclin1 levels were high in all of the chimeric strains, which did not have increased beclin1 expression after HS/R as shown in WT and caspase-1 $^{-/-}$ mice (Figure 25D). Since beclin1 increases during cell stress[178], the relatively unchanged beclin1 expression indicates increased stress at basal levels in chimeric livers, probably due to irradiation. Interestingly, WT/KO mice showed higher levels of liver injury compared to WT/WT and KO/WT mice (Figure 25B and 25C), suggesting that caspase-1 activation in parenchymal cells contributes to liver protection after HS/R.
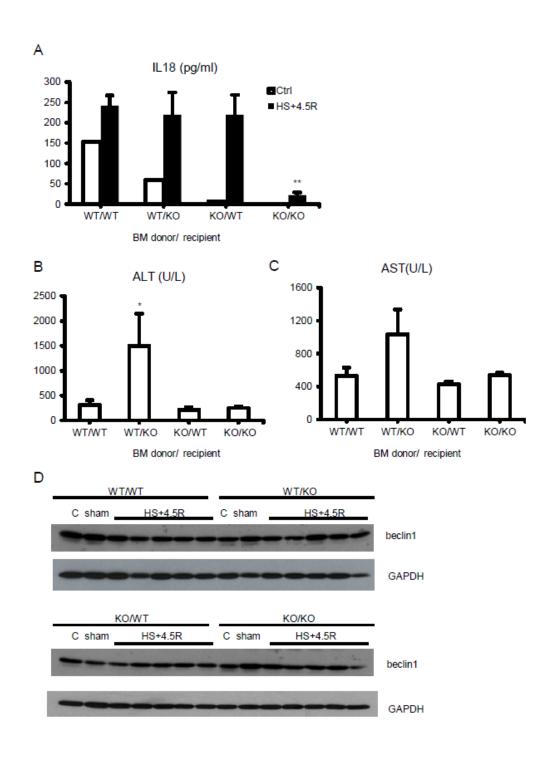
Figure 25: Generation of BM chimeric mice to determine the cell type responsible for the activation and protective effect of caspase-1 after HS/R

(A) Plasma IL18 in BM chimeric mice after control (Ctrl), HS + 4.5 hours of resuscitation (R) (n=1/ Ctrl group; n=5/experimental group; mean±SEM; **P<0.01). (B) Plasma ALT and (C) AST levels in chimeric mice after HS/R

(n=1 in control groups; n=5 in HS/R groups; mean±SEM*P<0.05). (D) Western blot of beclin1 levels in livers of control chimeric mice or mice subjected to HS+4.5R.

4.9 ACTIVATION AND PROTECTIVE EFFECT OF CASPASE-1 IS CASPASE-11 INDEPENDENT

Recent evidence has shown that caspase-1 $^{-/-}$ mice generated using strain 129 embryonic stem cells, which attenuate caspase-11 expression genetically, lack both caspase-1 and caspase-11[42]. Indeed, by Western blotting, we confirmed that peritoneal macrophages isolated from caspase-1 $^{-/-}$ mice were also caspase-11 deficient, whereas macrophages from strain 129 mice lack caspase-11 as expected (Figure 26A). Given that caspase-11 also mediates non-canonical inflammasome activation induced by cholera toxin B, *E. coli*, *C. rodentium,* and *V. cholerae*[42], we next determined whether the activation of caspase-1 in the liver after HS was mediated by caspase-11. As shown in Figure 26B, HS only, as well as HS/R, induced the activation of caspase-11. However, caspase-1 $^{-/-}$ liver also showed noticeably increased caspase-11 expression after HS (Figure 26B).

Since macrophages from strain 129 mice lack detectable caspase-11 protein, we utilized strain 129 mice to investigate the role of caspase-11 in mediating caspase-1 activation and liver protection, together with caspase-1 $^{-/-}$ and WT mice as controls. Caspase-1 $^{-/-}$ mice showed minimal levels of circulating IL-18 and a tendency towards increased liver injury as demonstrated previously (Figure 27). However, similar levels of liver injury and IL-18 release

75

were observed between strain 129 mice and WT (C57BL/6) mice, suggesting that the activation

and protective effect of caspase-1 in the liver is not dependent on caspase-11 after HS.
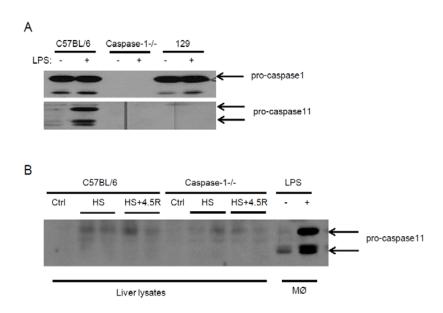
Figure 26: Caspase-1 $^{-/-}$ mice were caspase-1 $^{-/-}$ caspase-11 $^{-/-}$

(A) Peritoneal macrophages were isolated from WT (C57BL/6), caspase-1 $^{-/-}$, and strain 129 mice and the levels of

pro-caspase1 and pro-caspase11 in macrophages left unstimulated or stimulated with LPS were detected by Western

blot. (B) Levels of pro-caspase11 were detected by Western blot in liver lysates from control (Ctrl) mice or mice

treated with HS only or HS with 4.5 hours of resuscitation (HS+4.5R). Peritoneal macrophages treated with or

without LPS were used as controls (last two lanes).
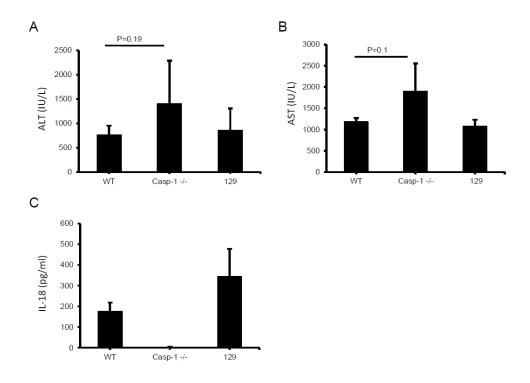
Figure 27: Strain 129 mice showed similar levels of liver injury and caspase-1 activation after HS

(A) ALT and (B) AST levels in WT (C56BL/6), casp-1 -/- and strain 129 mice treated with HS and 4.5 hours of resuscitation (mean±SEM; n=5 for HS+4.5R). (C) Circulating IL-18 levels in WT, casp-1 -/-, and strain 129 mice after HS and 4.5 hours of resuscitation.

5.0   RESULTS-THE AIM2 INFLAMMASOME MEDIATES ACTIVATION AND PROTECTIVE EFFECT OF CASPASE-1 IN HEPATOCYTES AFTER REDOX STRESS

5.1   THE PROTECTIVE EFFECT OF CASPASE-1 IN THE LIVER IS DEPENDENT ON AIM2 AFTER HS

In order to investigate the mechanism by which caspase-1 is activated and exerts protection after redox stress in the liver, we first assessed whether the activation of caspase-1 is mediated by the NLRP3 inflammasome. We subjected WT and NLRP3 $^{-/-}$ mice to HS with 4.5 hours of resuscitation, the time point associated with severe liver injury and excessive oxidative stress shown by our previous results[179]. As shown in Figure 28A, circulating IL-18 levels were similar in WT and NLRP3 $^{-/-}$ mice after HS/R, indicating that caspase-1 activation in immune cells is not NLRP3-dependent after redox stress induced by HS/R. Moreover, in contrast to caspase-1 $^{-/-}$ mice, NLRP3 $^{-/-}$ mice did not have a marked increase in liver damage compared with WT mice (Figure 28B). Taken together, the results suggest that the protective effect of caspase-1 in the liver is not mediated by the NLRP3 inflammasome.

Figure 28: Activation and protective effect of caspase-1 is not dependent on NLRP3 after HS/R

(A) Circulating IL-18 and (B) plasma ALT in WT and NLRP3 [-/-] mice after HS/R (n=2 in control groups; n=7-8 in HS/R groups; mean±SEM)

The NLRP1 inflammasome has been shown to mediate caspase-1 activation in a mouse model of cerebral ischemia[180]. Next, we determined whether the activation and protective effect of caspase-1 is dependent on the NLRP1 inflammasome after oxidative stress by *in vivo* knockdown of NLRP1a. Injection of siRNA against NLRP1a through tail vein significantly decreased the levels of NLRP1 in the liver at day 3, as determined by Western blot (Figure 29A). Knockdown of NLRP1a significantly suppressed the levels of circulating IL-18 after HS/R, suggesting the essential role of NLRP1a in mediating caspase-1activation in immune cells after HS/R (Figure 29B). However, mice treated with siNLRP1a showed similar levels of liver injury after HS/R compared with control siRNA treated mice as determined by ALT levels (Figure 29C), indicating that the protective effect of caspase-1 activation after oxidative stress in the liver is not mediated by the NLRP1 inflammasome.
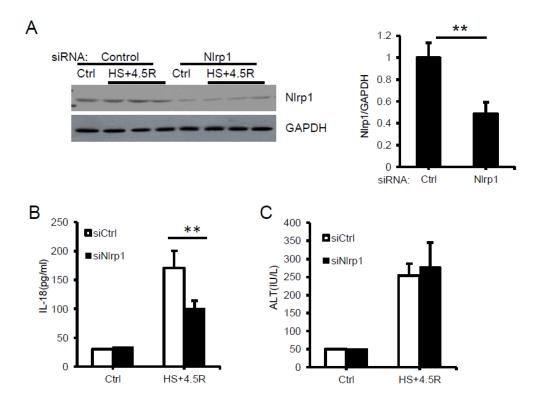
Figure 29: NLRP1 inflammasome mediates caspase-1 activation in immune cells, but not the protective effect of caspase-1

(A) Representative Western blot (left) and quantification (right) of NLRP1 expression in the liver in mice injected with control siRNA or NLRP1a siRNA two days before HS and 4.5 hours of resuscitation (HS+4.5R) treatment. (B) Circulating IL-18 and (C) plasma ALT in WT and NLRP1 siRNA treated mice after HS/R (n=1 in control groups; n=6-7 in HS/R groups; mean±SEM**P<0.01).

Since the AIM2 inflammasome can be activated by endogenous dsDNA[50], and mitochondrial DNA has been shown to be released after oxidative stress[37], we next hypothesized that the activation and protective effect of caspase-1 is mediated by the AIM2 inflammasome. AIM2 $^{-/-}$ mice had similar levels of plasma IL-18 as control mice, which ruled out the role of AIM2 in mediating caspase-1 activation in immune cells after HS/R (Figure 30A). AIM2 deficiency led to significantly elevated liver injury after HS/R, similar to that seen in caspase-1 $^{-/-}$ mice (Figure 30B). Altogether, these findings suggest a role for the NLRP1 inflammasome in

activating caspase-1 in immune cells, but the AIM2 inflammasome in mediating the protective

effect of caspase-1 in the liver after redox stress.
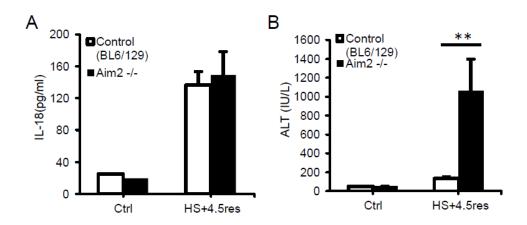
Figure 30: The protective effect of caspase-1 in the liver is dependent on AIM2 inflammasome after

HS/R

(A) Circulating IL-18 and (B) plasma ALT in Control and AIM2 $^{-/-}$ mice after HS/R (n=2 in control groups; n=7 in

HS/R groups; mean±SEM **P<0.01).

5.2 ACTIVATION AND THE PROTECTIVE EFFECT OF CASPASE-1 AFTER REDOX STRESS IS DEPENDENT ON AIM2 IN HEPATOCYTES.

To confirm the role of AIM2 in regulating caspase-1 activation and hepatocyte cell death after

redox stress, we subjected hepatocytes isolated from WT and AIM2 $^{-/-}$ mice to

hypoxia/reoxygenation in an *in vitro* model of HS/R[181]. Hypoxia-reoxygenation treatment

induced the activation of caspase-1 in WT hepatocytes as expected, whereas caspase-1 activity

stayed unchanged in AIM2 $^{-/-}$ hepatocytes (Figure 31A), suggesting a role for AIM2 in activating

caspase-1. To further confirm the activation of the AIM2 inflammasome in hepatocytes after

hypoxia-reoxygenation, we performed immunoprecipitation to assess the association of AIM2 and ASC, the adaptor protein required for the assembly of AIM2 inflammasome[50, 182]. AIM2 formed a complex with ASC in WT hepatocytes after hypoxia-reoxygenation as well as the treatment of poly(dA-dT):poly(dA-dT) [poly(dA:dT)], a synthetic form of dsDNA known to activate the AIM2 inflammasome[182] (Figure 31B). To determine if similar observations took place *in vivo*, we examined caspase-1 cleavage in the liver by Western blot. Similar to the *in vitro* results, caspase-1 was activated after HS/R in the WT liver, but the activity was not elevated in the AIM2 -/- liver after redox stress induced by HS/R (Figure 31C).

To investigate whether AIM2 is protective after redox stress in hepatocytes, we assessed hepatocyte apoptosis and necrosis by Annexin V/PI analysis. Consistent with the *in vivo* results showing increased liver cell death after HS/R, AIM2-deficiency resulted in higher levels of hepatocyte cell death after hypoxia-reoxygenation, which phenocopied caspase-1-deficient hepatocytes[179] (Figure 31D).
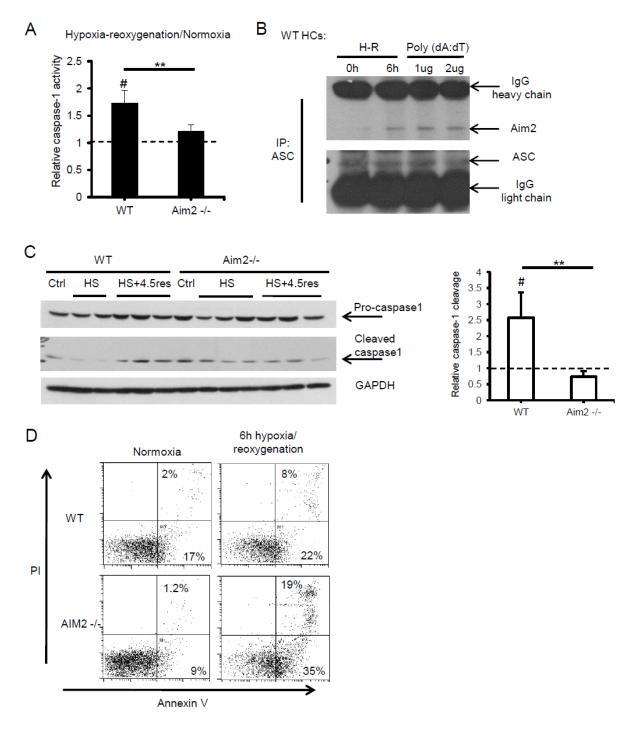
Figure 31: Activation and the protective effect of caspase-1 after redox stress is dependent on AIM2

in hepatocytes

(A) Relative caspase-1 activity in WT and AIM2 $^{-/-}$ hepatocytes after normoxia or six hours hypoxia and one hour

reoxygenation. Data are shown as percentage of normoxic levels (mean±SD n=3; $^{\#}P<0.05$, normoxia vs. hypoxia-

reoxygenation; $^{*}P<0.01$, WT vs. AIM2 $^{-/-}$). (B) WT hepatocytes were treated with six hours hypoxia and one hour

reoxygenation or poly (dA:dT) followed by immunoprecipitation with ASC and immunoblotting with AIM2. (C) Representative Western blot and quantification of pro- and cleaved caspase-1 in the livers of WT and AIM2 [-/-] mice after HS only or HS+4.5 hours resuscitation (HS+4.5R) (mean±SEM n=3; [#]P<0.05, HS+4.5R vs. Ctrl; *P<0.01, WT vs. AIM2 [-/-]).. (D) Representative Annexin V/PI flow cytometry dot plots for WT and AIM2 [-/-] hepatocytes cultured under normoxia or after six hours hypoxia/one hour reoxygenation.

5.3   DEFICIENCY IN AIM2 IMPAIRS BECLIN1 UPREGULATION AND MITOCHONDRIAL CLEARANCE AFTER HYPOXIA/REOXYGENATION.

We have shown that caspase-1 activation protects against cell death through upregulation of the autophagy initiator beclin1 and through the clearance of mitochondria through mitochondrial autophagy after oxidative stress[179]. Therefore, here we investigated whether AIM2 exerts protection in hepatocytes through the same mechanism. As shown in Figure 32A, beclin1 expression was induced in WT hepatocytes, but significantly lower in AIM2^{-/-} hepatocytes after hypoxia as well as poly(dA:dT) simulation, consistent with the results observed in caspase-1 [-/-] hepatocytes. AIM2 [-/-] cells had significantly increased mitochondrial content after hypoxia-reoxygenation compared with normoxia, whereas the levels remained unchanged in WT hepatocytes, as determined by measuring mtDNA copy number (Figure 32B). These results were also in line with what we have shown in caspase-1 [-/-] cells after redox stress. We also found that ROS production was greater in AIM2 [-/-] hepatocytes compared with WT cells after hypoxia-reoxygenation (Figure 32C), consistent with the central role of caspase-1 in regulating intracellular ROS production. Moreover, the role of AIM2 in regulating beclin1 expression was further confirmed by the decreased beclin1 levels in AIM2 [-/-] liver after HS/R compared with WT liver (Figure 32D). Taken together, AIM2 appears to protect hepatocytes from cell death

through the same mechanism as caspase-1, which is by upregulating mitochondrial clearance and thereby reducing intracellular ROS production after redox stress.
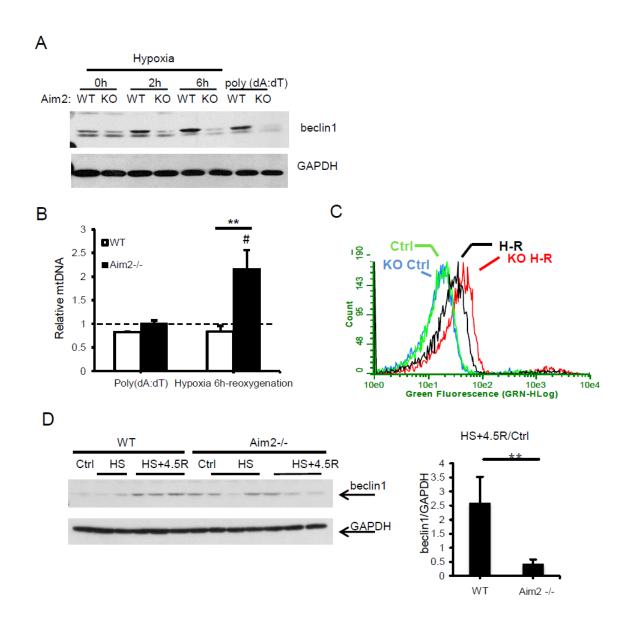
Figure 32: Beclin1 upregulation and mitochondrial clearance after redox stress is dependent on

AIM2 in hepatocytes

(A) Representative Western blot of beclin1 in WT and AIM2 [-/-] hepatocytes treated with poly (dA:dT) or cultured under normoxia or hypoxia for two or six hours. (B) Mitochondrial DNA copy number was shown as percentage of normoxic levels (mean±SEM; n=3; [#]P<0.05, normoxia vs. hypoxia-reoxygenation. *P<0.05, WT vs. AIM2 [-/-]). (C) DCF fluorescence measured by flow cytometry in WT and AIM2 [-/-] (KO) hepatocytes treated with six hours

hypoxia/one hour reoxygenation (H-R). Data shown are representative histograms from two independent experiments. (D) Western blot and quantification of beclin1 levels in control mice livers or mice subjected to HS alone or HS+4.5R (mean±SD; n=2 for control groups, n=5 for HS+4.5R groups; *P<0.05).

5.4   HMGB1 ASSOCIATES WITH AIM2 AFTER OXIDATIVE STRESS IN HEPATOCYTES

HMGB proteins have been shown to bind to all immunogenic nucleic acids and can function as universal sentinels for nucleic-acid-mediated innate immune responses, including the activation of TLR3, TLR7, and TLR9 by their cognate nucleic acids[183]. Therefore, we hypothesized that HMGB1 facilitates the sensing of dsDNA by AIM2, thereby enhancing the activation of the AIM2 inflammasome after redox stress. First, by immunoprecipitation, we showed an increased association of endogenous HMGB1 and AIM2 in WT hepatocytes after hypoxia-reoxygenation as well as poly(dA:dT) treatment. As expected, the association was not detectable in Aim -/- cells (Figure 33).
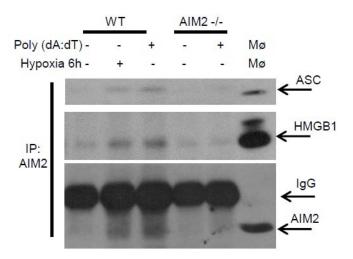
Figure 33: The association of HMGB1 and AIM2 after oxidative stress in hepatocytes

86

WT and AIM2 [-/-] hepatocytes were treated with six hours hypoxia and one hour reoxygenation or poly (dA:dT) followed by immunoprecipitation with AIM2 and immunoblotting with ASC or HMGB1. Cell lysate from LPS treated macrophages serve as control (last lane).

We next examined the possible interaction of HMGB1 and AIM2 in the liver after HS/R. Whereas HMGB1 is mainly localized in the nucleus, in the WT liver the released cytosolic HMGB1 co-localized with punctated cytoplasmic AIM2 after HS/R (Figure 34). Taken together, immunoprecipitation and immunofluorescence experiments indicate that HMGB1 associates with AIM2 in hepatocytes after redox stress.

Aim2   HMGB1   Merge
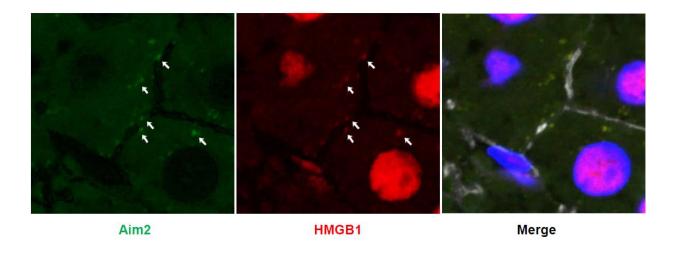
Figure 34: The association of HMGB1 and AIM2 after HS/R in the liver

The co-localization of AIM2 and HMGB1 (indicated by arrows) was determined by staining of AIM2 (green), HMGB1 (red), and nucleus (DAPI) in livers of mice subjected to HS and 4.5 hours of resuscitation.

5.5 HMGB1 IS PROTECTIVE AFTER OXIDATIVE STRESS IN HEPATOCYTES

To determine whether HMGB1^{-/-} hepatocytes recapitulate the phenotype of caspase-1^{-/-} and AIM2^{-/-} cells, we analyzed HMGB1^{-/-} cell death after hypoxia-reoxygenation. Consistent with our previous results showing increased cell death in caspase-1-deficient and AIM2-deficient hepatocytes, HMGB1-deficiency resulted in higher levels of hepatocyte apoptosis and necrosis after hypoxia/reoxygenation (Figure 35A). Moreover, HC-HMGB1^{-/-} mice had significantly higher levels of liver damage compared with WT mice after HS/R, suggesting an essential role of HMGB1 in protecting hepatocytes from cell death after redox stress (Figure 35B).
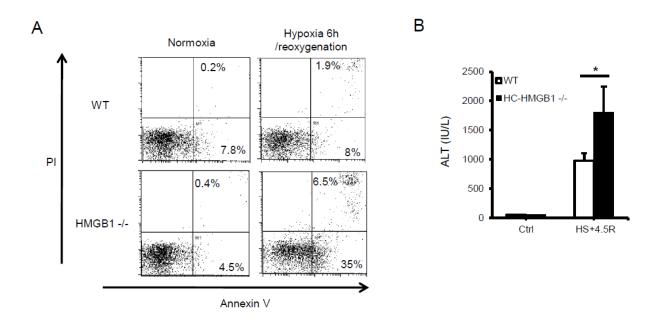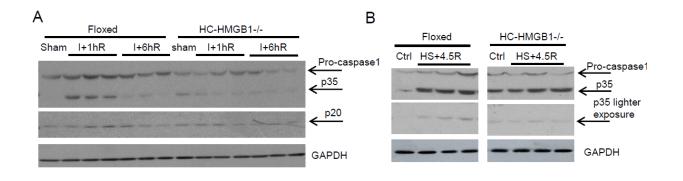
Figure 35: HMGB1 is protective after oxidative stress in hepatocytes

(A) Representative Annexin V/PI flow cytometry dot plots for WT and HMGB1^{-/-} hepatocytes cultured under normoxia or treated with six hours hypoxia/one hour reoxygenation. (B) Plasma ALT in mice after HS/R (n=2 in control groups; n=7 in HS+4.5R groups; mean±SEM; *P<0.05).

5.6   HMGB1 IS REQUIRED FOR CASPASE-1 ACTIVATION AND BECLIN1 UPREGULATION AFTER REDOX STRESS IN THE LIVER

To determine if AIM2 inflammasome activation is dependent on HMGB1 *in vivo*, we carried out experiments in liver I/R and HS/R models, both of which induce severe liver oxidative stress[136]. Caspase-1 was activated after one hour of liver ischemia, followed by one hour of reperfusion in WT mice, as shown by increased cleaved caspase-1 in the liver, but not in the HC-HMGB1$^{-/-}$ liver (Figure 36A). Similar results were also observed in the HS/R model, where WT but not HC-HMGB1$^{-/-}$ mice showed increased caspase-1 activation in the liver (Figure 36B), confirming a role for HMGB1 in regulating caspase-1 in hepatocytes after redox stress. Beclin1 levels were increased in WT livers following HS/R as shown before, but not in HC-HMGB1$^{-/-}$ livers, consistent with our findings in caspase-1-deficient and AIM2-deficient mice (Figure 36C). Our *in vitro* experiments also confirmed that HMGB1 in hepatocytes is required for the upregulation of beclin1 after hypoxia as well as synthetic dsDNA poly(dA:dT) (Figure 36D).
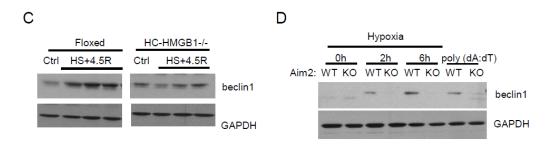
Figure 36: HMGB1 is required for caspase-1 activation and beclin1 upregulation after redox stress in the liver

(A) Representative Western blot of caspase-1 in liver of floxed and hepatocyte-specific HMGB1$^{-/-}$ (HC-HMGB1$^{-/-}$) mice after ischemia with one hour of reperfusion (I+1hR) or ischemia with six hours of reperfusion (I+6hR). (B) Representative Western blot of caspase-1 in liver of floxed and HC-HMGB1$^{-/-}$ mice after HS with 4.5 hours of resuscitation (HS+4.5R). (C) Western blot of beclin1 levels in livers of control mice or mice subjected to HS+4.5R. (D) Representative Western blot of beclin1 in WT and AIM2 $^{-/-}$ hepatocytes cultured under normoxia or treated with hypoxia for two and six hours or poly(dA:dT) for three hours.

6.0   DISCUSSION AND FUTURE DIRECTIONS

6.1   DISCUSSION: CASPASE-1 AND ADAPTIVE RESPONSES

This study was undertaken to determine the protective mechanisms of caspase-1 in the setting of redox stress in hepatocytes. Here, we show that caspase-1 deficiency or inhibition leads to enhanced mitochondrial ROS production and a failure to reduce mitochondrial content in hepatocytes subjected to hypoxia/reoxygenation. This was associated with a failure to upregulate beclin1 expression and subsequent mitochondrial autophagy, suggesting a previously unrecognized role of caspase-1 in the regulation of mitochondrial autophagy in hepatocytes. Using a model that induces oxidative stress in the liver[136, 184], HS/R, we show that similar events occur *in vivo*. Our results provide evidence that caspase-1 activation after HS/R leads to a reduction in oxidative stress, which in turn directly reduces hepatocellular cell death induced by I/R injury after HS/R.

Our findings in this study establish a mechanism to explain the paradoxical protective role of caspase-1 during HS/R. Our previous results and the results published here are in clear contrast to the detrimental effects of caspase-1 in more severe heart and kidney I/R injury models, which leave many cells anoxic rather than hypoxic and severely limit the initiation of adaptive survival responses. In these cases, caspase-1-mediated inflammation is detrimental[51, 55]. Our findings, although initially surprising, are consistent with our understanding of caspase-1-

91

mediated regulation of adaptive responses in non-myeloid cell types. Caspase-1 has been previously shown to regulate adaptive responses to stress, and is known to be important in preservation of epithelial integrity by increasing the proliferation of mucosal epithelial cells[150], mediating protein secretion in keratinocytes[60], and promoting membrane repair[7]. It now seems likely that caspase-1 activation promotes different effects in different cell types under varying stresses, including a protective role in the liver under conditions of oxidative stress. Indeed, recent studies provide evidence that caspase-1 can reduce the progression of hepatic steatosis[185], in which redox stress is one of the central mediators of the disease process[186, 187]. Our data could provide one of the mechanisms behind these effects.

6.2   DISCUSSION: DUAL ROLES OF CASPASE-1 IN IMMUNE CELLS VS. EPITHELIAL CELLS

Our work here demonstrates a novel role of caspase-1 and inflammasome in mediating protective responses in epithelial cells, in contrast to their well-established detrimental role in immune cells. We initially tried to investigate the role of caspase-1 in immune cells by luminex assay (data not shown). However we found that among the 20 cytokines and chemokines we measured, most of them were not significantly up-regulated in the circulation after HS/R. Some of those inflammatory mediators that stayed at low levels after HS/R include IL-1β and TNFα, which are associated with increased liver damage induced after oxidative stress[188, 189]. This together with the results from IL-18R $^{-/-}$ and IL-1R $^{-/-}$ mice (Figure 5) suggest that the protective effect of caspase-1 is most likely not mediated by its activation in immune cells. However, we still cannot

exclude the effect of cell-cell interaction. This effect can be further explored using cell-specific knockout mice.

6.3   DISCUSSION: MITOCHONDRIAL TURNOVER AND LIVER PROTECTION

We found that caspase-1 protects hepatocytes from hypoxia/reoxygenation-induced cell death by reducing ROS production, specifically in the mitochondria. During hypoxia, mitochondrial respiration is dramatically reduced because of oxygen deprivation. After reperfusion, reestablishment of mitochondrial aerobic respiration results in a burst of ROS production, which triggers the release of pro-apoptotic proteins such as cytochrome *c* and can subsequently result in cell death[135, 136, 190]. The inhibition of mitochondrial respiration during I/R and the removal of mitochondria to reduce ROS production upon reperfusion may confer protection against mitochondrial dysfunction and subsequent cell death[135, 168, 191, 192], and is a major cellular adaptive response to hypoxia[193]. Even though low ROS levels may be critical to signaling in cell stress and pre-conditioning responses[107], our study suggests high levels of mitochondrial ROS contribute directly to hepatocyte cell death during hypoxia/reoxygenation.

Importantly, our results suggest that caspase-1 induces mitochondrial autophagy in response to oxidative stress to promote mitochondrial turnover and maintain a healthy population of mitochondria, which in turn regulates ROS production and cell death. Our data also suggest that caspase-1 has no effect on regulating the expression of PGC-1α, which has been shown to contribute to increased mitochondrial biogenesis after hypoxia[194]. Autophagy has been shown to be essential for mitochondrial clearance, which leads to decreased ROS production by mitochondria[171, 195] and serves as a pro-survival mechanism[196, 197]. This autophagy-mediated

93

turnover of mitochondria may be particularly beneficial in the liver, where the half-life of mitochondria is only 1.83 days - much shorter than in organs such as heart and brain[198]. Given that lysosomal degradation is the major pathway for mitochondrial turnover [199], the shorter half-life of liver mitochondria suggests mitochondrial autophagy plays a significant role in mitochondrial quality control in the liver.

6.4   DISCUSSION: CASPASE-1 AND AUTOPHAGY

Our findings establish a previously unrecognized role for caspase-1 in the regulation of this cell-survival response through the regulation of autophagy and beclin1 expression. Autophagic flux is controlled by both induction and maturation/degradation of autophagosomes. To quantify autophagy, we inhibited lysosomal degradation and analyzed the accumulation of GFP-LC3 puncta by microscopy. This, together with assessment of steady-state autophagic vacuoles, allowed us to monitor changes in autophagic induction and degradation[172]. We show in this study that caspase-1$^{-/-}$ hepatocytes had a significantly reduced number of autophagic vacuoles after hypoxia/reoxygenation compared with WT cells, and no further accumulation was observed when lysosomal degradation was blocked, suggesting impaired induction of autophagy in caspase-1$^{-/-}$ hepatocytes.

These results are consistent with our subsequent findings that beclin1, a key protein involved in induction of autophagy, was expressed at significantly lower levels in caspase-1$^{-/-}$ hepatocytes compared with WT hepatocytes in response to oxidative stress from either HS/R or hypoxia/reoxygenation. Our results suggest that caspase-1 regulates mRNA levels of beclin1 as one mechanism for increasing its expression. Previous studies suggest that beclin1 can be

94

degraded after its ubiquitination and the process is regulated by ubiquitin-specific peptidases[101]. Beclin1 has been shown to confer protection during hypoxia/reoxygenation[177, 200], but here we demonstrate for the first time how beclin1 expression was regulated during hypoxia and in a clinically relevant model of HS/R. It was previously shown that beclin1 can be degraded by calpain during anoxia/reoxygenation and liver I/R[81], in contrast to being upregulated in our model of hypoxia/reoxygenation and HS/R. This discrepancy may relate to differences in the model, and further suggests that adaptive responses during HS/R are essential to protect the liver from further damage, whereas these adaptive responses may be absent during liver I/R. Beclin1 was previously shown to be cleaved and inactivated by caspase-8[174], but our study shows that during oxidative stress, beclin1 levels are upregulated by caspase-1, an inflammatory caspase, independent of caspase-8.

6.5 DISCUSSION: CASPASE-11-DEPENDENT NON-CANONICAL INFLAMMASOME ACTIVATION

Our previous microarray data showed that caspase-11 (also known as caspase-4) is among the most highly upregulated genes after HS (data not shown). Indeed, we found that caspase-11 protein expression was significantly increased after HS as well as after resuscitation, which suggests that caspase-11 might play a role during HS. Caspase-11 has been shown to mediate macrophage cell death after the infection of gram-negative bacteria[44, 201], but the upregulation of its expression does not seem to affect liver cell death after HS, indicated by our results from strain 129 mice which lack caspase-11[42, 202]. However, due to the strain difference, these results should be further confirmed with caspase-11 [-/-] mice generated on a C57BL/6 background.

Moreover, caspase-11 appears to be dispensable for the maturation of IL-18 after HS, which ruled out its role in caspase-1 activation in immune cells.

Consistent with the results demonstrated by the group of Vishva Dixit[42], we showed that peritoneal macrophages isolated from caspase-1 $^{-/-}$ mice lack both caspase-1 and caspase-11. However, our data also suggest that caspase-1 $^{-/-}$ mice still express caspase-11 in the liver, although at lower levels compared with WT mice. This discrepancy could be due to different expression levels in different cell types. However, the results need to be further confirmed using liver lysates from strain 129 mice as negative controls.

6.6   DISCUSSION: ACTIVATION OF AIM2 AFTER STERILE INJURY AND ITS ROLE IN REGULATING ADAPTIVE RESPONSE
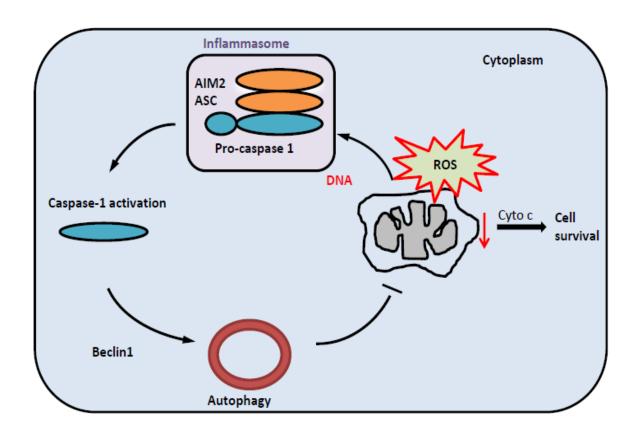
Figure 37: The role of AIM2 activation in regulating cellular adaptive response and cell death.

Here, we demonstrate for the first time that the assembly of AIM2 inflammasome is required for the activation of caspase-1 in hepatocytes after hypoxia-reoxygenation. The role of the AIM2 inflammasome in mediating the maturation of IL-18 and IL-1β has been extensively studied in immune cells after the infection of DNA virus and bacteria such as *Francisella tularensis*[203, 204, 205], *Legionella pneumophila*[206] and *Listeria monocytogenes*[207]. Moreover, evidence is emerging that AIM2 can be activated in the setting of sterile injury. AIM2 inflammasome was shown to mediate IL-1β and IL-18 release triggered by melittin, a component of honey bee venom, and

this may contribute to allergic responses induced by bee stings[208]. Mechanistically, melittin mediates the leakage of mitochondrial DNA into the cytosolic compartment, which can be sensed by AIM2 in keratinocytes. Furthermore, since autoimmune diseases, such as systemic lupus erythematosus, are characterized by increased antibody-DNA complexes derived from the host[209], several groups are actively investigating whether AIM2 is involved in the activation of inflammatory responses in lupus patients[210]. A study by Zhang *et al.* demonstrates that AIM2 facilitates macrophage activation induced by lymphocyte-derived apoptotic DNA[211]. However, much remains unknown about its physiological role in non-immune cells.

We show that AIM2 is hepatoprotective and this is associated with upregulation of beclin1 and mitochondrial clearance, leading to reduced ROS production after redox stress in hepatocytes. Our results shown here are in clear contrast to the detrimental effects of AIM2 in mediating macrophage cell death as suggested by previous studies[182, 212]. However, there is also emerging evidence that AIM2 can also play a protective role by regulating adaptive responses to stress. Panchanathan *et al.* showed that that AIM2 deficiency within immune cells contributes to increased susceptibility to lupus through upregulation of p202, a protein that inhibits AIM2 and caspase-1 activation[210, 213]. A study by Shi *et al.* has shown that the AIM2 inflammasome induces autophagy, which is consistent with what we have shown here[104]. It now seems likely that the formation of the AIM2 inflammasome leads to different effects in different cell types under varying stresses, including cellular protection in the liver under conditions of oxidative stress.

Although AIM2 has only been shown to be activated by dsDNA, it still remains unclear where the cytosolic dsDNA comes from to activate AIM2 in hepatocytes after hypoxia-reoxygenation. It has been well-established that during MPT, the release of mitochondrial

content including mtDNA is considered to be the irreversible point for cells to undergo cell death[214]. Similarly, the release of nuclear DNA into the cytosol has been shown to be associated with apoptotic cell death[215]. Provided that the cytosolic DNA in hepatocytes after hypoxia-reoxygenation is derived from mitochondria or nucleus of the same cells, our study here provides the first evidence that AIM2 activation by cytosolic DNA could initiate an adaptive and protective mechanism against cell death after redox stress. It seems like that the release of a sublethal amount of DNA into the cytosol can lead to the activation of AIM2 and subsequent clearance of mitochondria through mitochondrial autophagy, which can in turn limit the damage of mitochondria and further mtDNA release (Figure 37). Therefore, the pathway here seems to represent the tipping point for hepatocellular cell death. Whereas regulated release of DNA into the cytosol activates adaptive and protective responses after redox stress, high levels of cytosolic DNA that are passively released from mitochondria or nucleus are often associated with cell death.

6.7   DISCUSSION: THE ROLE OF HMGB1 IN MEDIATING INNATE IMMUNE RESPONSE AND AUTOPHAGY

HMGB proteins have been shown to bind to all immunogenic nucleic acids and can function as universal sentinels for nucleic-acid-mediated innate immune responses, including the activation of TLR3, TLR7, and TLR9 by their cognate nucleic acids[183]. Here, our findings establish a previously unrecognized role for HMGB1 in the regulation of AIM2 inflammasome assembly. HMGB1 has been demonstrated to co-localize and associate with TLR9 to mediate the CpG-DNA-induced inflammatory response[216]. Similarly, we show that HMGB1 interacts with AIM2

99

in hepatocytes after hypoxia-reoxygenation *in vitro* as well as HS *in vivo*. Mice lacking HMGB1 in hepatocytes show reduced activation of caspase-1 after HS, suggesting HMGB1 plays an important role in regulating inflammasome activation following redox stress.

In addition to the well-established role of HMGB1 as a cytokine to mediate the pro-inflammatory response[217], it was first known as an essential non-histone nuclear factor important for gene transcription and preserving chromosomal architecture[218]. Recent studies also implicate HMGB1 as a regulator of protective responses such as mitochondrial autophagy. Tang *et al.* have shown that in response to oxidative stress, increased cytosolic HMGB1 expression activates autophagy by binding to beclin1 and disrupting its association of Bcl-2[219, 220]. This HMGB1-mediated upregulation of autophagy serves as a protective mechanism against mitochondrial abnormality through increasing mitochondrial clearance in the settings of cellular stress[221]. Here, our preliminary data suggests that HMGB1 is required for the caspase-1-mediated upregulation of autophagy, which could provide an alternative mechanism for these previous observed effects of HMGB1.

6.8   FUTURE DIRECTIONS
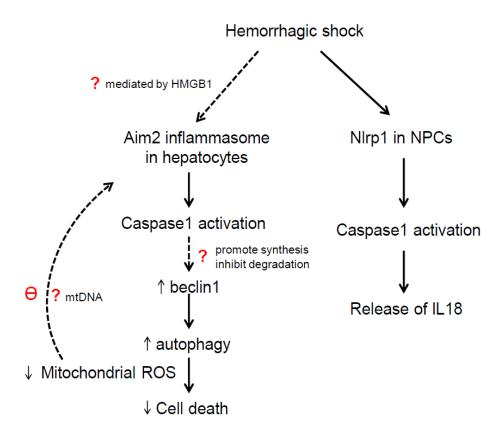
Figure 38: The role of caspase-1 in hepatocytes and immune cells after HS

HS/R induces caspase-1 activation through the formation of AIM2 inflammasome in hepatocytes, which further leads to induction of autophagy through upregulating beclin1 expression. Increased autophagic flux in these cells then clears dysfunctional mitochondria and leads to cell survival. On the other hand, caspase-1 activation was mediated by NLRP1 inflammasome in non-parenchymal cells after HS/R, which is responsible for IL-18 release by these cells. However, questions remain unanswered regarding these pathways: First, what is the mechanism by which caspase-1 regulates beclin1 expression in hepatocytes after redox stress? Second, where does the dsDNA that stimulates AIM2 activation come from? Third, is AIM2 activation in hepatocytes after HS/R mediated by HMGB1?

6.8.1   Regulation of beclin1 expression by caspase-1

Our findings establish a previously unrecognized role for caspase-1 in the regulation of this cell-survival response through the regulation of beclin1 expression. Our results also suggest that caspase-1 regulates mRNA levels of beclin1 as one mechanism for increasing its expression. However, since the changes of beclin1 protein expression after hypoxia are a lot greater than its upregulation at the mRNA level, we hypothesize that caspase-1 also regulates beclin1 expression at the post-transcriptional or post-translational level. Previous studies suggest that beclin1 can be degraded after its ubiquitination and the process is regulated by ubiquitin-specific peptidases[101]. Therefore, we will further explore whether caspase-1 activation affects beclin1 stability. Furthermore, given that caspase-1 is an aspartate-specific cysteine protease, it is reasonable to hypothesize that its substrate might inhibit the degradation of beclin1. To test this hypothesis, we will perform a diagonal gel method to identify the substrates of caspase-1 in hepatocytes after oxidative stress as previously characterized[70]. Although we can recapitulate the results from caspase-1 $^{-/-}$ hepatocytes with caspase-1 inhibitor, more definitive evidence needs to be provided to prove that caspase-1 activity rather than the expression itself is required for its downstream protective effect. To test that hypothesis, we will generate mutant caspase-1 with cysteine-to-serine mutation to abolish the activation of caspase-1.

6.8.2   Characterization of the hepatocyte-specific effect of caspase-1 activation

Our preliminary results using BM chimeric mice suggest that caspase-1 activation in parenchymal cells contributes to liver protection after HS/R. However, an increased stress response was found in the control chimeric mice without HS treatment, indicating that this

chimeric mice model is likely not ideal for studying cell-specific effects in the liver. Therefore, we will perform definitive experiments to investigate the role of individual liver cell types by generating hepatocyte-specific caspase-1$^{-/-}$ mice. To do this, we will make a caspase-1 LoxP construct that can be inserted into C57BL/6 mouse embryos. The resulting caspase-1 LoxP mice will then be further cross-bred with mice expressing cre-recombinase under a hepatocyte-specific promoter, albumin, to produce hepatocyte-specific caspase-1 $^{-/-}$ mice as described before[222].

6.8.3   The source of dsDNA that activates AIM2 inflammasome after redox stress: mitochondria or nuclei?

In this study, we demonstrate for the first time that the AIM2 inflammasome mediates the activation of caspase-1 *in vivo* and *in vitro* after oxidative stress. Since AIM2 has only been shown to be activated by dsDNA derived from either pathogen or host after sterile injury induced by HS, it is to be expected that the dsDNA responsible for AIM2 activation is from mitochondria or nuclei. Although we detected increased dsDNA in the cytosolic fraction of the liver after HS (data not shown), we cannot determine whether it is mitochondrial- or nuclear-derived using quantitative PCR. The reason could be that the method is not sensitive enough. As an alternative, we can transfect hepatocytes with mitochondrial or nuclear DNA to assess whether they can activate AIM2 inflammasome and caspase-1 to similar levels as seen after hypoxia-reoxygenation treatment. Furthermore, we can perform immuno-electron microscopy to investigate the exact cellular location of AIM2.

6.8.4   Interaction between AIM2 and HMGB1

We showed that HMGB1 co-localizes and associates with AIM2 to mediate caspase-1 activation in hepatocytes after redox stress. However, more definitive evidence needs to be provided to prove this novel interaction between AIM2 and HMGB1. One way is to overexpress epitope-tagged AIM2 and HMGB1 plasmid in Human Embryonic Kidney 293 cells. We will perform co-immunoprecipitation to assess the formation of AIM2-HMGB1 complex. We will also utilize Octet platform (Fortebio) to investigate kinetic characterization of AIM2-HMGB1 binding interaction.

6.8.5   The mechanism of HMGB1 release

We have previously shown that HMGB1 can be actively released and act as an early mediator of inflammation and organ damage after liver I/R, in contrast to being passively released from necrotic cells during sepsis[12]. It has been shown that the active release of HMGB1 after moderate oxidative stress is dependent on MAPK and chromosome region maintenance in macrophages[223], and its release potentially plays a protective role in these cells through the initiation of mitochondrial autophagy[219, 221]. Similarly, Evankovich et al. showed that HMGB1 can be actively released from the nucleus after oxidative stress in hepatocytes, which is mediated by decreased histone deacetylase activity[224]. In this study our work demonstrated that HMGB1 plays a protective role in hepatocytes by mediating the activation of AIM2 inflammasome and promoting mitochondrial autophagy through up-regulating beclin1, which is consistent with its protective role in macrophages when actively released[219, 221]. It would be of great interest to

assess whether HMGB1 is actively released in hepatocytes after hypoxia-reoxygenation and whether the process is mediated by a decrease in histone deacetylase activity as shown before.

6.8.6 Summary

Previous studies showed that in cells where autophagy was impaired, enhanced mitochondrial ROS promoted the activation of caspase-1[35, 37]. Our study provides an alternative mechanism of cellular protection in cells that produce little or no IL-1β/IL-18 cytokines, such as hepatocytes. In this scenario, caspase-1 is a central driver of mitochondrial autophagy, and the initiating factors leading to caspase-1 activation likely include DAMPs and ROS. Also, we further extended the story by showing that this activation and protective effect of caspase-1 is triggered by AIM2 inflammasome and this process in mediated by the nuclear protein HMGB1. In our investigations to better understand the function of inflammasome and caspase-1, we were most successful at generating more intriguing questions. Further studies are required to identify the mechanism of how caspase-1 activation upregulates beclin1, as well as provide definitive evidence to show the direct interaction between HMGB1 and AIM2.

REFERENCES

1.   Lemasters JJ, Theruvath TP, Zhong Z, Nieminen AL. Mitochondrial calcium and the permeability transition in cell death. *Biochim Biophys Acta*. 2009;1787:1395-1401

2.   James LP, Mayeux PR, Hinson JA. Acetaminophen-induced hepatotoxicity. *Drug Metab Dispos*. 2003;31:1499-1506

3.   Diesen DL, Kuo PC. Nitric oxide and redox regulation in the liver: Part i. General considerations and redox biology in hepatitis. *J Surg Res*. 2010;162:95-109

4.   Ahmed U, Latham PS, Oates PS. Interactions between hepatic iron and lipid metabolism with possible relevance to steatohepatitis. *World J Gastroentero*. 2012;18:4651-4658

5.   Chen GY, Nunez G. Sterile inflammation: Sensing and reacting to damage. *Nat Rev Immunol*. 2010;10:826-837

6.   Areschoug T, Gordon S. Pattern recognition receptors and their role in innate immunity: Focus on microbial protein ligands. *Contrib Microbiol*. 2008;15:45-60

7.   Gurcel L, Abrami L, Girardin S, Tschopp J, van der Goot FG. Caspase-1 activation of lipid metabolic pathways in response to bacterial pore-forming toxins promotes cell survival. *Cell*. 2006;126:1135-1145

8.   DeMaria EJ, Pellicane JV, Lee RB. Hemorrhagic shock in endotoxin-resistant mice: Improved survival unrelated to deficient production of tumor necrosis factor. *J Trauma*. 1993;35:720-724; discussion 724-725

9.   Chen LW, Chang WJ, Chen PH, Liu WC, Hsu CM. Tlr ligand decreases mesenteric ischemia and reperfusion injury-induced gut damage through tnf-alpha signaling. *Shock*. 2008;30:563-570

10. Zhai Y, Shen XD, O'Connell R, Gao F, Lassman C, Busuttil RW, Cheng G, Kupiec-Weglinski JW. Cutting edge: Tlr4 activation mediates liver ischemia/reperfusion inflammatory response via ifn regulatory factor 3-dependent myd88-independent pathway. *J Immunol*. 2004;173:7115-7119

11. Oka T, Hikoso S, Yamaguchi O, Taneike M, Takeda T, Tamai T, Oyabu J, Murakawa T, Nakayama H, Nishida K, Akira S, Yamamoto A, Komuro I, Otsu K. Mitochondrial DNA that escapes from autophagy causes inflammation and heart failure (vol 485, pg 251, 2012). *Nature*. 2012;490:292-292

12. Tsung A, Sahai R, Tanaka H, Nakao A, Fink MP, Lotze MT, Yang H, Li J, Tracey KJ, Geller DA, Billiar TR. The nuclear factor hmgb1 mediates hepatic injury after murine liver ischemia-reperfusion. *J Exp Med*. 2005;201:1135-1143

13. Tsung A, Klune JR, Zhang X, Jeyabalan G, Cao Z, Peng X, Stolz DB, Geller DA, Rosengart MR, Billiar TR. Hmgb1 release induced by liver ischemia involves toll-like receptor 4 dependent reactive oxygen species production and calcium-mediated signaling. *J Exp Med*. 2007;204:2913-2923

14.   Mariathasan S, Weiss DS, Newton K, McBride J, O'Rourke K, Roose-Girma M, Lee WP, Weinrauch Y, Monack DM, Dixit VM. Cryopyrin activates the inflammasome in response to toxins and atp. *Nature*. 2006;440:228-232

15.   Halle A, Hornung V, Petzold GC, Stewart CR, Monks BG, Reinheckel T, Fitzgerald KA, Latz E, Moore KJ, Golenbock DT. The nalp3 inflammasome is involved in the innate immune response to amyloid-beta. *Nat Immunol*. 2008;9:857-865

16.   Martinon F, Petrilli V, Mayor A, Tardivel A, Tschopp J. Gout-associated uric acid crystals activate the nalp3 inflammasome. *Nature*. 2006;440:237-241

17.   Griffith JW, Sun T, McIntosh MT, Bucala R. Pure hemozoin is inflammatory in vivo and activates the nalp3 inflammasome via release of uric acid. *J Immunol*. 2009;183:5208-5220

18.   Zhou R, Tardivel A, Thorens B, Choi I, Tschopp J. Thioredoxin-interacting protein links oxidative stress to inflammasome activation. *Nat Immunol*. 2010;11:136-140

19.   Yamasaki K, Muto J, Taylor KR, Cogen AL, Audish D, Bertin J, Grant EP, Coyle AJ, Misaghi A, Hoffman HM, Gallo RL. Nlrp3/cryopyrin is necessary for interleukin-1beta (il-1beta) release in response to hyaluronan, an endogenous trigger of inflammation in response to injury. *J Biol Chem*. 2009;284:12762-12771

20.   Davis BK, Wen H, Ting JP. The inflammasome nlrs in immunity, inflammation, and associated diseases. *Annu Rev Immunol*. 2011;29:707-735

21.   Schroder K, Tschopp J. The inflammasomes. *Cell*. 2010;140:821-832

22.   Troseid M, Seljeflot I, Arnesen H. The role of interleukin-18 in the metabolic syndrome. *Cardiovasc Diabetol*. 2010;9:11

23.   Takeuchi D, Yoshidome H, Kato A, Ito H, Kimura F, Shimizu H, Ohtsuka M, Morita Y, Miyazaki M. Interleukin 18 causes hepatic ischemia/reperfusion injury by suppressing anti-inflammatory cytokine expression in mice. *Hepatology*. 2004;39:699-710

24.   Hung J, McQuillan BM, Chapman CM, Thompson PL, Beilby JP. Elevated interleukin-18 levels are associated with the metabolic syndrome independent of obesity and insulin resistance. *Arterioscler Thromb Vasc Biol*. 2005;25:1268-1273

25.   Bruun JM, Stallknecht B, Helge JW, Richelsen B. Interleukin-18 in plasma and adipose tissue: Effects of obesity, insulin resistance, and weight loss. *Eur J Endocrinol*. 2007;157:465-471

26.   Sekine K, Fujishima S, Sasaki J, Ishizaka A, Aiso S, Aikawa N. In vivo il-18 supplementation ameliorates lethal acute lung injury in burn-primed endotoxemic mice: A novel anti-inflammatory role of il-18. *Shock*. 2009;32:554-562

27.   Arend WP, Palmer G, Gabay C. Il-1, il-18, and il-33 families of cytokines. *Immunol Rev*. 2008;223:20-38

28.   Fukumoto J, Fukumoto I, Parthasarathy PT, Cox R, Huynh B, Ramanathan GK, Venugopal RB, Allen-Gipson DS, Lockey RF, Kolliputi N. Nlrp3 deletion protects from hyperoxia-induced acute lung injury. *Am J Physiol Cell Physiol*. 2013

29.   Codolo G, Plotegher N, Pozzobon T, Brucale M, Tessari I, Bubacco L, de Bernard M. Triggering of inflammasome by aggregated alpha-synuclein, an inflammatory response in synucleinopathies. *PLoS One*. 2013;8:e55375

30.   Freeman D, Cedillos R, Choyke S, Lukic Z, McGuire K, Marvin S, Burrage AM, Sudholt S, Rana A, O'Connor C, Wiethoff CM, Campbell EM. Alpha-synuclein induces lysosomal rupture and cathepsin dependent reactive oxygen species following endocytosis. *PLoS One*. 2013;8:e62143

31. Shin MS, Kang Y, Lee N, Wahl ER, Kim SH, Kang KS, Lazova R, Kang I. Self double-stranded (ds)DNA induces il-1beta production from human monocytes by activating nlrp3 inflammasome in the presence of anti-dsdna antibodies. *J Immunol*. 2013;190:1407-1415

32. Amaral FA, Costa VV, Tavares LD, Sachs D, Coelho FM, Fagundes CT, Soriani FM, Silveira TN, Cunha LD, Zamboni DS, Quesniaux V, Peres RS, Cunha TM, Cunha FQ, Ryffel B, Souza DG, Teixeira MM. Nlrp3 inflammasome-mediated neutrophil recruitment and hypernociception depend on leukotriene b(4) in a murine model of gout. *Arthritis Rheum*. 2012;64:474-484

33. Jin C, Frayssinet P, Pelker R, Cwirka D, Hu B, Vignery A, Eisenbarth SC, Flavell RA. Nlrp3 inflammasome plays a critical role in the pathogenesis of hydroxyapatite-associated arthropathy. *Proc Natl Acad Sci U S A*. 2011;108:14867-14872

34. Gross O, Thomas CJ, Guarda G, Tschopp J. The inflammasome: An integrated view. *Immunol Rev*. 2011;243:136-151

35. Zhou R, Yazdi AS, Menu P, Tschopp J. A role for mitochondria in nlrp3 inflammasome activation. *Nature*. 2011;469:221-225

36. Green DR, Galluzzi L, Kroemer G. Mitochondria and the autophagy-inflammation-cell death axis in organismal aging. *Science*. 2011;333:1109-1112

37. Nakahira K, Haspel JA, Rathinam VA, Lee SJ, Dolinay T, Lam HC, Englert JA, Rabinovitch M, Cernadas M, Kim HP, Fitzgerald KA, Ryter SW, Choi AM. Autophagy proteins regulate innate immune responses by inhibiting the release of mitochondrial DNA mediated by the nalp3 inflammasome. *Nat Immunol*. 2011;12:222-230

38. Saitoh T, Fujita N, Jang MH, Uematsu S, Yang BG, Satoh T, Omori H, Noda T, Yamamoto N, Komatsu M, Tanaka K, Kawai T, Tsujimura T, Takeuchi O, Yoshimori T, Akira S. Loss of the autophagy protein atg16l1 enhances endotoxin-induced il-1beta production. *Nature*. 2008;456:264-268

39. Shimada K, Crother TR, Karlin J, Dagvadorj J, Chiba N, Chen S, Ramanujan VK, Wolf AJ, Vergnes L, Ojcius DM, Rentsendorj A, Vargas M, Guerrero C, Wang Y, Fitzgerald KA, Underhill DM, Town T, Arditi M. Oxidized mitochondrial DNA activates the nlrp3 inflammasome during apoptosis. *Immunity*. 2012;36:401-414

40. Bours MJ, Dagnelie PC, Giuliani AL, Wesselius A, Di Virgilio F. P2 receptors and extracellular atp: A novel homeostatic pathway in inflammation. *Front Biosci (Schol Ed)*. 2011;3:1443-1456

41. Wang S, Miura M, Jung YK, Zhu H, Li E, Yuan J. Murine caspase-11, an ice-interacting protease, is essential for the activation of ice. *Cell*. 1998;92:501-509

42. Kayagaki N, Warming S, Lamkanfi M, Vande Walle L, Louie S, Dong J, Newton K, Qu Y, Liu J, Heldens S, Zhang J, Lee WP, Roose-Girma M, Dixit VM. Non-canonical inflammasome activation targets caspase-11. *Nature*. 2011;479:117-121

43. Aachoui Y, Leaf IA, Hagar JA, Fontana MF, Campos CG, Zak DE, Tan MH, Cotter PA, Vance RE, Aderem A, Miao EA. Caspase-11 protects against bacteria that escape the vacuole. *Science*. 2013;339:975-978

44. Rathinam VA, Vanaja SK, Waggoner L, Sokolovska A, Becker C, Stuart LM, Leong JM, Fitzgerald KA. Trif licenses caspase-11-dependent nlrp3 inflammasome activation by gram-negative bacteria. *Cell*. 2012;150:606-619

45. Yazdi AS, Drexler SK, Tschopp J. The role of the inflammasome in nonmyeloid cells. *J Clin Immunol*. 2010;30:623-627

46.   Craven RR, Gao X, Allen IC, Gris D, Bubeck Wardenburg J, McElvania-Tekippe E, Ting JP, Duncan JA. Staphylococcus aureus alpha-hemolysin activates the nlrp3-inflammasome in human and mouse monocytic cells. *PLoS One*. 2009;4:e7446

47.   Lightfield KL, Persson J, Brubaker SW, Witte CE, von Moltke J, Dunipace EA, Henry T, Sun YH, Cado D, Dietrich WF, Monack DM, Tsolis RM, Vance RE. Critical function for naip5 in inflammasome activation by a conserved carboxy-terminal domain of flagellin. *Nat Immunol*. 2008;9:1171-1178

48.   Fink SL, Cookson BT. Caspase-1-dependent pore formation during pyroptosis leads to osmotic lysis of infected host macrophages. *Cell Microbiol*. 2006;8:1812-1825

49.   Hersh D, Monack DM, Smith MR, Ghori N, Falkow S, Zychlinsky A. The salmonella invasin sipb induces macrophage apoptosis by binding to caspase-1. *Proc Natl Acad Sci U S A*. 1999;96:2396-2401

50.   Fernandes-Alnemri T, Yu JW, Datta P, Wu J, Alnemri ES. Aim2 activates the inflammasome and cell death in response to cytoplasmic DNA. *Nature*. 2009;458:509-513

51.   Zhang WH, Wang X, Narayanan M, Zhang Y, Huo C, Reed JC, Friedlander RM. Fundamental role of the rip2/caspase-1 pathway in hypoxia and ischemia-induced neuronal cell death. *Proc Natl Acad Sci U S A*. 2003;100:16012-16017

52.   Liu XH, Kwon D, Schielke GP, Yang GY, Silverstein FS, Barks JD. Mice deficient in interleukin-1 converting enzyme are resistant to neonatal hypoxic-ischemic brain damage. *J Cereb Blood Flow Metab*. 1999;19:1099-1108

53.   Emsley HC, Smith CJ, Georgiou RF, Vail A, Hopkins SJ, Rothwell NJ, Tyrrell PJ. A randomised phase ii study of interleukin-1 receptor antagonist in acute stroke patients. *J Neurol Neurosurg Psychiatry*. 2005;76:1366-1372

54.   Guo H, Petrin D, Zhang Y, Bergeron C, Goodyer CG, LeBlanc AC. Caspase-1 activation of caspase-6 in human apoptotic neurons. *Cell Death Differ*. 2006;13:285-292

55.   Mezzaroma E, Toldo S, Farkas D, Seropian IM, Van Tassell BW, Salloum FN, Kannan HR, Menna AC, Voelkel NF, Abbate A. The inflammasome promotes adverse cardiac remodeling following acute myocardial infarction in the mouse. *Proc Natl Acad Sci U S A*. 2011;108:19725-19730

56.   Syed FM, Hahn HS, Odley A, Guo Y, Vallejo JG, Lynch RA, Mann DL, Bolli R, Dorn GW, 2nd. Proapoptotic effects of caspase-1/interleukin-converting enzyme dominate in myocardial ischemia. *Circ Res*. 2005;96:1103-1109

57.   Squires RC, Muehlbauer SM, Brojatsch J. Proteasomes control caspase-1 activation in anthrax lethal toxin-mediated cell killing. *J Biol Chem*. 2007;282:34260-34267

58.   Motani K, Kushiyama H, Imamura R, Kinoshita T, Nishiuchi T, Suda T. Caspase-1 protein induces apoptosis-associated speck-like protein containing a caspase recruitment domain (asc)-mediated necrosis independently of its catalytic activity. *J Biol Chem*. 2011;286:33963-33972

59.   Kelk P, Johansson A, Claesson R, Hanstrom L, Kalfas S. Caspase 1 involvement in human monocyte lysis induced by actinobacillus actinomycetemcomitans leukotoxin. *Infect Immun*. 2003;71:4448-4455

60.   Keller M, Ruegg A, Werner S, Beer HD. Active caspase-1 is a regulator of unconventional protein secretion. *Cell*. 2008;132:818-831

61.   Kim MJ, Yoo JY. Active caspase-1-mediated secretion of retinoic acid inducible gene-i. *J Immunol*. 2008;181:7324-7331

62. Gross O, Yazdi AS, Thomas CJ, Masin M, Heinz LX, Guarda G, Quadroni M, Drexler SK, Tschopp J. Inflammasome activators induce interleukin-1alpha secretion via distinct pathways with differential requirement for the protease function of caspase-1. *Immunity*. 2012;36:388-400

63. Qu Y, Franchi L, Nunez G, Dubyak GR. Nonclassical il-1 beta secretion stimulated by p2x7 receptors is dependent on inflammasome activation and correlated with exosome release in murine macrophages. *Journal of Immunology*. 2007;179:1913-1925

64. Rubartelli A, Cozzolino F, Talio M, Sitia R. A novel secretory pathway for interleukin-1 beta, a protein lacking a signal sequence. *EMBO J*. 1990;9:1503-1510

65. Lee P, Lee DJ, Chan C, Chen SW, Ch'en I, Jamora C. Dynamic expression of epidermal caspase 8 simulates a wound healing response. *Nature*. 2009;458:519-523

66. Chen CJ, Kono H, Golenbock D, Reed G, Akira S, Rock KL. Identification of a key pathway required for the sterile inflammatory response triggered by dying cells. *Nat Med*. 2007;13:851-856

67. Carruth LM, Demczuk S, Mizel SB. Involvement of a calpain-like protease in the processing of the murine interleukin 1 alpha precursor. *J Biol Chem*. 1991;266:12162-12167

68. Takahasi K, Yoneyama M, Nishihori T, Hirai R, Kumeta H, Narita R, Gale M, Jr., Inagaki F, Fujita T. Nonself rna-sensing mechanism of rig-i helicase and activation of antiviral immune responses. *Mol Cell*. 2008;29:428-440

69. Seth RB, Sun LJ, Ea CK, Chen ZJJ. Identification and characterization of mavs, a mitochondrial antiviral signaling protein that activates nf-kappa b and irf3. *Cell*. 2005;122:669-682

70. Shao W, Yeretssian G, Doiron K, Hussain SN, Saleh M. The caspase-1 digestome identifies the glycolysis pathway as a target during infection and septic shock. *J Biol Chem*. 2007;282:36321-36329

71. Chae JJ, Wood G, Richard K, Jaffe H, Colburn NT, Masters SL, Gumucio DL, Shoham NG, Kastner DL. The familial mediterranean fever protein, pyrin, is cleaved by caspase-1 and activates nf-kappa b through its n-terminal fragment. *Blood*. 2008;112:1794-1803

72. Chalkiadaki A, Guarente L. High-fat diet triggers inflammation-induced cleavage of sirt1 in adipose tissue to promote metabolic dysfunction. *Cell Metab*. 2012;16:180-188

73. Yu CY, Chiang RL, Chang TH, Liao CL, Lin YL. The interferon stimulator mitochondrial antiviral signaling protein facilitates cell death by disrupting the mitochondrial membrane potential and by activating caspases. *J Virol*. 2010;84:2421-2431

74. Lewis JS, Lee JA, Underwood JC, Harris AL, Lewis CE. Macrophage responses to hypoxia: Relevance to disease mechanisms. *J Leukoc Biol*. 1999;66:889-900

75. Biason-Lauber A, Boni-Schnetzler M, Hubbard BP, Bouzakri K, Brunner A, Cavelti-Weder C, Keller C, Meyer-Boni M, Meier DT, Brorsson C, Timper K, Leibowitz G, Patrignani A, Bruggmann R, Boily G, Zulewski H, Geier A, Cermak JM, Elliott P, Ellis JL, Westphal C, Knobel U, Eloranta JJ, Kerr-Conte J, Pattou F, Konrad D, Matter CM, Fontana A, Rogler G, Schlapbach R, Regairaz C, Carballido JM, Glaser B, McBurney MW, Pociot F, Sinclair DA, Donath MY. Identification of a sirt1 mutation in a family with type 1 diabetes. *Cell Metab*. 2013;17:448-455

76. Sun C, Zhang F, Ge X, Yan T, Chen X, Shi X, Zhai Q. Sirt1 improves insulin sensitivity under insulin-resistant conditions by repressing ptp1b. *Cell Metab*. 2007;6:307-319

77.   Stienstra R, Joosten LA, Koenen T, van Tits B, van Diepen JA, van den Berg SA, Rensen PC, Voshol PJ, Fantuzzi G, Hijmans A, Kersten S, Muller M, van den Berg WB, van Rooijen N, Wabitsch M, Kullberg BJ, van der Meer JW, Kanneganti T, Tack CJ, Netea MG. The inflammasome-mediated caspase-1 activation controls adipocyte differentiation and insulin sensitivity. *Cell Metab*. 2010;12:593-605

78.   Luzio JP, Pryor PR, Bright NA. Lysosomes: Fusion and function. *Nat Rev Mol Cell Biol*. 2007;8:622-632

79.   Amer A, Franchi L, Kanneganti TD, Body-Malapel M, Ozoren N, Brady G, Meshinchi S, Jagirdar R, Gewirtz A, Akira S, Nunez G. Regulation of legionella phagosome maturation and infection through flagellin and host ipaf. *J Biol Chem*. 2006;281:35217-35223

80.   Bergsbaken T, Fink SL, den Hartigh AB, Loomis WP, Cookson BT. Coordinated host responses during pyroptosis: Caspase-1-dependent lysosome exocytosis and inflammatory cytokine maturation. *J Immunol*. 2011;187:2748-2754

81.   Kim JS, Nitta T, Mohuczy D, O'Malley KA, Moldawer LL, Dunn WA, Jr., Behrns KE. Impaired autophagy: A mechanism of mitochondrial dysfunction in anoxic rat hepatocytes. *Hepatology*. 2008;47:1725-1736

82.   Klionsky DJ, Emr SD. Cell biology - autophagy as a regulated pathway of cellular degradation. *Science*. 2000;290:1717-1721

83.   Semenza GL. Hif-1: Upstream and downstream of cancer metabolism. *Curr Opin Genet Dev*. 2010;20:51-56

84.   Huang J, Canadien V, Lam GY, Steinberg BE, Dinauer MC, Magalhaes MA, Glogauer M, Grinstein S, Brumell JH. Activation of antibacterial autophagy by nadph oxidases. *Proc Natl Acad Sci U S A*. 2009;106:6226-6231

85.   Gutierrez MG, Master SS, Singh SB, Taylor GA, Colombo MI, Deretic V. Autophagy is a defense mechanism inhibiting bcg and mycobacterium tuberculosis survival in infected macrophages. *Cell*. 2004;119:753-766

86.   Zhao YO, Khaminets A, Hunn JP, Howard JC. Disruption of the toxoplasma gondii parasitophorous vacuole by ifngamma-inducible immunity-related gtpases (irg proteins) triggers necrotic cell death. *PLoS Pathog*. 2009;5:e1000288

87.   He Y, Wan S, Hua Y, Keep RF, Xi G. Autophagy after experimental intracerebral hemorrhage. *J Cereb Blood Flow Metab*. 2008;28:897-905

88.   Cardinal J, Pan PH, Dhupar R, Ross M, Nakao A, Lotze M, Billiar T, Geller D, Tsung A. Cisplatin prevents high mobility group box 1 release and is protective in a murine model of hepatic ischemia/reperfusion injury. *Hepatology*. 2009;50:565-574

89.   Band M, Joel A, Hernandez A, Avivi A. Hypoxia-induced bnip3 expression and mitophagy: In vivo comparison of the rat and the hypoxia-tolerant mole rat, spalax ehrenbergi. *Faseb J*. 2009;23:2327-2335

90.   Gustafsson AB, Gottlieb RA. Autophagy in ischemic heart disease. *Circ Res*. 2009;104:150-158

91.   Hamacher-Brady A, Brady NR, Gottlieb RA. Enhancing macroautophagy protects against ischemia/reperfusion injury in cardiac myocytes. *J Biol Chem*. 2006;281:29776-29787

92.   Abrahamsen H, Stenmark H, Platta HW. Ubiquitination and phosphorylation of beclin 1 and its binding partners: Tuning class iii phosphatidylinositol 3-kinase activity and tumor suppression. *FEBS Lett*. 2012;586:1584-1591

93.   Kiyono K, Suzuki HI, Matsuyama H, Morishita Y, Komuro A, Kano MR, Sugimoto K, Miyazono K. Autophagy is activated by tgf-beta and potentiates tgf-beta-mediated growth inhibition in human hepatocellular carcinoma cells. *Cancer Res*. 2009;69:8844-8852

94.   Shrivastava S, Chowdhury JB, Steele R, Ray R, Ray RB. Hepatitis c virus upregulates beclin1 for induction of autophagy and activates mtor signaling. *J Virol*. 2012;86:8705-8712

95.   Jiang QA, Wang YH, Li TJ, Shi KJ, Li ZS, Ma YS, Li F, Luo H, Yang Y, Xu CM. Heat shock protein 90-mediated inactivation of nuclear factor-kappa b switches autophagy to apoptosis through becn1 transcriptional inhibition in selenite-induced nb4 cells. *Mol Biol Cell*. 2011;22:1167-1180

96.   Pattingre S, Tassa A, Qu X, Garuti R, Liang XH, Mizushima N, Packer M, Schneider MD, Levine B. Bcl-2 antiapoptotic proteins inhibit beclin 1-dependent autophagy. *Cell*. 2005;122:927-939

97.   Liang C, Lee JS, Inn KS, Gack MU, Li Q, Roberts EA, Vergne I, Deretic V, Feng P, Akazawa C, Jung JU. Beclin1-binding uvrag targets the class c vps complex to coordinate autophagosome maturation and endocytic trafficking. *Nat Cell Biol*. 2008;10:776-787

98.   Fimia GM, Stoykova A, Romagnoli A, Giunta L, Di Bartolomeo S, Nardacci R, Corazzari M, Fuoco C, Ucar A, Schwartz P, Gruss P, Piacentini M, Chowdhury K, Cecconi F. Ambra1 regulates autophagy and development of the nervous system. *Nature*. 2007;447:1121-1125

99.   Zhong Y, Wang QJ, Li X, Yan Y, Backer JM, Chait BT, Heintz N, Yue Z. Distinct regulation of autophagic activity by atg14l and rubicon associated with beclin 1-phosphatidylinositol-3-kinase complex. *Nat Cell Biol*. 2009;11:468-476

100.   Platta HW, Abrahamsen H, Thoresen SB, Stenmark H. Nedd4-dependent lysine-11-linked polyubiquitination of the tumour suppressor beclin 1. *Biochem J*. 2012;441:399-406

101.   Liu J, Xia H, Kim M, Xu L, Li Y, Zhang L, Cai Y, Norberg HV, Zhang T, Furuya T, Jin M, Zhu Z, Wang H, Yu J, Hao Y, Choi A, Ke H, Ma D, Yuan J. Beclin1 controls the levels of p53 by regulating the deubiquitination activity of usp10 and usp13. *Cell*. 2011;147:223-234

102.   Xu C, Liu J, Hsu LC, Luo Y, Xiang R, Chuang TH. Functional interaction of heat shock protein 90 and beclin 1 modulates toll-like receptor-mediated autophagy. *Faseb J*. 2011;25:2700-2710

103.   Suzuki T, Franchi L, Toma C, Ashida H, Ogawa M, Yoshikawa Y, Mimuro H, Inohara N, Sasakawa C, Nunez G. Differential regulation of caspase-1 activation, pyroptosis, and autophagy via ipaf and asc in shigella-infected macrophages. *PLoS Pathog*. 2007;3:e111

104.   Shi CS, Shenderov K, Huang NN, Kabat J, Abu-Asab M, Fitzgerald KA, Sher A, Kehrl JH. Activation of autophagy by inflammatory signals limits il-1beta production by targeting ubiquitinated inflammasomes for destruction. *Nat Immunol*. 2012;13:255-263

105.   Bodemann BO, Orvedahl A, Cheng T, Ram RR, Ou YH, Formstecher E, Maiti M, Hazelett CC, Wauson EM, Balakireva M, Camonis JH, Yeaman C, Levine B, White MA. Ralb and the exocyst mediate the cellular starvation response by direct activation of autophagosome assembly. *Cell*. 2011;144:253-267

106. Piantadosi CA, Suliman HB. Transcriptional control of mitochondrial biogenesis and its interface with inflammatory processes. *Biochim Biophys Acta*. 2012;1820:532-541

107. Pagliaro P, Moro F, Tullio F, Perrelli MG, Penna C. Cardioprotective pathways during reperfusion: Focus on redox signaling and other modalities of cell signaling. *Antioxid Redox Signal*. 2011;14:833-850

108. Finkel T. Signal transduction by mitochondrial oxidants. *J Biol Chem*. 2012;287:4434-4440

109. Halle A, Hornung V, Petzold GC, Stewart CR, Monks BG, Reinheckel T, Fitzgerald KA, Latz E, Moore KJ, Golenbock DT. The nalp3 inflammasome is involved in the innate immune response to amyloid-beta. *Nature Immunology*. 2008;9:857-865

110. Zhou RB, Tardivel A, Thorens B, Choi I, Tschopp J. Thioredoxin-interacting protein links oxidative stress to inflammasome activation. *Nature Immunology*. 2010;11:136-U151

111. Yamasaki K, Muto J, Taylor KR, Cogen AL, Audish D, Bertin J, Grant EP, Coyle AJ, Misaghi A, Hoffman HM, Gallo RL. Nlrp3/cryopyrin is necessary for interleukin-1 beta (il-1 beta) release in response to hyaluronan, an endogenous trigger of inflammation in response to injury. *Journal of Biological Chemistry*. 2009;284:12762-12771

112. Cassel SL, Eisenbarth SC, Iyer SS, Sadler JJ, Colegio OR, Tephly LA, Carter AB, Rothman PB, Flavell RA, Sutterwala FS. The nalp3 inflammasome is essential for the development of silicosis. *P Natl Acad Sci USA*. 2008;105:9035-9040

113. Dostert C, Petrilli V, Van Bruggen R, Steele C, Mossman BT, Tschopp J. Innate immune activation through nalp3 inflammasome sensing of asbestos and silica. *Science*. 2008;320:674-677

114. Rathinam VAK, Jiang ZZ, Waggoner SN, Sharma S, Cole LE, Waggoner L, Vanaja SK, Monks BG, Ganesan S, Latz E, Hornung V, Vogel SN, Szomolanyi-Tsuda E, Fitzgerald KA. The aim2 inflammasome is essential for host defense against cytosolic bacteria and DNA viruses. *Nature Immunology*. 2010;11:395-403

115. Bulua AC, Simon A, Maddipati R, Pelletier M, Park H, Kim KY, Sack MN, Kastner DL, Siegel RM. Mitochondrial reactive oxygen species promote production of proinflammatory cytokines and are elevated in tnfr1-associated periodic syndrome (traps). *J Exp Med*. 2011;208:519-533

116. Morgan MJ, Liu ZG. Crosstalk of reactive oxygen species and nf-kappab signaling. *Cell Res*. 2011;21:103-115

117. Naik E, Dixit VM. Mitochondrial reactive oxygen species drive proinflammatory cytokine production. *J Exp Med*. 2011;208:417-420

118. Imbert V, Rupec RA, Livolsi A, Pahl HL, Traenckner EB, Mueller-Dieckmann C, Farahifar D, Rossi B, Auberger P, Baeuerle PA, Peyron JF. Tyrosine phosphorylation of i kappa b-alpha activates nf-kappa b without proteolytic degradation of i kappa b-alpha. *Cell*. 1996;86:787-798

119. Fan C, Li Q, Ross D, Engelhardt JF. Tyrosine phosphorylation of i kappa b alpha activates nf kappa b through a redox-regulated and c-src-dependent mechanism following hypoxia/reoxygenation. *J Biol Chem*. 2003;278:2072-2080

120. Galluzzi L, Kroemer G. Necroptosis: A specialized pathway of programmed necrosis. *Cell*. 2008;135:1161-1163

121. Lim SY, Davidson SM, Hausenloy DJ, Yellon DM. Preconditioning and postconditioning: The essential role of the mitochondrial dc permeability transition pore. *Cardiovasc Res*. 2007;75:530-535

122. Kim JS, He L, Lemasters JJ. Mitochondrial permeability transition: A common pathway to necrosis and apoptosis. *Biochem Biophys Res Commun*. 2003;304:463-470

123. Lee HC, Wei YH. Mitochondrial biogenesis and mitochondrial DNA maintenance of mammalian cells under oxidative stress. *Int J Biochem Cell Biol*. 2005;37:822-834

124. Fernandez-Marcos PJ, Auwerx J. Regulation of pgc-1alpha, a nodal regulator of mitochondrial biogenesis. *Am J Clin Nutr*. 2011;93:884S-890

125. Liang H, Ward WF. Pgc-1alpha: A key regulator of energy metabolism. *Adv Physiol Educ*. 2006;30:145-151

126. Saxena S, Shukla D, Bansal A. Augmentation of aerobic respiration and mitochondrial biogenesis in skeletal muscle by hypoxia preconditioning with cobalt chloride. *Toxicol Appl Pharmacol*. 2012;264:324-334

127. Ramjiawan A, Bagchi RA, Blant A, Albak L, Cavasin MA, Horn TR, McKinsey TA, Czubryt MP. Roles of histone deacetylation and amp kinase in regulation of cardiomyocyte pgc-1alpha gene expression in hypoxia. *Am J Physiol Cell Physiol*. 2013

128. Valle I, Alvarez-Barrientos A, Arza E, Lamas S, Monsalve M. Pgc-1alpha regulates the mitochondrial antioxidant defense system in vascular endothelial cells. *Cardiovasc Res*. 2005;66:562-573

129. Dewar D, Moore FA, Moore EE, Balogh Z. Postinjury multiple organ failure. *Injury*. 2009;40:912-918

130. Lichtman SN, Lemasters JJ. Role of cytokines and cytokine-producing cells in reperfusion injury to the liver. *Semin Liver Dis*. 1999;19:171-187

131. Helling TS. The liver and hemorrhagic shock. *J Am Coll Surg*. 2005;201:774-783

132. Glantzounis GK, Salacinski HJ, Yang WX, Davidson BR, Seifalian AM. The contemporary role of antioxidant therapy in attenuating liver ischemia-reperfusion injury: A review. *Liver Transplant*. 2005;11:1031-1047

133. Jaeschke H, Lemasters JJ. Apoptosis versus oncotic necrosis in hepatic ischemia/reperfusion injury. *Gastroenterology*. 2003;125:1246-1257

134. van Golen RF, van Gulik TM, Heger M. The sterile immune response during hepatic ischemia/reperfusion. *Cytokine Growth F R*. 2012;23:69-84

135. Burwell LS, Nadtochiy SM, Brookes PS. Cardioprotection by metabolic shut-down and gradual wake-up. *J Mol Cell Cardiol*. 2009;46:804-810

136. Malhi H, Gores GJ, Lemasters JJ. Apoptosis and necrosis in the liver: A tale of two deaths? *Hepatology*. 2006;43:S31-44

137. Kim JS, Qian T, Lemasters JJ. Mitochondrial permeability transition in the switch from necrotic to apoptotic cell death in ischemic rat hepatocytes. *Gastroenterology*. 2003;124:494-503

138. Jaeschke H. Molecular mechanisms of hepatic ischemia-reperfusion injury and preconditioning. *Am J Physiol Gastrointest Liver Physiol*. 2003;284:G15-26

139. Shokolenko I, Venediktova N, Bochkareva A, Wilson GL, Alexeyev MF. Oxidative stress induces degradation of mitochondrial DNA. *Nucleic Acids Res*. 2009;37:2539-2548

140. Berndt C, Lillig CH, Holmgren A. Thiol-based mechanisms of the thioredoxin and glutaredoxin systems: Implications for diseases in the cardiovascular system. *Am J Physiol Heart Circ Physiol*. 2007;292:H1227-1236

141. Zuo Y, Xiang B, Yang J, Sun X, Wang Y, Cang H, Yi J. Oxidative modification of caspase-9 facilitates its activation via disulfide-mediated interaction with apaf-1. *Cell Res*. 2009;19:449-457

142. Gill R, Tsung A, Billiar T. Linking oxidative stress to inflammation: Toll-like receptors. *Free Radic Biol Med*. 2010;48:1121-1132

143. Prince JM, Levy RM, Yang R, Mollen KP, Fink MP, Vodovotz Y, Billiar TR. Toll-like receptor-4 signaling mediates hepatic injury and systemic inflammation in hemorrhagic shock. *J Am Coll Surg*. 2006;202:407-417

144. Meng X, Ao L, Song Y, Raeburn CD, Fullerton DA, Harken AH. Signaling for myocardial depression in hemorrhagic shock: Roles of toll-like receptor 4 and p55 tnf-alpha receptor. *Am J Physiol Regul Integr Comp Physiol*. 2005;288:R600-606

145. Liu Y, Yuan Y, Li Y, Zhang J, Xiao G, Vodovotz Y, Billiar TR, Wilson MA, Fan J. Interacting neuroendocrine and innate and acquired immune pathways regulate neutrophil mobilization from bone marrow following hemorrhagic shock. *J Immunol*. 2009;182:572-580

146. Mollen KP, Levy RM, Prince JM, Hoffman RA, Scott MJ, Kaczorowski DJ, Vallabhaneni R, Vodovotz Y, Billiar TR. Systemic inflammation and end organ damage following trauma involves functional tlr4 signaling in both bone marrow-derived cells and parenchymal cells. *J Leukoc Biol*. 2008;83:80-88

147. Pomerantz BJ, Reznikov LL, Harken AH, Dinarello CA. Inhibition of caspase 1 reduces human myocardial ischemic dysfunction via inhibition of il-18 and il-1beta. *Proc Natl Acad Sci U S A*. 2001;98:2871-2876

148. Melnikov VY, Ecder T, Fantuzzi G, Siegmund B, Lucia MS, Dinarello CA, Schrier RW, Edelstein CL. Impaired il-18 processing protects caspase-1-deficient mice from ischemic acute renal failure. *J Clin Invest*. 2001;107:1145-1152

149. Menzel CL, Sun Q, Loughran PA, Pape HC, Billiar TR, Scott MJ. Caspase-1 is hepatoprotective during trauma and hemorrhagic shock by reducing liver injury and inflammation. *Mol Med*. 2011;17:1031-1038

150. Zaki MH, Boyd KL, Vogel P, Kastan MB, Lamkanfi M, Kanneganti TD. The nlrp3 inflammasome protects against loss of epithelial integrity and mortality during experimental colitis. *Immunity*. 2010;32:379-391

151. Csak T, Ganz M, Pespisa J, Kodys K, Dolganiuc A, Szabo G. Fatty acid and endotoxin activate inflammasomes in mouse hepatocytes that release danger signals to stimulate immune cells. *Hepatology*. 2011;54:133-144

152. Prince JM, Ming MJ, Levy RM, Liu S, Pinsky DJ, Vodovotz Y, Billiar TR. Early growth response 1 mediates the systemic and hepatic inflammatory response initiated by hemorrhagic shock. *Shock*. 2007;27:157-164

153. Carchman EH, Rao J, Loughran PA, Rosengart MR, Zuckerbraun BS. Heme oxygenase-1-mediated autophagy protects against hepatocyte cell death and hepatic injury from infection/sepsis in mice. *Hepatology*. 2011;53:2053-2062

154. Kim JS, Ohshima S, Pediaditakis P, Lemasters JJ. Nitric oxide protects rat hepatocytes against reperfusion injury mediated by the mitochondrial permeability transition. *Hepatology*. 2004;39:1533-1543

155. Lagoa CE, Vodovotz Y, Stolz DB, Lhuillier F, McCloskey C, Gallo D, Yang R, Ustinova E, Fink MP, Billiar TR, Mars WM. The role of hepatic type 1 plasminogen activator inhibitor (pai-1) during murine hemorrhagic shock. *Hepatology*. 2005;42:390-399

156. Evans ZP, Palanisamy AP, Sutter AG, Ellett JD, Ramshesh VK, Attaway H, Schmidt MG, Schnellmann RG, Chavin KD. Mitochondrial uncoupling protein-2 deficiency protects steatotic mouse hepatocytes from hypoxia/reoxygenation. *Am J Physiol Gastrointest Liver Physiol*. 2012;302:G336-342

157. Stolz DB, Ross MA, Salem HM, Mars WM, Michalopoulos GK, Enomoto K. Cationic colloidal silica membrane perturbation as a means of examining changes at the sinusoidal surface during liver regeneration. *Am J Pathol*. 1999;155:1487-1498

158. Choi SW, Gerencser AA, Lee DW, Rajagopalan S, Nicholls DG, Andersen JK, Brand MD. Intrinsic bioenergetic properties and stress sensitivity of dopaminergic synaptosomes. *J Neurosci*. 2011;31:4524-4534

159. Santos JH, Meyer JN, Mandavilli BS, Van Houten B. Quantitative pcr-based measurement of nuclear and mitochondrial DNA damage and repair in mammalian cells. *Methods Mol Biol*. 2006;314:183-199

160. Gusdon AM, Chen J, Votyakova TV, Mathews CE. Chapter 24 quantification, localization, and tissue specificities of mouse mitochondrial reactive oxygen species production. *Methods Enzymol*. 2009;456:439-457

161. Gusdon AM, Zhu JH, Van Houten B, Chu CT. Atp13a2 regulates mitochondrial bioenergetics through macroautophagy. *Neurobiology of Disease*. 2012;45:962-972

162. Lemasters JJ, Ramshesh VK. Imaging of mitochondrial polarization and depolarization with cationic fluorophores. *Methods Cell Biol*. 2007;80:283-295

163. Jarrar D, Wang P, Cioffi WG, Bland KI, Chaudry IH. Critical role of oxygen radicals in the initiation of hepatic depression after trauma hemorrhage. *J Trauma*. 2000;49:879-885

164. Rensing H, Bauer I, Peters I, Wein T, Silomon M, Jaeschke H, Bauer M. Role of reactive oxygen species for hepatocellular injury and heme oxygenase-1 gene expression after hemorrhage and resuscitation. *Shock*. 1999;12:300-308

165. Li C, Jackson RM. Reactive species mechanisms of cellular hypoxia-reoxygenation injury. *Am J Physiol Cell Physiol*. 2002;282:C227-241

166. Belousov VV, Fradkov AF, Lukyanov KA, Staroverov DB, Shakhbazov KS, Terskikh AV, Lukyanov S. Genetically encoded fluorescent indicator for intracellular hydrogen peroxide. *Nat Methods*. 2006;3:281-286

167. Faulkner KM, Liochev SI, Fridovich I. Stable mn(iii) porphyrins mimic superoxide dismutase in vitro and substitute for it in vivo. *J Biol Chem*. 1994;269:23471-23476

168. Yoshioka J, Chutkow WA, Lee S, Kim JB, Yan J, Tian R, Lindsey ML, Feener EP, Seidman CE, Seidman JG, Lee RT. Deletion of thioredoxin-interacting protein in mice impairs mitochondrial function but protects the myocardium from ischemia-reperfusion injury. *J Clin Invest*. 2012;122:267-279

169. Hoppeler H, Vogt M, Weibel ER, Fluck M. Response of skeletal muscle mitochondria to hypoxia. *Exp Physiol*. 2003;88:109-119

170. Liu L, Feng D, Chen G, Chen M, Zheng Q, Song P, Ma Q, Zhu C, Wang R, Qi W, Huang L, Xue P, Li B, Wang X, Jin H, Wang J, Yang F, Liu P, Zhu Y, Sui S, Chen Q. Mitochondrial outer-membrane protein fundc1 mediates hypoxia-induced mitophagy in mammalian cells. *Nat Cell Biol*. 2012;14:177-185

171. Pua HH, Guo J, Komatsu M, He YW. Autophagy is essential for mitochondrial clearance in mature t lymphocytes. *J Immunol*. 2009;182:4046-4055

172. Klionsky DJ, Abeliovich H, Agostinis P, Agrawal DK, Aliev G, Askew DS, Baba M, Baehrecke EH, Bahr BA, Ballabio A, Bamber BA, Bassham DC, Bergamini E, Bi XN,

Biard-Piechaczyk M, Blum JS, Breclesen DE, Brodsky JL, Brumell JH, Brunk UT, Bursch W, Camougrand N, Cebollero E, Cecconi F, Chen YY, Chin LS, Choi A, Chu CT, Chung JK, Clarke PGH, Clark RSB, Clarke SG, Clave C, Cleveland JL, Codogno P, Colombo MI, Coto-Montes A, Cregg JM, Cuervo AM, Debnath J, Demarchi F, Dennis PB, Dennis PA, Deretic V, Devenish RJ, Di Sano F, Dice JF, DiFiglia M, Dinesh-Kumar S, Distelhorst CW, Djavaheri-Mergny M, Dorsey FC, Droge W, Dron M, Dunn WA, Duszenko M, Eissa NT, Elazar Z, Esclatine A, Eskelinen EL, Fesues L, Finley KD, Fuentes JM, Fueyo J, Fujisaki K, Galliot B, Gao FB, Gewirtz DA, Gibson SB, Gohla A, Goldberg AL, Gonzalez R, Gonzalez-Estevez C, Gorski S, Gottlieb RA, Haussinger D, He YW, Heidenreich K, Hill JA, Hoyer-Hansen M, Hu X, Huang WP, Iwasaki A, Jaattela M, Jackson WT, Jiang X, Jin SK, Johansen T, Jung JU, Kadowaki M, Kang C, Kelekar A, Kessel DH, Kiel JAKW, Kim HP, Kimchi A, Kinsella TJ, Kiselyov K, Kitamoto K, Knecht E, Komatsu M, Kominami E, Konclo S, Kovacs AL, Kroemer G, Kuan CY, Kumar R, Kundu M, Landry J, Laporte M, Le WD, Lei HY, Lenardo MJ, Levine B, Lieberman A, Lim KL, Lin FC, Liou W, Liu LF, Lopez-Berestein G, Lopez-Otin C, Lu B, Macleod KF, Malorni W, Martinet W, Matsuoka K, Mautner J, Meijer AJ, Melendez A, Michels P, Miotto G, Mistiaen WP, Mizushima N, Mograbi B, Monastyrska I, Moore MN, Moreira PI, Moriyasu Y, Motyl T, Munz C, Murphy LO, Naqvi NI, Neufeld TP, Nishino I, Nixon RA, Noda T, Nurnberg B, Ogawa M, Oleinick NL, Olsen LJ, Ozpolat B, Paglin S, Palmer GE, Papassideri I, Parkes M, Perlmutter DH, Perry G, Piacentini M, Pinkas-Kramarski R, Prescott M, Proikas-Cezanne T, Raben N, Rami A, Reggiori F, Rohrer B, Rubinsztein DC, Ryan KM, Sadoshima J, Sakagami H, Sakai Y, Sandri M, Sasakawa C, Sass M, Schneider C, Seglen PO, Seleverstov O, Settleman J, Shacka JJ, Shapiro IM, Sibirny A, Silva-Zacarin ECM, Simon HU, Simone C, Simonsen A, Smith MA, Spanel-Borowski K, Srinivas V, Steeves M, Stenmark H, Stromhaug PE, Subauste CS, Sugimoto S, Sulzer D, Suzuki T, Swanson MS, Takeshita F, Talbot NJ, Talloczy Z, Tanaka K, Tanaka K, Tanida I, Taylor GS, Taylor JP, Terman A, Tettamanti G, Thompson CB, Thumm M, Tolkovsky AM, Tooze SA, Truant R, Tumanovska LV, Uchiyama Y, Ueno T, Uzcategui NL, van der Klei I, Vaquero EC, Vellai T, Vogel MW, Wang HG, Webster P, Wiley JW, Xi ZJ, Xiao G, Yahalom J, Yang JM, Yap G, Yin XM, Yoshimori T, Yu L, Yue ZY, Yuzaki M, Zabirnyk O, Zheng XX, Zhu X, Deter RL, Tabas I. Guidelines for the use and interpretation of assays for monitoring autophagy in higher eukaryotes. *Autophagy*. 2008;4:151-175

173. Kimura S, Noda T, Yoshimori T. Dissection of the autophagosome maturation process by a novel reporter protein, tandem fluorescent-tagged lc3. *Autophagy*. 2007;3:452-460

174. Li H, Wang P, Sun QH, Ding WX, Yin XM, Sobol RW, Stolz DB, Yu J, Zhang L. Following cytochrome c release, autophagy is inhibited during chemotherapy-induced apoptosis by caspase 8-mediated cleavage of beclin 1. *Cancer Res*. 2011;71:3625-3634

175. Yoritaka A, Hattori N, Uchida K, Tanaka M, Stadtman ER, Mizuno Y. Immunohistochemical detection of 4-hydroxynonenal protein adducts in parkinson disease. *Proc Natl Acad Sci U S A*. 1996;93:2696-2701

176. Venkatraman A, Shiva S, Davis AJ, Bailey SM, Brookes PS, Darley-Usmar VM. Chronic alcohol consumption increases the sensitivity of rat liver mitochondrial respiration to inhibition by nitric oxide. *Hepatology*. 2003;38:141-147

177. Hamacher-Brady A, Brady NR, Gottlieb RA. Enhancing macroautophagy protects against ischemia/reperfusion injury in cardiac myocytes. *J Biol Chem*. 2006;281:29776-29787

178. Kang R, Zeh HJ, Lotze MT, Tang D. The beclin 1 network regulates autophagy and apoptosis. *Cell Death Differ*. 2011;18:571-580

179. Sun Q, Gao W, Loughran P, Shapiro R, Fan J, Billiar TR, Scott MJ. Caspase-1 activation is protective against hepatocyte cell death by up-regulating beclin1 and mitochondrial autophagy in the setting of redox stress. *J Biol Chem*. 2013

180. Abulafia DP, de Rivero Vaccari JP, Lozano JD, Lotocki G, Keane RW, Dietrich WD. Inhibition of the inflammasome complex reduces the inflammatory response after thromboembolic stroke in mice. *J Cereb Blood Flow Metab*. 2009;29:534-544

181. McCloskey CA, Kameneva MV, Uryash A, Gallo DJ, Billiar TR. Tissue hypoxia activates jnk in the liver during hemorrhagic shock. *Shock*. 2004;22:380-386

182. Hornung V, Ablasser A, Charrel-Dennis M, Bauernfeind F, Horvath G, Caffrey DR, Latz E, Fitzgerald KA. Aim2 recognizes cytosolic dsdna and forms a caspase-1-activating inflammasome with asc. *Nature*. 2009;458:514-518

183. Yanai H, Ban T, Wang ZC, Choi MK, Kawamura T, Negishi H, Nakasato M, Lu Y, Hangai S, Koshiba R, Savitsky D, Ronfani L, Akira S, Bianchi ME, Honda K, Tamura T, Kodama T, Taniguchi T. Hmgb proteins function as universal sentinels for nucleic-acid-mediated innate immune responses. *Nature*. 2009;462:99-U110

184. Glantzounis GK, Salacinski HJ, Yang W, Davidson BR, Seifalian AM. The contemporary role of antioxidant therapy in attenuating liver ischemia-reperfusion injury: A review. *Liver Transpl*. 2005;11:1031-1047

185. Henao-Mejia J, Elinav E, Jin C, Hao L, Mehal WZ, Strowig T, Thaiss CA, Kau AL, Eisenbarth SC, Jurczak MJ, Camporez JP, Shulman GI, Gordon JI, Hoffman HM, Flavell RA. Inflammasome-mediated dysbiosis regulates progression of nafld and obesity. *Nature*. 2012;482:179-185

186. Pessayre D, Mansouri A, Fromenty B. Nonalcoholic steatosis and steatohepatitis. V. Mitochondrial dysfunction in steatohepatitis. *Am J Physiol Gastrointest Liver Physiol*. 2002;282:G193-199

187. Mehta K, Van Thiel DH, Shah N, Mobarhan S. Nonalcoholic fatty liver disease: Pathogenesis and the role of antioxidants. *Nutr Rev*. 2002;60:289-293

188. Imaeda AB, Watanabe A, Sohail MA, Mahmood S, Mohamadnejad M, Sutterwala FS, Flavell RA, Mehall WZ. Acetaminophen-induced hepatotoxicity in mice is dependent on tlr9 and the nalp3 inflammasome. *Journal of Clinical Investigation*. 2009;119:305-314

189. Gao B. Hepatoprotective and anti-inflammatory cytokines in alcoholic liver disease. *J Gastroen Hepatol*. 2012;27:89-93

190. Chen Q, Camara AK, Stowe DF, Hoppel CL, Lesnefsky EJ. Modulation of electron transport protects cardiac mitochondria and decreases myocardial injury during ischemia and reperfusion. *Am J Physiol Cell Physiol*. 2007;292:C137-147

191. Vallabhaneni R, Kaczorowski DJ, Yaakovian MD, Rao J, Zuckerbraun BS. Heme oxygenase 1 protects against hepatic hypoxia and injury from hemorrhage via regulation of cellular respiration. *Shock*. 2010;33:274-281

192. Aragones J, Schneider M, Van Geyte K, Fraisl P, Dresselaers T, Mazzone M, Dirkx R, Zacchigna S, Lemieux H, Jeoung NH, Lambrechts D, Bishop T, Lafuste P, Diez-Juan A, Harten SK, Van Noten P, De Bock K, Willam C, Tjwa M, Grosfeld A, Navet R, Moons

L, Vandendriessche T, Deroose C, Wijeyekoon B, Nuyts J, Jordan B, Silasi-Mansat R, Lupu F, Dewerchin M, Pugh C, Salmon P, Mortelmans L, Gallez B, Gorus F, Buyse J, Sluse F, Harris RA, Gnaiger E, Hespel P, Van Hecke P, Schuit F, Van Veldhoven P, Ratcliffe P, Baes M, Maxwell P, Carmeliet P. Deficiency or inhibition of oxygen sensor phd1 induces hypoxia tolerance by reprogramming basal metabolism. *Nat Genet*. 2008;40:170-180

193. Kelly DP. Hypoxic reprogramming. *Nat Genet*. 2008;40:132-134
194. Zhu L, Wang Q, Zhang L, Fang Z, Zhao F, Lv Z, Gu Z, Zhang J, Wang J, Zen K, Xiang Y, Wang D, Zhang CY. Hypoxia induces pgc-1alpha expression and mitochondrial biogenesis in the myocardium of tof patients. *Cell Res*. 2010;20:676-687
195. Gusdon AM, Zhu J, Van Houten B, Chu CT. Atp13a2 regulates mitochondrial bioenergetics through macroautophagy. *Neurobiol Dis*. 2012;45:962-972
196. Terman A, Dalen H, Eaton JW, Neuzil J, Brunk UT. Mitochondrial recycling and aging of cardiac myocytes: The role of autophagocytosis. *Exp Gerontol*. 2003;38:863-876
197. Ravikumar B, Berger Z, Vacher C, O'Kane CJ, Rubinsztein DC. Rapamycin pre-treatment protects against apoptosis. *Hum Mol Genet*. 2006;15:1209-1216
198. Miwa S, Lawless C, von Zglinicki T. Mitochondrial turnover in liver is fast in vivo and is accelerated by dietary restriction: Application of a simple dynamic model. *Aging Cell*. 2008;7:920-923
199. Diaz F, Moraes CT. Mitochondrial biogenesis and turnover. *Cell Calcium*. 2008;44:24-35
200. Bellot G, Garcia-Medina R, Gounon P, Chiche J, Roux D, Pouyssegur J, Mazure NM. Hypoxia-induced autophagy is mediated through hypoxia-inducible factor induction of bnip3 and bnip3l via their bh3 domains. *Mol Cell Biol*. 2009;29:2570-2581
201. Broz P, Ruby T, Belhocine K, Bouley DM, Kayagaki N, Dixit VM, Monack DM. Caspase-11 increases susceptibility to salmonella infection in the absence of caspase-1. *Nature*. 2012;490:288-291
202. Broz P, Monack DM. Noncanonical inflammasomes: Caspase-11 activation and effector mechanisms. *PLoS Pathog*. 2013;9:e1003144
203. Belhocine K, Monack DM. Francisella infection triggers activation of the aim2 inflammasome in murine dendritic cells. *Cell Microbiol*. 2012;14:71-80
204. Jones JW, Broz P, Monack DM. Innate immune recognition of francisella tularensis: Activation of type-i interferons and the inflammasome. *Front Microbiol*. 2011;2:16
205. Fernandes-Alnemri T, Yu JW, Juliana C, Solorzano L, Kang S, Wu J, Datta P, McCormick M, Huang L, McDermott E, Eisenlohr L, Landel CP, Alnemri ES. The aim2 inflammasome is critical for innate immunity to francisella tularensis. *Nat Immunol*. 2010;11:385-393
206. Ge J, Gong YN, Xu Y, Shao F. Preventing bacterial DNA release and absent in melanoma 2 inflammasome activation by a legionella effector functioning in membrane trafficking. *Proc Natl Acad Sci U S A*. 2012;109:6193-6198
207. Tsuchiya K, Hara H, Kawamura I, Nomura T, Yamamoto T, Daim S, Dewamitta SR, Shen Y, Fang R, Mitsuyama M. Involvement of absent in melanoma 2 in inflammasome activation in macrophages infected with listeria monocytogenes. *J Immunol*. 2010;185:1186-1195
208. Dombrowski Y, Peric M, Koglin S, Kaymakanov N, Schmezer V, Reinholz M, Ruzicka T, Schauber J. Honey bee (apis mellifera) venom induces aim2 inflammasome activation in human keratinocytes. *Allergy*. 2012;67:1400-1407

209. Sun KH, Yu CL, Tang SJ, Sun GH. Monoclonal anti-double-stranded DNA autoantibody stimulates the expression and release of il-1beta, il-6, il-8, il-10 and tnf-alpha from normal human mononuclear cells involving in the lupus pathogenesis. *Immunology*. 2000;99:352-360

210. Panchanathan R, Duan X, Shen H, Rathinam VA, Erickson LD, Fitzgerald KA, Choubey D. Aim2 deficiency stimulates the expression of ifn-inducible ifi202, a lupus susceptibility murine gene within the nba2 autoimmune susceptibility locus. *J Immunol*. 2010;185:7385-7393

211. Zhang W, Cai Y, Xu W, Yin Z, Gao X, Xiong S. Aim2 facilitates the apoptotic DNA-induced systemic lupus erythematosus via arbitrating macrophage functional maturation. *J Clin Immunol*. 2013

212. Roberts TL, Idris A, Dunn JA, Kelly GM, Burnton CM, Hodgson S, Hardy LL, Garceau V, Sweet MJ, Ross IL, Hume DA, Stacey KJ. Hin-200 proteins regulate caspase activation in response to foreign cytoplasmic DNA. *Science*. 2009;323:1057-1060

213. Panchanathan R, Shen H, Duan X, Rathinam VA, Erickson LD, Fitzgerald KA, Choubey D. Aim2 deficiency in mice suppresses the expression of the inhibitory fcgamma receptor (fcgammariib) through the induction of the ifn-inducible p202, a lupus susceptibility protein. *J Immunol*. 2011;186:6762-6770

214. Weiss JN, Korge P, Honda HM, Ping P. Role of the mitochondrial permeability transition in myocardial disease. *Circ Res*. 2003;93:292-301

215. Collins JA, Schandl CA, Young KK, Vesely J, Willingham MC. Major DNA fragmentation is a late event in apoptosis. *J Histochem Cytochem*. 1997;45:923-934

216. Ivanov S, Dragoi AM, Wang X, Dallacosta C, Louten J, Musco G, Sitia G, Yap GS, Wan Y, Biron CA, Bianchi ME, Wang H, Chu WM. A novel role for hmgb1 in tlr9-mediated inflammatory responses to cpg-DNA. *Blood*. 2007;110:1970-1981

217. Yang H, Wang H, Czura CJ, Tracey KJ. The cytokine activity of hmgb1. *J Leukoc Biol*. 2005;78:1-8

218. Lotze MT, Tracey KJ. High-mobility group box 1 protein (hmgb1): Nuclear weapon in the immune arsenal. *Nat Rev Immunol*. 2005;5:331-342

219. Tang D, Kang R, Livesey KM, Cheh CW, Farkas A, Loughran P, Hoppe G, Bianchi ME, Tracey KJ, Zeh HJ, 3rd, Lotze MT. Endogenous hmgb1 regulates autophagy. *J Cell Biol*. 2010;190:881-892

220. Tang D, Kang R, Livesey KM, Zeh HJ, 3rd, Lotze MT. High mobility group box 1 (hmgb1) activates an autophagic response to oxidative stress. *Antioxid Redox Signal*. 2011;15:2185-2195

221. Tang D, Kang R, Livesey KM, Kroemer G, Billiar TR, Van Houten B, Zeh HJ, 3rd, Lotze MT. High-mobility group box 1 is essential for mitochondrial quality control. *Cell Metab*. 2011;13:701-711

222. Rajewsky K, Gu H, Kuhn R, Betz UA, Muller W, Roes J, Schwenk F. Conditional gene targeting. *J Clin Invest*. 1996;98:600-603

223. Tang D, Shi Y, Kang R, Li T, Xiao W, Wang H, Xiao X. Hydrogen peroxide stimulates macrophages and monocytes to actively release hmgb1. *J Leukoc Biol*. 2007;81:741-747

224. Evankovich J, Cho SW, Zhang R, Cardinal J, Dhupar R, Zhang L, Klune JR, Zlotnicki J, Billiar T, Tsung A. High mobility group box 1 release from hepatocytes during ischemia and reperfusion injury is mediated by decreased histone deacetylase activity. *J Biol Chem*. 2010;285:39888-39897

QIAN SUN

qis7@pitt.edu

EDUCATION and TRAINING

GRADUATE:

2008-	University of Pittsburgh, Pittsburgh	PhD Expected graduation: 2013	Cellular and Molecular Pathology

UNDERGRADUATE:

2003-2008	Medical Center of Fudan University, Shanghai, China	Bachelor of Medicine, 2008	Basic Medical Sciences

_____

POSITIONS

2008 -	Graduate Student Research	University of Pittsburgh, Cellular & Molecular Pathology; Laboratory of Dr. Timothy Billiar
2007 – 2008	Undergraduate Research	Fudan University, Department of Molecular and Cellular Biology; Laboratory of Dr. Luanfeng Pan

_____

ACADEMIC AND PROFESSIONAL HONORS

Travel Award	Seahorse Bioscience-Keystone Metabolic Control of Inflammation	2013
Travel Award	Graduate and Professional Student Association	2013
Travel Award	Keystone Autophagy Meeting	2011

Best Poster Presentation	Surgical Research Day	2011
People's Scholarship	Fudan University	2005-2007
Tuition Scholarship	Fudan University	2003-2007
Excellent Student	Summer research program in Molecular Medicine Key Lab	2005

_____

ORGANIZATIONAL ACTIVITIES

University of Pittsburgh	Housing helper for incoming student	2011-2012
Fudan University	Volunteer for Chinese Red Ribbon	2005
Fudan University	Volunteer at Shanghai No.1 Social Welfare Institution	2005

_____

PROFESSIONAL SOCIETY MEMBERSHIPS

| American Association of Immunologists (AAI) | 2012-2013 |
| Society for Leukocyte Biology | 2011-2013 |

_____

ORAL PRESENTATIONS

1. Caspase-1 is Hepatoprotective after Hemorrhagic Shock. 8th World Congress on Trauma, Shock, Inflammation and Sepsis, Munich, Germany, 2010

2. Regulation of Autophagy and Apoptosis by Caspase-1 after Hemorrhagic Shock in Mice. 30th Surgical Infection Society, Las Vegas, Nevada, 2010

3. Regulation of Autophagy by Caspase-1 in Hepatocytes after Oxidative Stress. 33th Shock Conference, Portland, Oregon, 2010

4. Caspase-1 is hepatoprotective by reducing ROS production in the liver after hemorrhagic shock, 1st Regional Translational Research in Mitochondria, Aging and Disease, Pittsburgh, Pennsylvania, 2011

PEER-REVIEWED PUBLICATIONS

1. **Sun Q**, Gao W, Loughran P, Shapiro R, Fan J, Biliar TR, Scott MJ. Caspase-1 activation is protective against hepatocyte cell death by up-regulating beclin1 and mitochondrial autophagy in the setting of redox stress. J Biol Chem. 2013 Apr 15. [Epub ahead of print]

2. Menzel CL, **Sun Q**, Loughran PA, Pape HC, Billiar TR, Scott MJ. Caspase-1 is hepatoprotective during trauma and hemorrhagic shock by reducing liver injury and inflammation. Mol Med. 17;9-10(2011):1031-8

3. Scott MJ, Chen C, **Sun Q**, Billiar TR. Hepatocytes express functional NOD1 and NOD2 receptors: A role for NOD1 in hepatocyte CC and CXC chemokine production. Journal of Hepatology 53;4 (2010):693-701

4. Marongiu F, Gramignoli R, **Sun Q**, Tahan V, Miki T, Dorko K, Ellis E, Strom SC. Isolation of amniotic mesenchymal stem cells. Curr Protoc Stem Cell Biol. 2010 Mar; Chapter 1: Unit 1E.5. PMID: 20200854

PUBLISHED ABSTRACTS

1. **Sun Q**, Billiar TR, Scott MJ. Caspase-1 blocks regulates induction of autophagy after hemorrhagic shock in mice. Shock. 33;7 Suppl 1 (2010) Published Abstract

2. **Sun Q**, Billiar TR, Scott MJ. Hypoxia-induced upregulation of autophagy in mouse hepatocytes is dependent on caspase-1. Surgical Infections. 11;2 (2010) Published Abstract

3. Menzel C, **Sun Q**, Pape H, Billiar TR, Scott MJ. Caspase-1 is protective during trauma and hemorrhagic shock in mice. Cytokine. 48; 59 (2009) Published Abstract